FLASHOVER MECHANISM AND LABORATORY EVALUATION OF POLLUTED INSULATORS UNDER DC VOLTAGE

BY

Fernando A. Chagas

A THESIS

Submitted to the Faculty of Graduate Studies in partial fulfillment of the requirements for the degree of

DOCTOR OF PHILOSOPHY

Department of Electrical and Computer Engineering

The University of Manitoba

Winnipeg, Manitoba, Canada

DECEMBER 1996

ISBN 0-612-16110-2

Name POLLUTED INSULATOR

Dissertation Abstracts International and *Masters Abstracts International* are arranged by broad, general subject categories. Please select the one subject which most nearly describes the content of your dissertation or thesis. Enter the corresponding four-digit code in the spaces provided.

SUBJECT TERM

Electronics Engineering

SUBJECT CODE 0544

UMI

Subject Categories

THE HUMANITIES AND SOCIAL SCIENCES

COMMUNICATIONS AND THE ARTS
- Architecture 0729
- Art History 0377
- Cinema 0900
- Dance 0378
- Design and Decorative Arts 0389
- Fine Arts 0357
- Information Science 0723
- Journalism 0391
- Landscape Architecture 0390
- Library Science 0399
- Mass Communications 0708
- Music 0413
- Speech Communication 0459
- Theater 0465

EDUCATION
- General 0515
- Administration 0514
- Adult and Continuing 0516
- Agricultural 0517
- Art 0273
- Bilingual and Multicultural 0282
- Business 0688
- Community College 0275
- Curriculum and Instruction 0727
- Early Childhood 0518
- Elementary 0524
- Educational Psychology 0525
- Finance 0277
- Guidance and Counseling 0519
- Health 0680
- Higher 0745
- History of 0520
- Home Economics 0278
- Industrial 0521
- Language and Literature 0279
- Mathematics 0280
- Music 0522
- Philosophy of 0998
- Physical 0523
- Reading 0535
- Religious 0527
- Sciences 0714
- Secondary 0533
- Social Sciences 0534
- Sociology of 0340
- Special 0529
- Teacher Training 0530
- Technology 0710
- Tests and Measurements 0288
- Vocational 0747

LANGUAGE, LITERATURE AND LINGUISTICS
- Language
  - General 0679
  - Ancient 0289
  - Linguistics 0290
  - Modern 0291
  - Rhetoric and Composition 0681
- Literature
  - General 0401
  - Classical 0294
  - Comparative 0295
  - Medieval 0297
  - Modern 0298
  - African 0316
  - American 0591
  - Asian 0305
  - Canadian (English) 0352
  - Canadian (French) 0355
  - Caribbean 0360
  - English 0593
  - Germanic 0311
  - Latin American 0312
  - Middle Eastern 0315
  - Romance 0313
  - Slavic and East European 0314

PHILOSOPHY, RELIGION AND THEOLOGY
- Philosophy 0422
- Religion
  - General 0318
  - Biblical Studies 0321
  - Clergy 0319
  - History of 0320
  - Philosophy of 0322
- Theology 0469

SOCIAL SCIENCES
- American Studies 0323
- Anthropology
  - Archaeology 0324
  - Cultural 0326
  - Physical 0327
- Business Administration
  - General 0310
  - Accounting 0272
  - Banking 0770
  - Management 0454
  - Marketing 0338
- Canadian Studies 0385
- Economics
  - General 0501
  - Agricultural 0503
  - Commerce-Business 0505
  - Finance 0508
  - History 0509
  - Labor 0510
  - Theory 0511
- Folklore 0358
- Geography 0366
- Gerontology 0351
- History
  - General 0578
  - Ancient 0579
  - Medieval 0581
  - Modern 0582
  - Church 0330
  - Black 0328
  - African 0331
  - Asia, Australia and Oceania 0332
  - Canadian 0334
  - European 0335
  - Latin American 0336
  - Middle Eastern 0333
  - United States 0337
- History of Science 0585
- Law 0398
- Political Science
  - General 0615
  - International Law and Relations 0616
  - Public Administration 0617
- Recreation 0814
- Social Work 0452
- Sociology
  - General 0626
  - Criminology and Penology 0627
  - Demography 0938
  - Ethnic and Racial Studies 0631
  - Individual and Family Studies 0628
  - Industrial and Labor Relations 0629
  - Public and Social Welfare 0630
  - Social Structure and Development 0700
  - Theory and Methods 0344
- Transportation 0709
- Urban and Regional Planning 0999
- Women's Studies 0453

THE SCIENCES AND ENGINEERING

BIOLOGICAL SCIENCES
- Agriculture
  - General 0473
  - Agronomy 0285
  - Animal Culture and Nutrition 0475
  - Animal Pathology 0476
  - Fisheries and Aquaculture 0792
  - Food Science and Technology 0359
  - Forestry and Wildlife 0478
  - Plant Culture 0479
  - Plant Pathology 0480
  - Range Management 0777
  - Soil Science 0481
  - Wood Technology 0746
- Biology
  - General 0306
  - Anatomy 0287
  - Animal Physiology 0433
  - Biostatistics 0308
  - Botany 0309
  - Cell 0379
  - Ecology 0329
  - Entomology 0353
  - Genetics 0369
  - Limnology 0793
  - Microbiology 0410
  - Molecular 0307
  - Neuroscience 0317
  - Oceanography 0416
  - Plant Physiology 0817
  - Veterinary Science 0778
  - Zoology 0472
- Biophysics
  - General 0786
  - Medical 0760

EARTH SCIENCES
- Biogeochemistry 0425
- Geochemistry 0996
- Geodesy 0370
- Geology 0372
- Geophysics 0373
- Hydrology 0388
- Mineralogy 0411
- Paleobotany 0345
- Paleoecology 0426
- Paleontology 0418
- Paleozoology 0985
- Palynology 0427
- Physical Geography 0368
- Physical Oceanography 0415

HEALTH AND ENVIRONMENTAL SCIENCES
- Environmental Sciences 0768
- Health Sciences
  - General 0566
  - Audiology 0300
  - Dentistry 0567
  - Education 0350
  - Administration, Health Care 0769
  - Human Development 0758
  - Immunology 0982
  - Medicine and Surgery 0564
  - Mental Health 0347
  - Nursing 0569
  - Nutrition 0570
  - Obstetrics and Gynecology 0380
  - Occupational Health and Safety 0354
  - Oncology 0992
  - Ophthalmology 0381
  - Pathology 0571
  - Pharmacology 0419
  - Pharmacy 0572
  - Public Health 0573
  - Radiology 0574
  - Recreation 0575
  - Rehabilitaion and Therapy 0382
  - Speech Pathology 0460
  - Toxicology 0383
- Home Economics 0386

PHYSICAL SCIENCES

Pure Sciences
- Chemistry
  - General 0485
  - Agricultural 0749
  - Analytical 0486
  - Biochemistry 0487
  - Inorganic 0488
  - Nuclear 0738
  - Organic 0490
  - Pharmaceutical 0491
  - Physical 0494
  - Polymer 0495
  - Radiation 0754
- Mathematics 0405
- Physics
  - General 0605
  - Acoustics 0986
  - Astronomy and Astrophysics 0606
  - Atmospheric Science 0608
  - Atomic 0748
  - Condensed Matter 0611
  - Electricity and Magnetism 0607
  - Elementary Particles and High Energy 0798
  - Fluid and Plasma 0759
  - Molecular 0609
  - Nuclear 0610
  - Optics 0752
  - Radiation 0756
- Statistics 0463

Applied Sciences
- Applied Mechanics 0346
- Computer Science 0984
- Engineering
  - General 0537
  - Aerospace 0538
  - Agricultural 0539
  - Automotive 0540
  - Biomedical 0541
  - Chemical 0542
  - Civil 0543
  - Electronics and Electrical 0544
  - Environmental 0775
  - Industrial 0546
  - Marine and Ocean 0547
  - Materials Science 0794
  - Mechanical 0548
  - Metallurgy 0743
  - Mining 0551
  - Nuclear 0552
  - Packaging 0549
  - Petroleum 0765
  - Sanitary and Municipal 0554
  - System Science 0790
- Geotechnology 0428
- Operations Research 0796
- Plastics Technology 0795
- Textile Technology 0994

PSYCHOLOGY
- General 0621
- Behavioral 0384
- Clinical 0622
- Cognitive 0633
- Developmental 0620
- Experimental 0623
- Industrial 0624
- Personality 0625
- Physiological 0989
- Psychobiology 0349
- Psychometrics 0632
- Social 0451

THE UNIVERSITY OF MANITOBA

FACULTY OF GRADUATE STUDIES

COPYRIGHT PERMISSION

FLASHOVER MECHANISM AND LABORATORY EVALUATION OF POLLUTED INSULATORS UNDER DC VOLTAGE

BY

FERNANDO A. CHAGAS

A Thesis/Practicum submitted to the Faculty of Graduate Studies of the University of Manitoba in partial fulfillment of the requirements for the degree of

DOCTOR OF PHILOSOPHY

ABSTRACT

HVDC constitutes an economical alternative when huge blocks of power need to be transmitted over long distances.

Factors which influence the mechanism of pollution flashover under dc voltages must be carefully studied if a representative test is to be proposed, as test results are dependent on various factors, such as source capacity. Two test procedures for HVDC insulator testing are currently being analyzed for international standardization: the salt fog procedure and the solid layer procedure followed by steam fog or cold fog for wetting of the pollution layer.

This thesis presents the results of extensive tests conducted to verify the effect of the voltage source on the critical flashover voltage of dc insulators under pollution. Tests, with the solid layer method using the steam fog for wetting of pollution layer, were performed. A data acquisition system was used to record all current pulses above a certain pre selected current level and the corresponding voltage evolution during current pulse duration, which made possible a complete analysis of current pulses and voltage drops characteristics during the flashover process.

The information obtained provides a better understanding of the flashover process of dc insulation under pollution and may be used to improve the existing testing guidelines.

An analysis of a recent model for simulation of the flashover process of polluted dc insulation was performed. The model was used to estimate the flashover voltage for the insulators tested with reasonable results. An improvement of the model has been proposed and verified.

ACKNOWLEDGEMENT

The author wishes to express his sincere gratitude to his advisor Dr. E. Kuffel for his encouragement, guidance and valuable discussions during the course of this work and to Dr. M. R. Raghuveer for his support and kind help during the revision of the Thesis.

The author expresses his thanks to Dr. João G. C. Barros and Mr. Jose Carlos de Medeiros for their support and encouragement to initiate and conclude this work.

The author is grateful to Mr. Agenor O. F. Mundim who took over his duties in CEPEL - Electrical Energy Research Center during the periods when he was at The University of Manitoba and during the one year period when he was planning and performing the experiments at CEPEL Pollution Laboratory and also to Mr. Edegard Gomes Jr. from the High Voltage Unit of CEPEL for the valuable technical discussions.

The help of Mr. Daniel Silveira, Mr. Marcelo Carvalhaes and Carlos Fontes, technicians from the High Voltage Unit of CEPEL, during the testing period is also acknowledge.

The sponsorship of CNPq - Brazilian National Research Council and CEPEL is gratefully acknowledged.

Finally, the author expresses his sincere appreciation to his wife, Adriana, and children Thiago, Felipe and Carolina for their understanding, support and encouragement.

TABLE OF CONTENTS

LIST OF FIGURES

LIST OF TABLES

LIST OF PHOTOS

CHAPTER 1

GENERAL

1.1 - INTRODUCTION

Insulations of both ac and dc lines are subjected to overvoltages due to lightning discharges, overvoltages generated internally in the system and also normal continuous operating voltage. Internal overvoltages on dc systems are much lower than on ac systems, as in dc systems fault clearing can be obtained by action on the control system of rectifiers. Internal and external overvoltages normally impose requirements on the length of insulator strings, post insulators or bushings whereas the continuous overvoltage stress defines the needed leakage or creepage distance.

Pollution has a notable effect on the performance of external insulation under dc voltage. In fact, the pollution performance of the insulation is the first criterion for insulation design in HVDC systems. In the recent years a number of HVDC transmission systems were put in operation in different countries. Generally the HVDC alternative for transmission is economical when huge blocks of power have to be transmitted over long distances. In Brazil, HVDC transmission at ±600kV or ± 800kV levels are being considered as alternatives for the transmission of power to be generated by future power stations in the Amazon Region to the large load centers in the southeast and northeast of the country. The planned transmission lines are expected to cover distances from 1,800 to 2,500 km. The correct choice of insulators for these systems will have an important impact on cost and operational reliability.

Due to the lack of experience and understanding of the mechanisms which govern the flashover process on polluted insulators under dc voltage, HVDC insulators are designed and tested following guidelines which are well established for ac insulation; but specifications may be changed as new information on dc artificial pollution tests becomes available. The first HVDC stations had insulators with stress level of the order of 24 mm/kV(Creep). For the majority of new stations the stress level lies between 30 to 35 mm/kV, whereas for bushings, creepage lengths up to 50 mm/kV have been used.

Several insulator flashovers have been reported in HVDC stations due to inadequate insulator contamination design. Many of these flashovers were related to uneven wetting of insulators and bushings even when the surface was clean or very low level of pollution was present. Studies are being conducted in various countries in order to get a better understanding of the performance of insulation under dc stress. These studies have identified important differences in the pollution performance of dc insulators subjected to natural or artificial tests, when compared to ac insulators.

1.2 - OBJECTIVES OF THE PRESENT RESEARCH

The objectives are:

1. to obtain extensive experimental data in order to verify if the proposed criteria for dc voltage source to be used for pollution testing have general application;

2. to obtain additional information on the characteristics of pulse currents and related voltage drops during dc pollution tests. This information is important for the design of components of HVDC test sources;

3. to obtain experimental data to contribute to the standardization of HVDC insulator pollution test under consideration by IEC and IEEE;

4. from the experimental data obtained, perform an analysis of a recent model for HVDC insulator pollution flashover in order to verify if any improvement to this model can be proposed.

CHAPTER 2

LITERATURE REVIEW

2.1 - OPERATING EXPERIENCE ON EXISTING DC SYSTEMS

Reference [1] presents the operational experience over 10 years on both station and line insulation for the Sylmar Converter Station and the Pacific HVDC Line near Los Angeles. An excessive number of insulation flashovers has occurred since the system has started operation in 1970. During 9 years 196 flashovers occurred at ± 400kV. More than half of these occurred during the first two years of operation. The flashover rates were about the same for both polarities (55% at positive and 45% at negative polarity). Several measures were taken to reduce the flashover incidence. In [1] it is reported that the station insulators and the line insulators of the first 16 km of the line close to the station had to be subjected to washing every two months to get satisfactory operational reliability.

Reference [2] also gives information about insulation performance of dc systems in operation until 1982. The pollution failure rate is reported to be low but washing and coating had been introduced in nearly all stations, which has certainly a negative economic effect on the system operational costs. The number of flashovers at voltage levels > 300kV is much higher than at lower levels. For the higher operating voltages(± 400kV), 80 station flashovers are reported, 65% of these refer to wall bushings.

HVDC wall bushings performance appears to be more critical at system voltages above ±400kV. The increase in specific leakage length from 25 mm/kV used in ±400kV Pacific Intertie to

40mm/kV for the ±500kV system did not improve the bushing performance. After the ±600kV Brazilian Itaipu system was put in operation, 23 flashovers on wall bushings and transducers bushings occurred during the first 4 years, all reported during light rain, 18 under negative and 5 under positive polarity. In Itaipu, the ESDD(Equivalent Salt Deposit Density) levels measured on the bushings were light, in the range 3-5 $\mu g/cm^2$, which is too low to explain flashover occurrence by a conventional pollution flashover mechanism.

It is reported that prior to the failure, no scintillation was observed on the bushings' surfaces, although careful observation was made during rainy periods. Also in some few cases puncture of the bushing porcelain occurred. It was demonstrated by laboratory tests that these bushing failures occur due to non uniformity of the wetting process under rain.

The above information emphasizes the importance of contamination performance of external insulation under dc voltage and the need for further research in the dc flashover process (i.e. contamination collection, wetting and flashover development) in order that a better understanding can be acquired, new design and solutions can be proposed and also more representative test methods can be adopted.

2.2- POLLUTION FLASHOVER MECHANISM UNDER DC

The surface flashover of polluted insulation is a complex phenomenon, involving several variables. The flashover process develops in 5 main stages:

1- surface contamination and deposition;

2- wetting of the contamination layer with consequent formation of a conductive layer on insulator surface;

3- formation of dry bands associated with the drying effect of surface leakage currents with non uniform density along the insulator surface;

4- partial arc formation bridging the dry band;

5- arc elongation to complete short-circuit of the insulation.

Although basic knowledge has been developed during the last decades on some of the physical mechanisms involved in each of the stages of the breakdown process, and mathematical models have been proposed for the representation of some of these stages, the dielectric design of high voltage insulators is in practice an experimental art.

In the following, each one of the stages of the breakdown process will be briefly reviewed.

2.2.1 Surface contamination deposition - contamination pattern of dc insulators

The first stage of the flashover process under pollution is the accumulation of contaminants over the surface of the insulation under voltage. Information can be found in the literature about the types and degrees of contamination observed in some installations in USA and Japan are reviewed below. Comparisons are made with the ac experience when possible.

The first results presented were obtained at the Sylmar dc Converter Station [4], southern terminal of the ± 400kV HVDC Pacific Intertie, situated next to a busy interstate highway and within a farming area. An outdoor insulator testing rack of 11 insulator strings was constructed and energized directly from a pole of the operating transmission line. The insulators were subjected to the outages, voltages amplitudes and polarity changes required during the operation of the transmission system. Glass and porcelain suspension insulators were tested. Also a string

of dc suspension insulators was energized, at the same location, at 230 kVac at an approximately equivalent voltage stress as for the dc energized insulators, for the same period.

The following observations were made:

- for the dc energized insulators the amount of soluble contaminants (expressed in ESDD) collected by the bottom surface of an insulator was much higher than that collected by the top surface. After 2 years the bottom surface accumulated 3 times more contaminant then the top one. After 3 years this ratio increased to 10 times;

- rain has an effective cleaning action on the top surface but the effect of natural cleaning on bottom surface is much reduced. After rainfall the amount of soluble contaminant level decreased more than 5 times at the top surface but to half of the previous level at the bottom surface. Figure 2.1[4] shows a curve with the data obtained for one specific string tested;

- nitrate salts accounted for over 50% of the total contamination, probably due to automobile emission and agricultural pollution;

- the amount of contaminants collected was different for insulator positions along the string. This pattern is noted mainly in the bottom surface of the insulators. Under normal stress the insulators close to the energized and ground terminals collected much more contaminants than those in the middle of the string. Figure 2.2[4] shows the distribution for two different insulator strings;

- the energized ac string presented an entirely different pattern. The top surfaces, on average, accumulated 50% more contaminant than the bottom ones. The amount of collected contaminant, however, was much less than for the dc string during the same time and

location. Table 2.1[4] shows the ESDD values measured. It is also shown the ESDD level for a non energized string placed close to the test set-up, situated in the dc field. It is supposed that under dc the electrostatic forces have a dominating role, whereas, under ac forces due to wind and gravity are predominating on particles deposition over the surfaces of insulators;

- for the dc strings the amount of collected contaminants increases with the voltage stress. The glass insulators collected more contaminant then the porcelain ones, even when the voltage stress was lower.

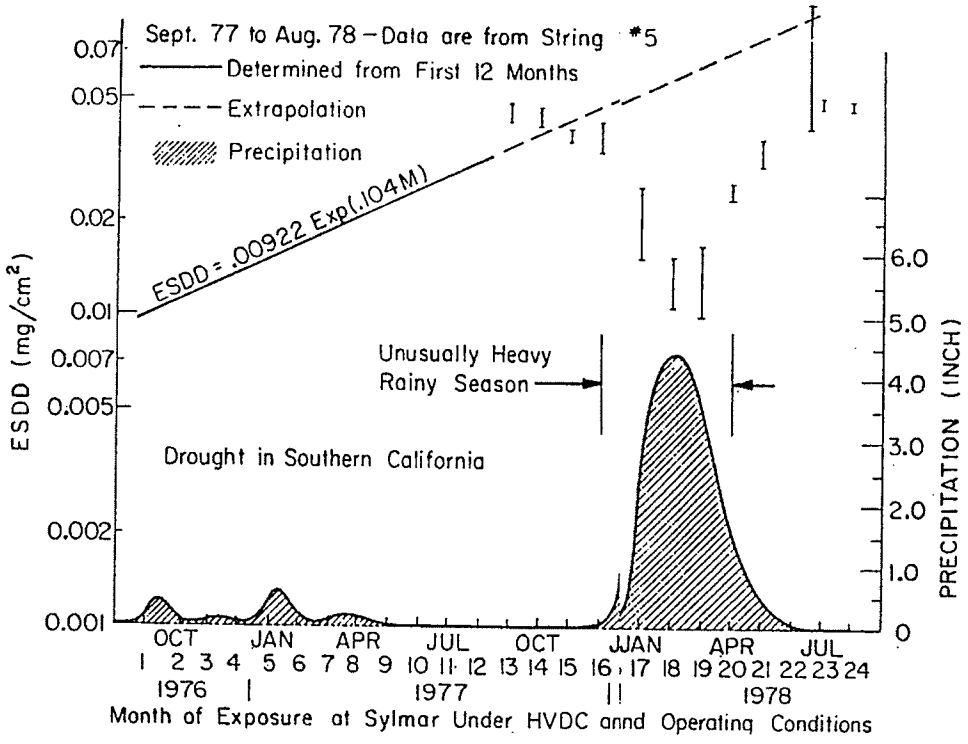

Figure 2.1[4]. Accumulation of contamination of the bottom surface of insulator and the amount of rainfall.

- the amount of contaminant collected by the bottom part of sheds was in average 35% higher than that for the top surface of sheds. The distribution of contamination on the bottom surfaces of the sheds was practically uniform along the column;

- The contamination deposition was uniform around the circumference of the insulator;

- no difference was observed between positively and negatively energized insulators;

- the accumulation of contaminants increases more than linearly with the applied stress; for insulators subjected to the same average stress, those energized with higher voltages collect more pollution.

In order to measure the degree of contamination collected by dc insulators in Japan, 4 testing stations were mounted, 3 close to the sea and one inland [6,7]. The applied voltage was ± 250kV in one station (Takeyama, close to the coast) and ± 280kV in the other three. Some of the insulators were energized for more than 5 years. The main information obtained from the measurements were:

Coastal Stations

- no significant difference was obtained between contamination levels collected by energized and deenergized insulators. The supposed reason is that, close to the sea, the contamination process is a fast one, defined by strong winds from the sea which carry the salt to be deposited;

- for short periods (some days) of observation the contamination layer was almost constant along the insulator strings. However, when long periods are considered (some years) there was an increase in the pollution level of insulators close to the energized terminal as seen in Figure 2.3[6].

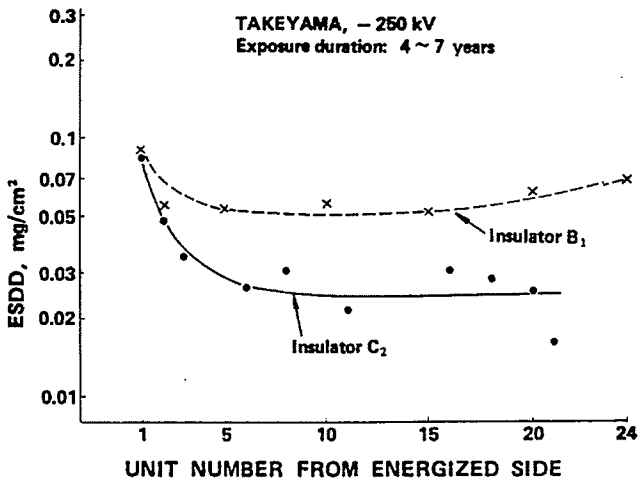

Figure 2.3[6]. ESDD distribution along insulators strings by long-term natural pollution tests.

- for short periods (some days) of observation there was no significant difference between the top and bottom surface contamination levels. However after 1 to 3 months there was an increase in the contamination level on the bottom surfaces as compared to the top ones, 2 to 5 times higher at bottom surfaces, in average.

Inland Station (Yonezawa testing station, 70km from the coast)

This station is located in a rural area far from any industrial contamination source.

- the effect of dc voltage on the contamination collection was observed only on insulators close to the energized and ground end of the string under test. No practical effect was identified in the middle of the string. See Figures 2.4[7] and 2.5[7], and Table 2.2[7];

- the amounts of insoluble contaminants on the bottom surface of the dc energized insulators was 1.2 to 1.4 greater than that for non energized ones. This value has a tendency to increase as the exposure period becomes shorter. The contamination levels (ESDD) on the bottom surfaces were 3 to 5 times those observed on the top surfaces for those insulators close to the strings ends, whereas no practical difference was observed for the units in the middle of the string;

- an increase in the voltage stress from 90kV/m to 120kV/m had no significant influence on the contamination levels;

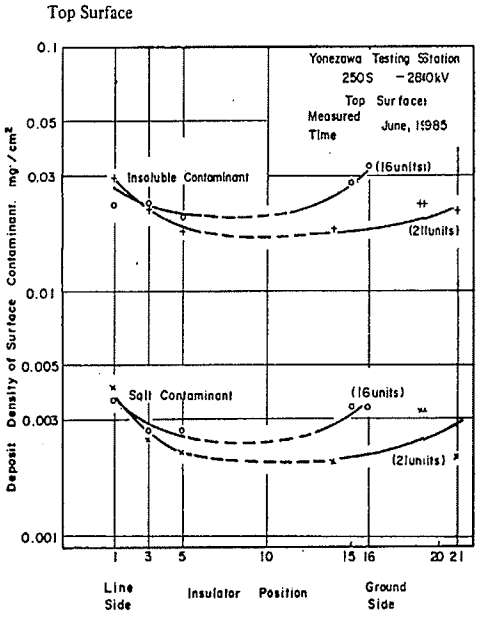

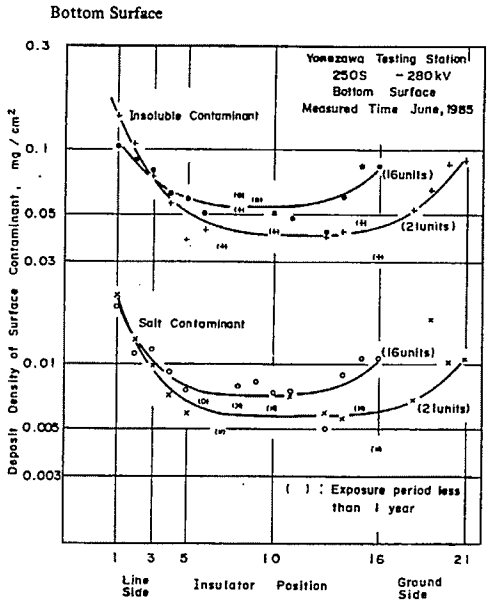

Figure 2.4[7]. Top surface

Figure 2.5[7]. Bottom surface

Distributions of contaminant along insulator string with -280kV dc voltage after 2 year exposure.

Table 2.2[7] - Effect of dc voltage application on deposit of contaminant(middle part of insulator string).

Type of contaminant	Insulator	Ratio of deposit density of contamination with dc voltage to that without voltage			
		Exposure period over 18 months		6-10 months exposure period	
		Average Value	Standard deviation(%)	Average Value	Standard deviation(%)
Salt contaminant	320DCF	1.11	5.3	1.40	23.6
	250S	0.97	28.2	0.83	34.9
Insoluble contaminant	320DCF	1.43	16.5	2.03	14.6
	250S	1.23	28.9	1.50	19.7

- the chemical components of the soluble contamination layer was different during each measurement period. In one measurement chloride salts accounted for 50% to 60% (weight) followed by sulfates. Nitrate salts accounted for 10% to 20%. Measurements conducted 2 years later indicated sulfate salt content of 65% to 90% while chlorides constituted less than 5% of the total soluble contaminants.

- Table 2.3[7] shows chemical analysis of results of insoluble contaminants on bottom surfaces.

Table 2.3[7] - Chemical analysis results of insoluble contaminant on bottom surface(middle part of insulator string).

Testing station	Voltage application	Exposure period	Weight ratio of each component to total weight of insoluble contaminant, %, ( ) shows the standard deviation, %			
			C	SiO_2	Al_2O_3	Fe_2O_3
Yonezawa	-280kV	1y ~ 3y2m	10(1.9)	41(21.4)	14(12.3)	0.1 ~ 5.7
	No voltage	1y ~ 4y8m	5.4(26.2)	45(24.0)	15(15.3)	0.2 ~ 4.6
Takeyama	-250kV	10m ~ 3y2m	10(19.0)	41(15.4)	15(10.4)	10
	No voltage	1y ~ 2y	9(10.6)	40(8.8)	14	9 ~ 11

- it is noted that the pollution levels in stations close to the sea were much higher than that in the inland station. Table 2.4 [7] shows the results of leakage current measurements;

Table 2.4[7] - Maximum value of leakage current under natural conditions(Yonezawa, -280kVdc)

Insulator type	Energized number of units	Suspension type	Maximum leakage current		Weather	Rainfall intensity (mm/min.)	Average value of leakage current (mA)	Measured period
			Max. Value (mA)	Measured time				
250S	20 ~21	Vertical	1.8	1983 - 7	Rain	0.67	0.18	1981-1985
250S	21	Tension	2.5	1983 - 12	Sleet	0.03	0.51	1981-1985
250S	16	Vertical	2.7	1984 - 7	Rain	0.32	0.31	1983-1985
3200DCF	17	Tension	1.7	1982 - 7	Rain	0.25	0.18	1981-1983

- no flashover was observed in these installations during the test period although no information was given about the dc source used at Yonezawa. A diagram of the circuit of the source used at one coastal station is presented, a single wave rectifier circuit with 1.5 μF output capacitor.

Another significant natural pollution study was performed in the USA by BPA and ASEA in a test rack at the Big Eddy Test Center[8]. Tests were performed on different types of station insulators using a ± 600kV source, with 1.5A continuous rating and voltage drop less than 5% when 100mA pulses are drawn by the load. Insulators were energized at different voltage levels: -100kV, +250kV and ±500kV. The following main results were obtained:

- pollution distribution was uneven along the insulators and around their circumference due to electric field and wind effects. Higher concentration occurs at ends of the strings;

- energized insulators collected approximately 3 times more contaminants than non energized ones;

- highly stressed insulators (≥ 20mm/kV) collect more pollution. See Figure 2.6 [8];

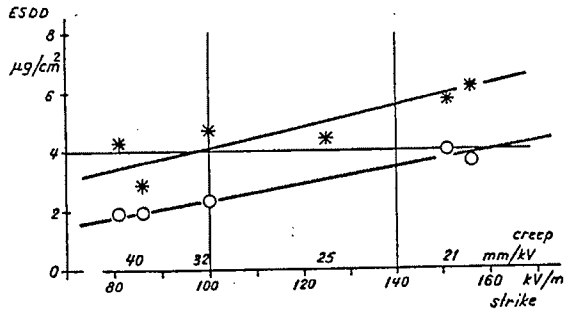

Figure 2.6[8]. ESDD as a function of stress - o - after 1 year;- ∗ - after 18 months.

- larger diameter insulators collect less pollution. See Figure 2.7 [8];

- RTV and non ceramic insulators collect 1,5 to 2,0 times more pollution than porcelain insulators but are more easily cleaned by wind and rain;

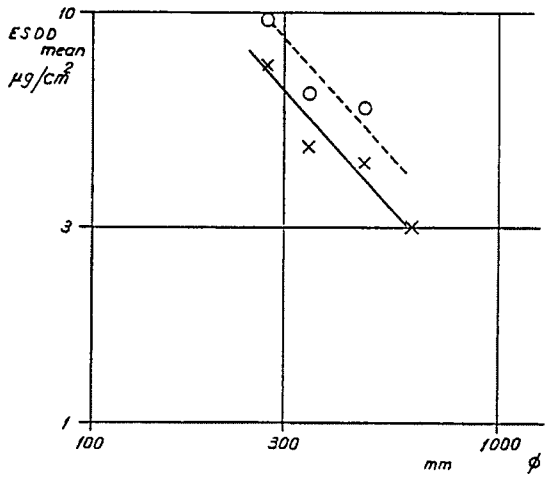

Figure 2.7[8]. Diameter influence on ESDD- - x - 32 mm/kV;- o - 15 mm/kV.

- the pollution level on the top and bottom of sheds are different and change with insulator type. Figure 2.8[8] shows the distribution obtained one month after any measurable rain precipitation;

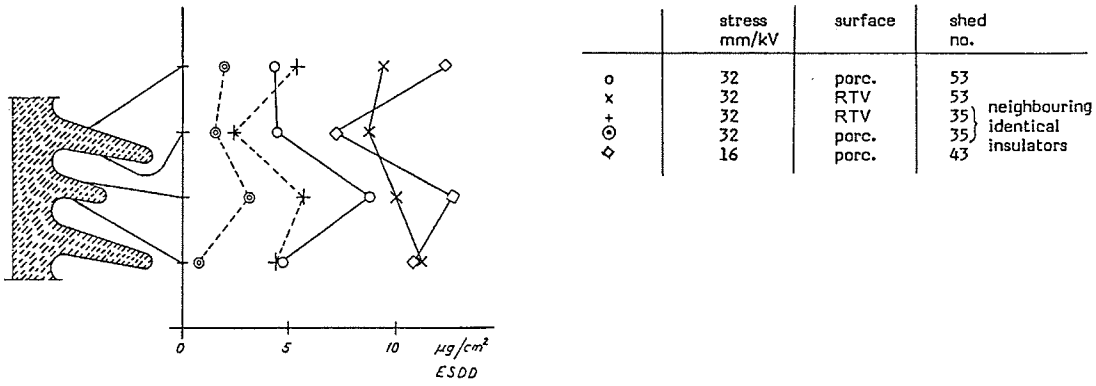

Figure 2.8[8]. Pollution distribution along shed profile after 3 months.

- the measured pollution levels and leakage currents were very low. Even during adverse weather conditions, current pulses were below 1mA. However, several flashovers were obtained during the experiments. Those flashovers occurred preferably under heavy rain in combination with wind gusts on highly stressed insulators. Some occurred also under ice conditions at low pollution levels.

In conclusion to this section it can be said that the experiments conducted at different locations are, in general, in agreement and the findings may be summarized as follows:

1. insulators energized with dc voltage collected much more contamination than those energized with ac voltage under the same voltage stress;

2. the amount of collected contaminant increased more than linearly with the voltage stress; the amount of soluble contaminants(expressed in ESDD) collected by the bottom surface of

tested insulators was much higher than that collected by the top one. Rain had an effective cleaning action on the top surface but the effect of natural cleaning on the bottom surface was found to be much reduced;

3. the amount of contaminants collected was different for different insulator positions along the string. Insulators close to the energized and ground terminals collected much more contaminants than those in the middle of the string;

4. glass insulators collected more contaminants than porcelain ones;

5. RTV and non ceramic insulators collected more contaminants than porcelain but are more easily cleaned by wind and rain.

2.2.2 Mechanisms of contamination layer wetting

A polluted insulator under dry condition has electrical strength very close to that of a clean insulator. Only when the pollution layer is wetted, the surface resistance decreases, increasing the surface current and eventually a flashover may develop. In practice, it is observed that polluted insulators flashover under very humid conditions, such as those under dew, drizzle or fog. Three main processes occur which cause wetting of the insulation contamination layer:

- the first is the moisture absorption by the soluble and non soluble components of the pollution layer. The rate of moisture absorption depends on the chemical constitution of the pollution layer [9]. For example, NaCl rapidly absorbs moisture at ambient humidity higher than 75%. Other salts or salts composition can have even higher hygroscopy than NaCl[10];

- the second process is the condensation of water on the insulator surface when the ambient temperature is higher than that of the insulator one. This process is mainly influenced by the temperature difference between the insulator and the ambient;

- the third process is wetting by collision of water droplets with the insulator surface.

Figure 2.9[9] shows an example of the variation of impedance of an insulator, for ac system, uniformly polluted in the laboratory and submitted to natural wetting process. As seen in this Figure, at the beginning of the process, the humidity (H) is low, the insulator temperature (T(S)) is higher than the ambient temperature (T(A)). After sun set the humidity increases, the temperature changes and after some time the insulator has a lower temperature than the ambient. Figure 2.9 shows the variation of the insulator static resistance when low voltage is applied, together with the dynamic surface impedance which is the one measured when the insulator is energized at full voltage. The dynamic resistance variation is a function of the wetting rate and drying effect caused by the leakage current which flows when the insulator is under voltage. Figure 2.10[9] shows the variation of surface impedance of the same insulator, equally polluted, but now subjected to the humidification process in the laboratory using the steam-fog method. The curves from the two figures have similar shapes but the times involved are different, the natural humidification process being much slower.

In the laboratory two methods are generally used to wet the previously polluted insulator surface: the cold fog method and the steam fog method.

With standard equipment for cold fog generation, water droplets are produced with average radius of 31.4 μm and radius dispersion 16.6 μm[11]. The main wetting mechanism is the collision of water droplets with the insulator surface, wetting by condensation being minimal as there is no practical temperature difference between the insulator and the fog (in general the insulator temperature is even a little bit higher than that of the fog). The maximum humidification of the

pollution layer is attained in a shorter time. Also the washing process of the pollution layer is faster.

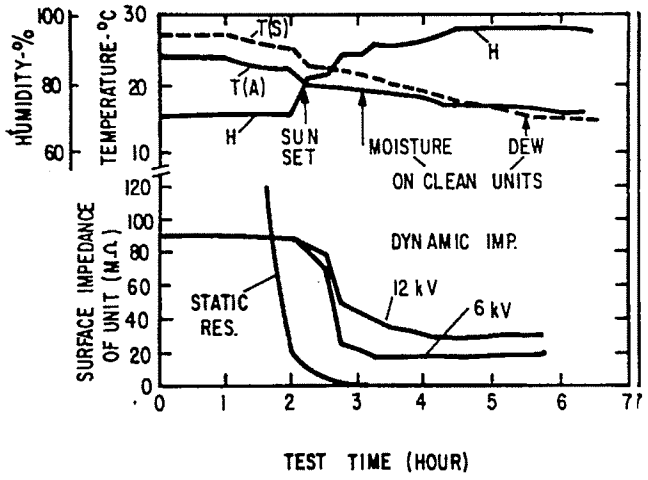

Figure 2.9[9]. Transient climatic conditions and surface impedance of type A11 insulators contaminated with K-1, 40g/l. Mixture, at a SDD of 0.07mg/cm^2 in a natural wetting condition.

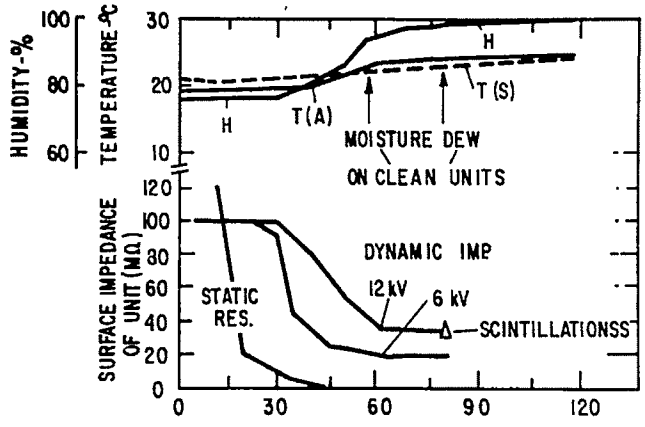

Figure 2.10[9]. Transient climatic conditions and surface impedance of type A11 insulators contaminated with K-1, 40g/l. Mixture, at a SDD of 0.07mg/cm^2 in a regular fog test of Project UHV.

During the steam-fog wetting method, similar phenomena occur as those in nature. The three main humidification processes are present, but condensation due to the temperature difference between insulator and fog is the major wetting mechanism. During this wetting process the water

droplets have more uniform dimensions and are of smaller sizes than those obtained during the cold fog method, with an average radius of 10.3 μm and a radius dispersion of 4.6 μm[11]. The time to obtain maximum humidification, or minimum resistance of insulator, is longer and the washing process is also slower. Due to these characteristics, the steam fog method is preferred and it results in lower flashover voltages with less dispersion than the cold fog method.

For ac insulators, information in the literature[9] confirms that the steam fog method correlates well with the natural wetting process, as the flashover voltages are in good agreement with the minimum values obtained for the same insulator strings, with the same pollution level humidified naturally.

2.2.3 Dry band formation

The voltage gradient to initiate a discharge process in air is about 30 kV/cm. HVDC insulators are designed with average voltage gradient of about 330 V/cm(creepage distance which results in about 30 mm/kV) or even less as is the case with bushings where creepage distances up to 50 mm/kV are used. So to initiate a flashover under pollution, it can be concluded that the voltage distribution along the insulator must be highly non uniform. Some non uniformity is expected from the shape of the insulator but the main factor which causes the highly non uniform voltage distribution and consequently the appearance of highly stressed dielectric areas is the formation of dry bands.

When the pollution layer becomes wet, the resistance decreases and the surface leakage current increases. The current density is higher at some areas of the insulator surface, usually, where the insulator has a smaller diameter. In these areas, the drying effect of the leakage current overcomes the wetting effect of the fog and a dry band is formed, whose length can increase with time. On suspension insulators the dry band usually starts forming around the pin. As the resistance of the dry band is much higher than the resistance of the conductive layer across the

rest of the insulating distance, almost all voltage is applied across the dry band. When the dry band can not sustain the voltage across it, a partial arc is triggered and bridges the dry band. The applied voltage is then distributed across the wetted area. Eventually the arc propagates across the rest of the insulating distance leading to a flashover.

Figure 2.11[12] shows qualitatively the process of dry band formation and breakdown in a polluted insulating strip.

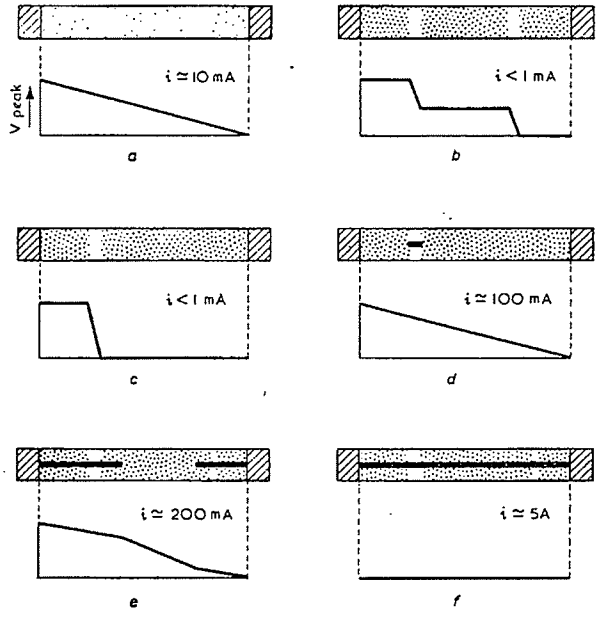

Figure 2.11[12]. Typical voltage distribution on a polluted strip: a-wetting begins; b-dry bands form; c-one dry band predominates; d-dry band flashes over; e-arcs extend; f-flashover complete.

One or more dry bands are formed even when the electrodes and the insulator are designed so as to give uniform current density along the insulating distance. This occurs due to local non uniformity of the pollution layer and wetting process.

In [13] an analytical model for dry band growth is presented. The model assumes a linear resistivity distribution along the dry band and a constant resisitivity for the series wetted polluted layer. Equations are formulated for the temperature distribution and the rate of its growth along

the dry band. These are formulated based on the heat equations for the dry band and wet region and on the equation for power generated per unit volume at the dry band. The analytical model gave results which agreed with experimental results obtained by tests on samples with cylindrical shapes contaminated with different pollution layers composition.

2.2.4 Models for arcing phenomena on polluted insulating surfaces under dc

Various theories have been presented in the last 40 years in an attempt to explain the arcing phenomena along contaminated surfaces. In [14] a critical review of the main mathematical models for pollution flashover has been presented. These include models for sustaining dc arcs and criteria for dc arc motion along contaminated surfaces. Following is a summary of these models.

Due to the complexity of the arcing phenomena along contaminated surface, the models presented are based on experiments with very simple insulators shapes(cylinder, rectangular plate, circular plate) and many simplified assumptions had to be made in order that the mathematical model could be obtained.

The flashover voltage of a polluted insulator is a statistical variable with significant dispersion, even when obtained in tests under apparently controlled conditions. Some of the simplified assumptions avoid complex effects or characteristics of the phenomenon which occur on real insulators, such as: complexity of the insulator shape; non uniformity of the pollution layer; variability of surface resistivity due to the thermal process and non uniform wetting; multiple arcs burning in series or in parallel; influence of the supply circuit parameters (HVDC test source) on the insulator behavior during artificial tests.

Arc modeling has to take into account three aspects: a criterion to determine the minimum voltage necessary to trigger the partial arc across the dry band; a criterion to determine the minimum

voltage necessary to maintain the partial arc in series with the wetted contaminated layer; a criterion for arc propagation along the insulator surface.

In 1958 Obenaus proposed a quantitative model for flashover on polluted surfaces. The model of the flashover process is represented by an arc in series with a resistance as seen in *Figure 2.12*[15]. The arc represents the partial flashover which bridges the dry band and the series resistance represents the series unbridged wetted polluted portion of the insulator.

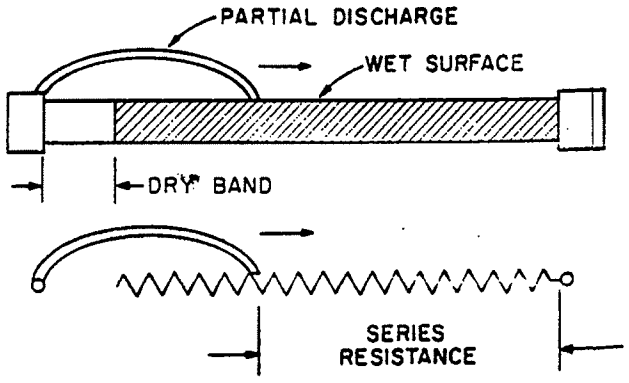

Figure 2.12[15].Obenaus model for pollution flashover.

The arc voltage can be expressed as:

$$U_{arc} = x.N.i^{-n} + U_e \qquad (1)$$

where **n** and **N** are constants for the static arc characteristic in air, **x** is the arc length, U_e is the electrode voltage drop, the sum of cathode and anode arc voltage drops, which, for an electrolyte, was measured to be ~ 830V. Normally, this voltage drop can be neglected, except for multiple arc burning in series. Then:

$$U = x.N.i^{-n} + i.R_p, \text{ or}$$

$$x=(i^n/N).(U - i.R_p) \quad (2)$$

where R_p is the series resistance which represents the series unbridged wetted polluted portion of the insulator and **U** is the total voltage applied to the insulator.

The maximum arc length that can be sustained in this circuit is determined by differentiating **x** with regard to **i** and equating to zero, obtaining the critical current i_{cx}:

$$i_{cx}=U^n/R_p^{n+1} \quad (3)$$

The critical arc length is given by substitution of (3) in (2):

$$x_c=(1/R_p)(U^{n+1}/N)(n^n/(n+1)^{n+1}) \quad (4)$$

Now the minimum direct voltage U_{cx} necessary to sustain an arc of length **x** in series with the resistance R_p can be determined from(4):

$$U_{cx}=x^{1/(n+1)} . N^{1/(n+1)} . R_p^{n/(n+1)} . (n+1)/(n^{n/(n+1)}) \quad (5)$$

In[16] the same model as that proposed by Obenaus is used but substituting the fixed series resistance (which represents just one single position of the arc root on the insulating surface) by a variable resistance:

$$R_p=r_p.(L-x), \quad (6)$$

where r_p represents an uniform pollution resistance per unit leakage path, **L** is the total leakage path length and **x** is the arc length.

The applied voltage can be expressed as:

$$U=x.N.i^{-n} + i.r_p.(L-x) \quad (7)$$

The minimum voltage necessary to maintain an arc of length **x** can be calculated by differentiating **U** with regard to **i** and equating zero. The following expression is obtained for the corresponding current:

$$i_{cx}=[(n.N.x)/(r_p.L - r_p.x)]^{1/(n+1)} \quad (8)$$

The critical voltage can be calculated by substituting (8) in (7) and is given by:

$$U_{cx}=(n+1).(N.x)^{1/(n+1)}.[r_p.(L-x)/n]^{n/(n+1)} \quad (9)$$

Figure 2.13[16] shows a curve for this relation between U_{cx} and **x**.

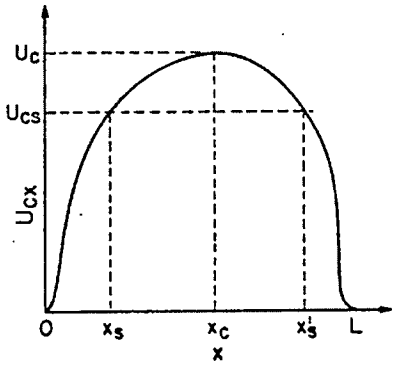

Figure 2.13[16]. Dependence of the critical voltage necessary to sustain a dc arc on the arc length according to Alston-Zoledziowski.

The maximum value for U_{cx} can be calculated by maximizing U_{cx} in relation to x, $dU_{cx}/dx=0$, which results in:

$$x_c=L/(n+1) \quad (10)$$

The maximum voltage U_c is then given by:

$$U_c=L.N^{1/(n+1)}.r_p^{n/(n+1)} \quad (11)$$

If a voltage U_{cs} is applied to the insulator, the discharge being quite short initially, the discharge could grow until $x=x_s$, it cannot grow further because the voltage required to maintain conduction exceeds U_{cs}. However, if the discharge length exceeds x_s' initially, further increase in x would reduce the burning voltage so that the discharge would grow to a flashover. From (10) and (8) the critical current can be obtained:

$$i_c=(N/r_p)^{1/(n+1)} \quad (12)$$

Which shows that the critical current is independent of the arc length and of the leakage length L.

Arc motion criteria

Hampton[12] studied the condition for arc propagation along a conductive surface with uniform resistance per unit length, using measurements in a water column (which maintains a constant resistance per unit length). The necessary condition established for flashover is that the gradient along the water column E_p should exceed that in the arc column E_a. In other words, an arc rooted on a cylinder having constant resistivity will propagate along the surface if the voltage gradient in the arc column E_a is less than that along the resistive surface E_p. Therefore the criterion for arc motion is:

$$E_a < E_p \qquad (13)$$

This criterion has been further generalized by Hesketh[17], who assumed that the arc burning in series with the wet polluted layer adjusts itself to draw the maximum current from the supply.

$$di/dx > 0 \qquad (14)$$

An advance of the arc root δ_s, see *Figure 2.14*[17], will occur only if this results in an increase in the current, which means that the relation **di/dx>0** has to be valid for all positions of the arc path.

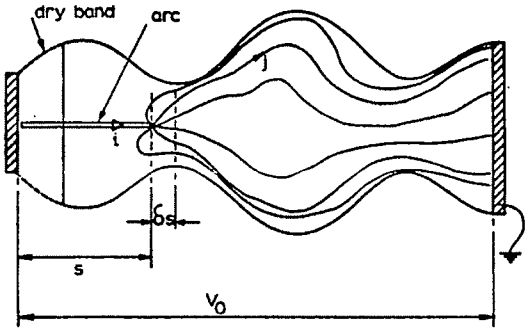

Figure 2.14[17]. Developed surface of arbitrary insulator with arc spanning distance s.

If in *Figure 2.14*[17] **x** is the arc length, $\mathbf{R_p}$ the resistance between arc root and electrode, $\mathbf{R_s}$ the internal resistance of the voltage supply, **U** the total applied voltage, $\mathbf{U_c}$ the cathode fall in arc, $\mathbf{U_a}$ the anode fall in arc, $\mathbf{E_a}$ the voltage gradient in arc column and **i** the current:

$$U = U_c + U_a + E_a.x + i.(R_s + R_p) \qquad (15)$$

Differentiating with respect to **x**:

$$0 = x.dE_a/dx + E_a + (R_s + R_p).di/dx + i.dR_p/dx$$

But,

$$dE_a/dx=(dE_a/di)(di/dx)$$

The following relation is obtained:

$$di/dx=-(E_a+i.dR_p/dx)/(x.dE_a/di+R_s+R_p)$$

For a complete flashover, as $di/dx>0$:

$$(E_a+i.dR_p/dx)/(x.dE_a/di+R_s+R_p)<0 \qquad (16)$$

In the case studied by Hampton[12], a uniform water jet of length **l**, with the resistance per unit length of the column constant, an axial flow of the current can be considered, so $-i.dR_p/dx$ is equal to the voltage gradient along the water column or $E_p=dU/dx=-i.dR_p/dx$ and equation(16) can be written as:

$$(Ea-Ep)/(x.dE_a/di+R_p+R_s)<0 \qquad (17)$$

which, provided the denominator is positive, will be identical to Hampton's criterion. It can also be shown that for uniform pollution layer resistance per unit length, Hampton's criterion for arc motion results in critical current and critical stress which are the same as those obtained by the criterion to maintain a dc arc. Under critical condition equation 17 can be written as:

$$E_a=E_p \qquad (18)$$

but, $E_p=r_p.i_c$ and $E_a=N.i_c^{-n}$, then $r_p.i_c=N.i_c^{-n}$ or,

$$i_c=(N/r_p)^{1/(n+1)} \qquad (19)$$

This equation is identical to equation 12. Substituting this expression for i_c in the equation for E_a above, results:

$E_a=E_p=U/L$, Then $U_c=L.E_a$, or

$$U_c=L.N^{1/(n+1)}.r_p^{\,n/(n+1)} \qquad (20)$$

This equation is identical to equation 11.

These criteria do not describe the physical mechanism by which the arc actually moves once the criteria are satisfied. Also no information is available about the propagation velocity.

Wilkins and Al-Baghdadi[18] proposed a mechanism for arc propagation which they designated as "elongation by ionization and successive root formation". *Figure 2.15*[18] is used to explain this mechanism. They proposed that elongation is produced by new ionization paths created at the tip of the discharge. Just in front of the discharge root the probability of ionization is higher because of the high voltage gradient and high temperature in this region.

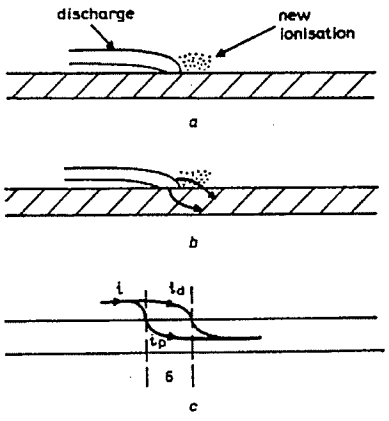

Figure 2.15[18]. Proposed mechanism for arc elongation. a - ionization in front of discharge tip; b - possible current paths; c - simplified model for analysis.

Some current may then flow through the new ionized path in front of the discharge tip. The conductivity of the new path increases with the current, while the electrolyte path maintains its conductivity and the total current gradually will circulate trough the new path as its resistance becomes lower than that of the previous path which includes the resistance of the length δ of the path over the pollution layer. This produces an elongation δ of the discharge. The elongation is not stepwise as shown in Figure 15 but is a continuous process. The mathematical criteria can be derived as follows, assuming $\mathbf{i_d}$ is the current in the new path ahead of the discharge tip, $\mathbf{i_p}$ the current along the resistive pollution layer and **i** the total current. So,

$$\mathbf{i=i_p+i_d} \qquad \textbf{(21)}$$

The voltage drop across both parallel paths must be the same or:

$$\mathbf{N.i_d^{-n}.\delta=i_p.r_p.\delta} \qquad \textbf{(22)}$$

Elimination of $\mathbf{i_p}$ gives:

$$\mathbf{i=(N/r_p).i_d^{-n}+i_d} \qquad \textbf{(23)}$$

The minimum value for **i** can be calculated by differentiating it with respect to $\mathbf{i_d}$ and equating to zero: $\mathbf{di/di_d=-(N/r_p).n.i_d^{-n-1}+1=0}$, then:

$$\mathbf{i_d=(N.n/r_p)^{1/(n+1)}} \qquad \textbf{(24)}$$

The minimum value for **i** is that given by substitution of equation 24 in equation 23, or:

$$\mathbf{i_{min}=n^{1/(n+1)}.(1+1/n).(N/r_p)^{1/(n+1)}} \qquad \textbf{(25)}$$

If the current **i** is less than $\mathbf{i_{min}}$ the parallel discharge path will be not stable and will extinguish. So to get the elongation, in each point the current shall be greater than $\mathbf{i_{min}}$.

Al-Baghdadi also proposed an empirical expression to calculate the arc speed **v**, based on high speed camera studies of arc propagation along polluted surfaces under dc.

$\mathbf{v=1.54.10^{-4}.r_p^{2.5}.(i^4 - i_c^4)}$, where: **v** is the velocity in cm/s, **i** is the arc current in A, r_p is the pollution layer resistance per unit length in Ω/cm and $\mathbf{i_c}$ the critical arc current in A.

Several other theories were proposed to account for arc motion along polluted surfaces; including drying, thermal forces electrostatic forces, magnetic forces and partial electrical breakdown ahead of the arc tip.

Also some papers propose refinements to the dc models presented, as:

- composite layer model, in order to represent better the flashover on a polluted long-rod insulator, two resistive layers corresponding to the stem and sheds with constant but different resistance per unit length(r_{p1} and r_{p2}) and partial arc leakage lengths(L_1 and L_2);

- current concentration at arc root points, in order to determine the resistance of the polluted layer, one paper[14] represented the arc root as a half circle at the boundary of the dry band; another[19] represented the arc root as circular;

- large diameter insulators, when multiple arc can burn in parallel along the dry band;

- arc electrode voltage drops, which can not be neglected when heavy pollution is present or multiple arc are burning in series.

Rizk[20] proposed models for polluted insulator flashover based on dimensional analysis. He obtained expressions for the critical current $\mathbf{i_c}$ and critical voltage $\mathbf{U_c}$ which are generalized versions of those presented here.

Recently a dynamic model which takes into account the instantaneous changes in the arc parameters during the flashover, and also the actual geometry of the insulator was proposed [33,34]. However, the proposed model does not take into account the real current distribution over the insulator surface during the flashover process. This model will be analyzed in more detail when the data obtained in this experimental work are presented.

2.3 - ARTIFICIAL POLLUTION TESTS

In this section a brief review of the international experience on dc testing of polluted insulators is presented.

2.3.1 Test procedures for HVDC insulators under pollution; some results from tests

The existing experience and knowledge on ac pollution testing should not be applied directly to dc insulator design. The existing methods should be studied in order to establish correlation between the natural contamination performance and the laboratory performance.

Two test procedures have been used for dc insulator testing:

- the salt-fog method, in which a clean insulator is energized at high voltage and then subjected to a defined ambient pollution simulated by a salt-fog;

- the solid layer method, in which an insulator subjected to dry, uniform layer of a defined solid pollution is energized at high voltage and then humidified using steam fog or cold fog.

Experience from ac tests shows that the steam fog method gives much more reproducible results than the cold fog method.

A laboratory test procedure has to be[24]:

- repeatable - this means, it produces the same results in the same laboratory when the test is repeated;

- reproducible - this means, it produces the same result in different laboratories;

- representative - this means, the laboratory test simulates service conditions.

Several aspects of the pollution performance of dc insulators have been carefully studied in order to develop representative tests.

Below an analysis of the influence of different factors on the flashover voltage of polluted insulators under dc, from recent experimental studies, is presented:

- the type of salts present on the contamination layer. Careful study was made of the influence of the type of salt on the ac flashover voltage of polluted insulators. A similar study is recommended to be made for dc;

- the type of non soluble materials present in the contamination layer. Some tests results show that contrary to ac tests, the amount and type of non soluble material has a remarkable effect on dc test results[25], as can be seen from *Figure 2.16*[25]. Another test result is reported in reference 24, where Kaolin and Tonoko were used as inert materials. The flashover voltage with Tonoko was 13 to 26% higher than with Kaolin. This difference was attributed to the

different particle size distribution of the two components. Kaolin is constituted of much smaller particles. In this same reference differences in test results were obtained even when the same material from different sources was used;

- the shape of insulators. In dc tests the shape has a strong effect on the insulator performance, much more than for ac tests, where the leakage distance can be used as a first approximation parameter when comparing two different insulators designs. Some dc test results show that insulators with the same leakage distance, but different designs can have flashover voltages with ratio up 2 to 1[26];

- the test source capacity. This aspect has been studied extensively in this project and is analyzed in Chapter 4;

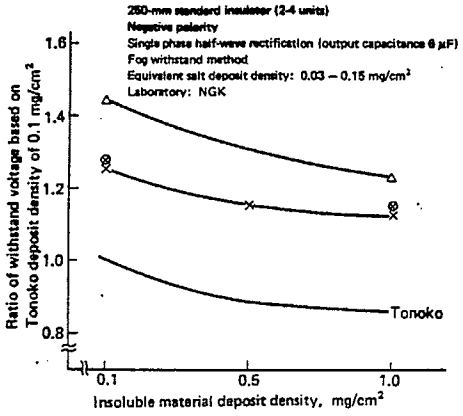

Figure 2.16[25]- Influence of kind of insoluble material on withstand voltage
Insoluble materials: Δ - Carbon; × - Soot; ⊗ - Soot+Tonoko(1:1)

- the effect of polarity. Most of the test results presented show that negative polarity gives lower flashover voltage than positive polarity, although some results are presented where both give similar values. The effect of polarity may also be dependent on the insulator type. Some authors relate this difference to the configuration of electrodes of the insulator [27];

- the effect of non uniformity of the pollution layer. Tests were performed with different top/bottom pollution ratios. It was shown that if the pollution is uniform the flashover voltage

is lower when compared to a non uniform pollution layer with the same average ESDD, as seen in *Figure 2.17*[25]. *Figure 2.18*[6] show tests performed on insulator strings with non uniform pollution along the string. The test results are the same for a string uniformly polluted with the same average ESDD. *Figure 2.19*[27] shows a comparison between the performance of naturally polluted insulators of specific designs and the performance of the same insulators uniformly polluted in the laboratory. As seen the flashover withstand voltage of the naturally polluted insulator has a large dispersion and all results are above a minimum limiting line which is the one obtained for uniform polluted insulator. This large dispersion is attributed to factors reported before, such as: non uniformity of the pollution layer, different soluble and non soluble materials, non uniformity of wetting in the natural atmosphere, etc.. Reference 27 concludes that an artificial pollution test can give more consistent results, by stricter control of testing conditions. In fact this can be concluded from the results of *Figure 2.19*, but the selection of insulators using the results of a laboratory test can be conservative.

- relation between length of insulator string and withstand voltage. *Figure 2.20*[28] shows the results of tests in different laboratories on strings consisting of standard 250mm insulators. The relation between the flashover voltage and length of insulator string is linear. This is an important result and if it can be experimentally proved for other insulators types, tests in laboratory could be performed at lower voltages using cheaper test equipment and installations.

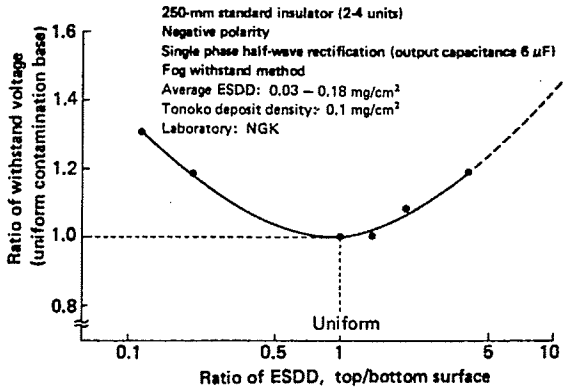

Figure 2.17[25]- Ratio of withstand voltage in case of non-uniform contamination on top and bottom surface.

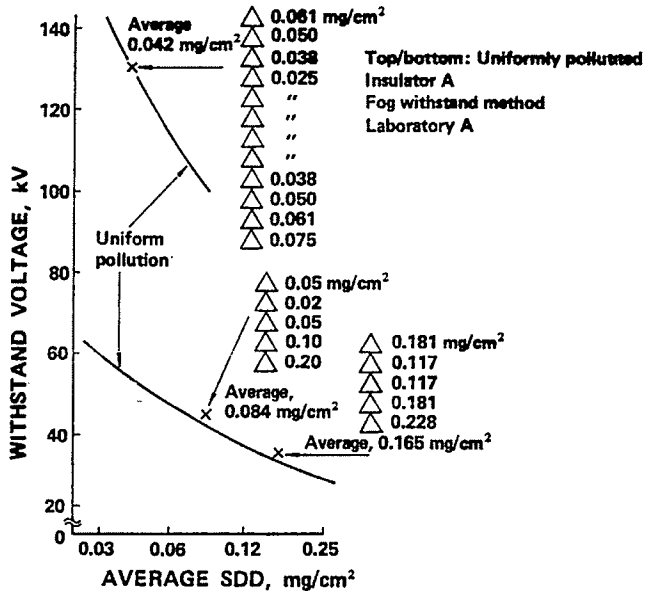

Figure 2.18[6]. Withstand voltage performance of the insulator polluted non-uniformly along the insulator string

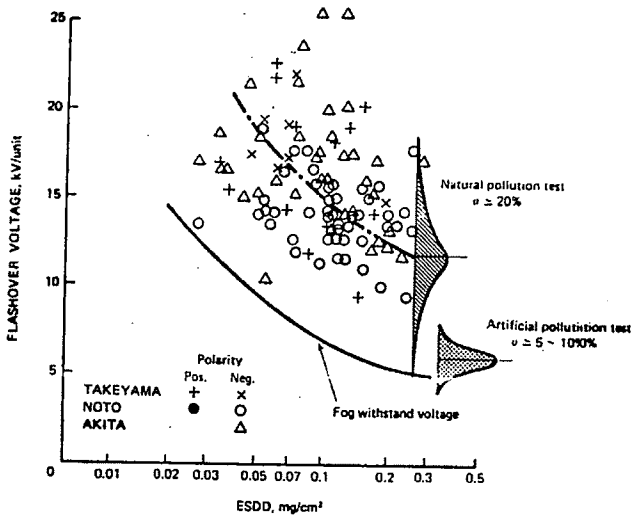

Figure 2.19[27]. Dispersion of flashover voltage of naturally and artificially polluted insulators.

Recently a round-robin test was organized by CIGRÉ(Task Force 33.04.04) and IEEE(WG on Insulator Contamination), with participation of six laboratories(IREQ-Canada, CEPEL-Brazil, NGK-Japan, HVTRC-USA, CESI-Italy and STRI-Sweden), aiming at standardization of artificial test method on HVDC insulators under pollution. Three types of specimens were tested, strings of minimum 5 units of IEEE suspension insulators; strings of minimum 5 units of anti-fog

suspension insulators; a station post insulator, using two tests procedures: the salt fog procedure and the solid layer method followed by steam fog method for wetting the layer.

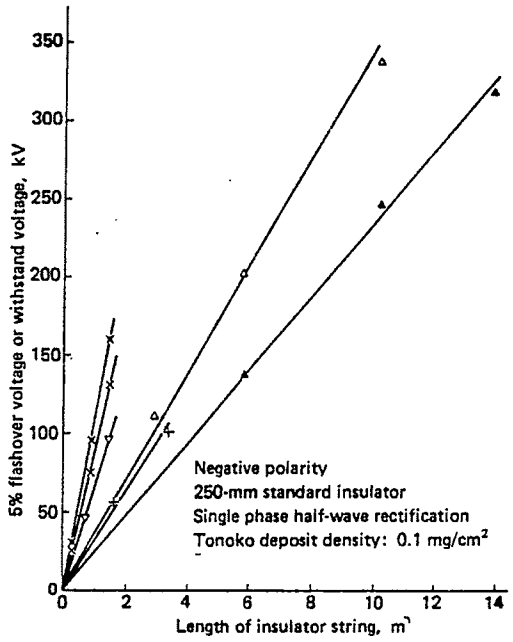

Figure 2.20[28]. Relation between length of insulator string and withstand voltage

The main conclusions of this experimental study conducted by CIGRÉ-IEEE are presented in Reference 35 and are:

- the results for the salt fog procedure were not reproducible. Further investigation is necessary in order to get a reproducible and repetitive salt fog test procedure to be used as standard for dc insulators;

- the influence of the non-soluble material and fog rate on test results were confirmed. Different non-soluble materials(American Kaolin, Brazilian Kaolin and Tonoko) gave different results. Differences up 20% in flashover voltage results were obtained in tests performed at the same laboratory. The fog rate has also an influence in the test results; increasing the fog rate seems to result in lower flashover voltage;

- if the non-soluble material is specified, the results for solid layer method with steam fog seem to be reproducible. The scatter obtained among the different participants is in order of that obtained in standardized artificial pollution tests on HVAC insulators;

- information is now available to prepare provisional specifications for standardization for the solid layer method.

2.3.2 - Requirements for HVDC sources for pollution testing

As discussed earlier, the process of flashover of a polluted insulator has various stages: pollution layer is wetted leading to the leakage current flow and consequent formation of the dry band; partial arc bridging the dry band; arc propagation and spanning all the insulating distance.

In high voltage dc tests there is an important interaction between the discharge process and the power supply. The test source must not inhibit arc growth to reach the critical length and further final flashover process.

In other words, the test source shall be powerful enough to supply the leakage current pulses without excessive voltage drops, which can inhibit the critical conditions which lead to the complete flashover.

Various circuits are used in laboratories to perform dc pollution tests on insulation. *Figure 2.21*[21] presents the most frequently used.

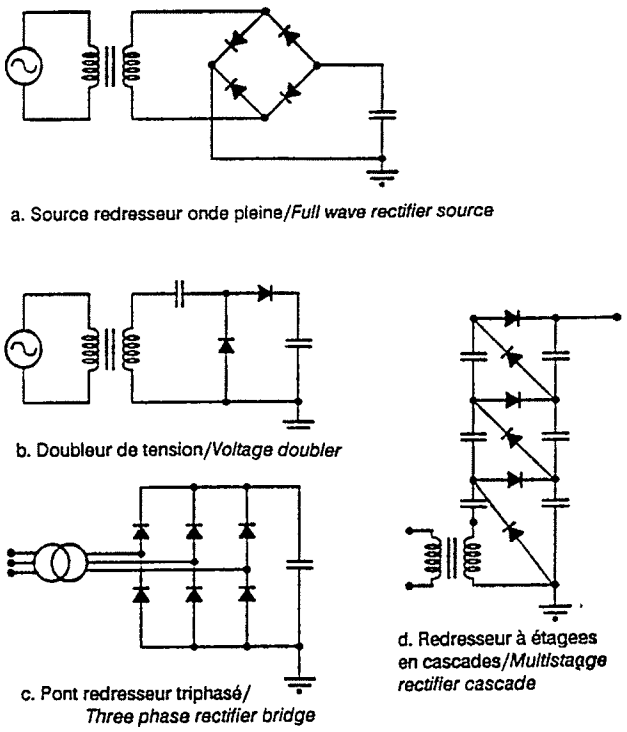

Figure 2.21[21]. Different HVDC pollution tests circuits

The information published so far on pollution testing of bushing and insulators give some indications on the main characteristics (risetime, amplitude, duration, decay time and repetition rate) of typical leakage current pulses occurring prior to a flashover during a dc test pollution. It is important to note that all these characteristics must be considered when HVDC sources are being discussed [22].

Figure 2.22[21] shows leakage current measurements(I_H is the current pulse with highest amplitude at critical voltage level, the maximum voltage level which does not lead to flashover of the insulator) on 16 different suspension insulators strings. Tests were performed with SDD from very light up to 0.5mg/cm^2, at -350kV. Maximum value for I_H of 500mA was obtained.

Figure 2.23[21] shows leakage currents amplitude-duration curves obtained during tests on large porcelain shells. From this figure it can be seen that leakage currents with peaks up to 800mA and duration as long as 3s were measured. To supply such types of current pulses with no significant voltage drop is the main requirement for the test source. For the test circuits presented in *Figure 2.21*[21], with a component rating normally found in HV laboratories, this requirement cannot be met unless output capacitors of extremely high capacitance are used. The limitation of these circuits is that as the leakage current has a long duration, its charge content is very high and is continuously drained from the output capacitor. The charging of the output capacitors occurs only during a short period in each cycle or each half cycle, depending on the type of circuit used, and the charging current is limited by the impedance of the ac source and diode protecting resistors. When the charge given by the ac source to the output capacitor is smaller than that taken from the capacitor by the test sample, the output voltage drops. If the leakage current has a long duration, the output voltage will drop, reducing the amplitude of the current, until an equilibrium is reached (charge in = charge out).

An alternative to rectifiers with very high output capacitors is the use of a controlled HVDC circuit. One example of such a circuit is shown in *Figure 2.24*[21]. As soon as the output voltage starts to decrease the control system changes the firing angle of the SCR on the low voltage side of the feeding transformer, increasing the applied input voltage to the rectifier, increasing consequently the charge transferred to the output capacitor.

Figures 2.25[22] and 2.26[22] show a simulation of a 3 phases, 3 stages multiplier circuit with and without the automatic regulating system. Without the automatic regulating system a voltage drop of 14% was obtained when a certain current pulse was drawn by the load. With the automatic regulating system the voltage drop was less then 3%.

Another point to be discussed if a source with automatic regulation is used, is that when the leakage pulse decreases to zero, the test object will be subjected to an overvoltage the value of

which depends on the way the current decreases to zero, see *Figure 2.26*[22]. Further analysis is needed to clarify the effect of this overvoltage on the test results, in order that a requirement can be specified for this parameter.

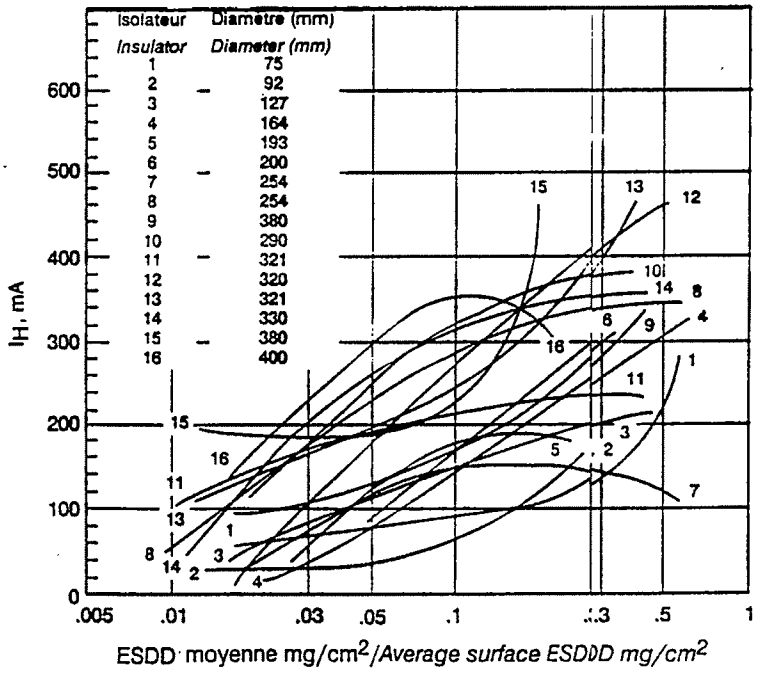

Figure 2.22[21]. Highest leakage current pulse not leading to flashover, I_H, for different dc suspension Insulators.

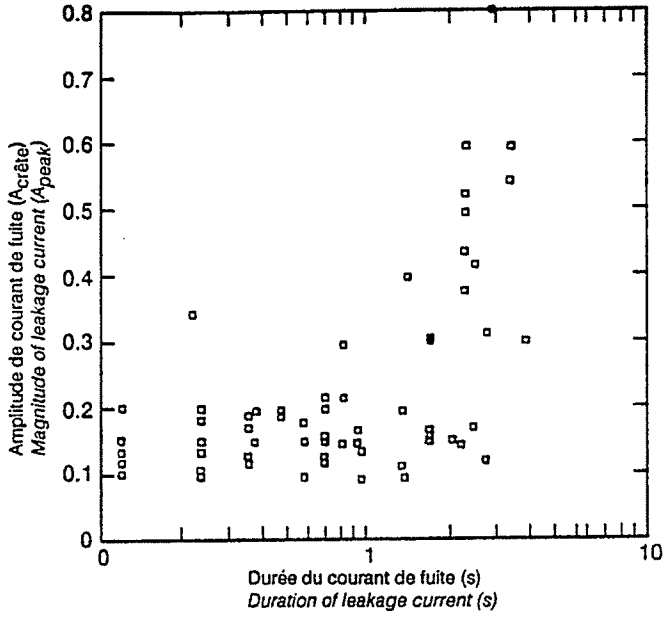

Figure 2.23[21]. Relationship between leakage current pulse amplitude and duration in clean fog withstand tests on a bushing shell. ESDD = 0.12mg/cm^2 . Average shell diameter 1015mm. Test voltage 550kV.

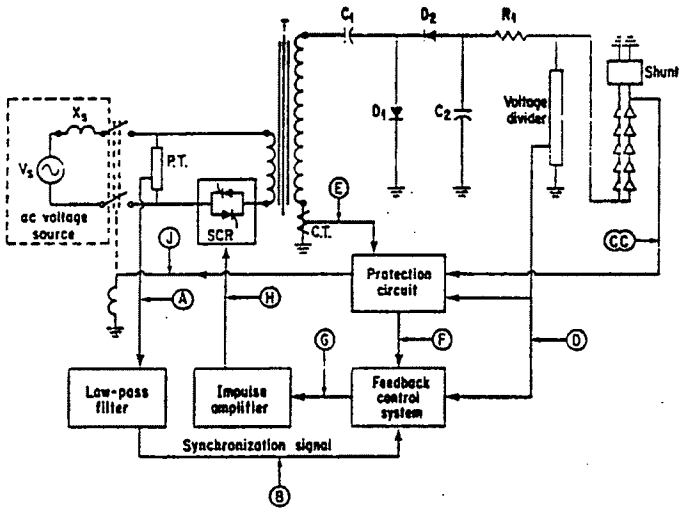

Figure 2.24[21]. General arrangement of a controlled HVDC voltage doubler circuit.

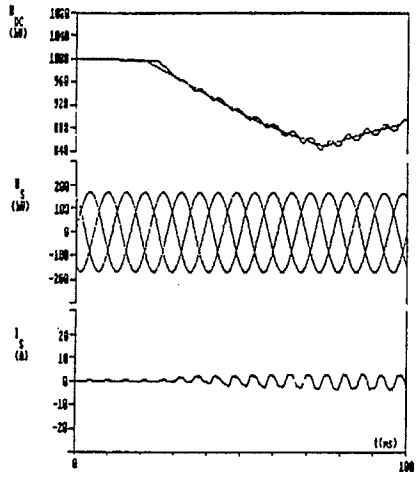

Figure 2.25[22]. 3 phases, 3 stages rectifier without automatic regulation under trapezoidal shape load current of 1.3A.
U_{DC}: output dc voltage with superimposed ripple
U_S: phase voltages on feeding transformers primary.
I_S: composition of phase currents, $I_{\phi 1}+I_{\phi 2}+I_{\phi 3}$

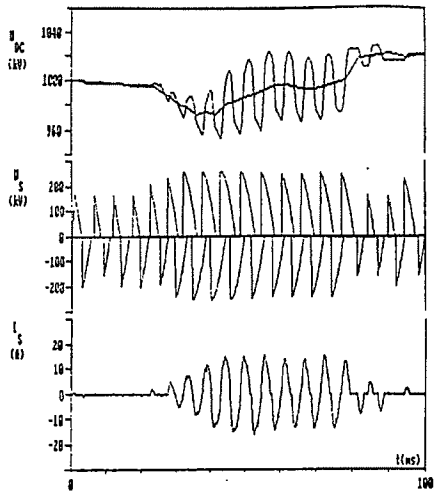

Figure 2.26[22]. 3 phases, 3 stages rectifier with automatic regulation under trapezoidal shape load current of 1.3A.
U_{DC}: output dc voltage with superimposed ripple
U_S: phase voltages on feeding transformers primary.
I_S: composition of phase currents, $I_{\phi 1}+I_{\phi 2}+I_{\phi 3}$

Figure 2.27[21] shows the influence of the output capacitor, when a single phase half-wave circuit is used, in comparison to a source with an automatic regulating system. The results of flashover voltage are the same for the sources are the same when high capacitance output capacitor is used for the non-controlled source.

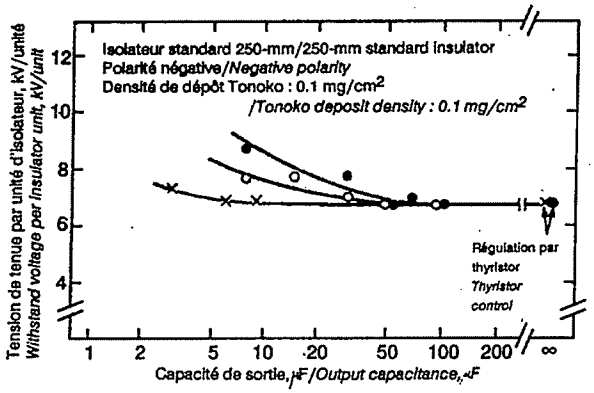

Symbol	Laboratory	ESDD mg/cm²	No. of insulators	Test method	Rectification system
●	ETL	0.074	3	Repeated flashover	Single phase half-wave
○		0.074	3		Single phase full-wave
×	NGK	0.16	6	Fog withstand	Single phase half-wave

Figure 2.27[21]. Influence of output capacitance on flashover voltage

Another type of solution found in the literature is presented in *Figure 2.28*[23]. It is a twelve pulse rectifier fed by a powerful ac source.

The V-I characteristic of the source is shown in Figure 2.29[23]. It is seen that the characteristic has two distinct slopes. It is beneficial to operate on the characteristic with the lower slope to have better regulation. To achieve that the author introduces a load resistance which brings the operation of the rectifier to a point closer to the high current region. The disadvantage of this method is that high power is dissipated in this load resistor. For example, operation close to the knee means that the load current is 70 mA which implies a 49 kW rating for the load resistor at full output voltage.

Figure 2.30[21] shows, for simulation purposes, the leakage current and insulator voltage, corresponding to a critical test. I_H represents the critical leakage current which here is defined as that current pulse with highest amplitude at critical voltage level, the maximum voltage level which does not lead to flashover of the insulator.

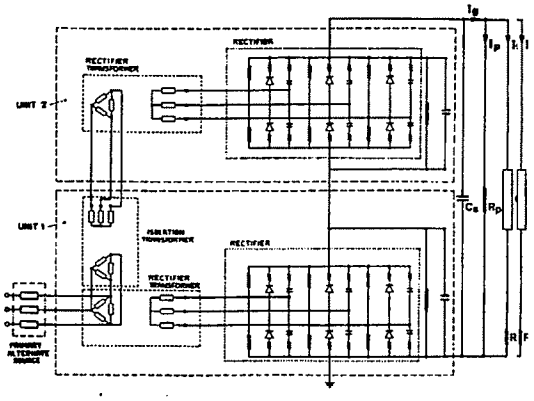

Figure 2.28[23]. Electrical circuit used for modeling the generator

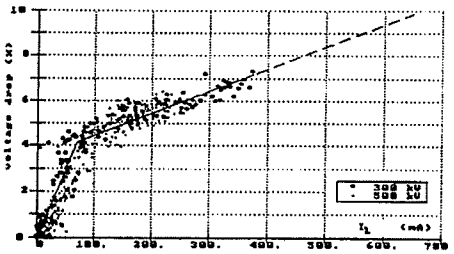

Figure 2.29[23]. Voltage drop, in percentage, vs. leakage current. Values measured with the 50Hz source. I_P = 30mA

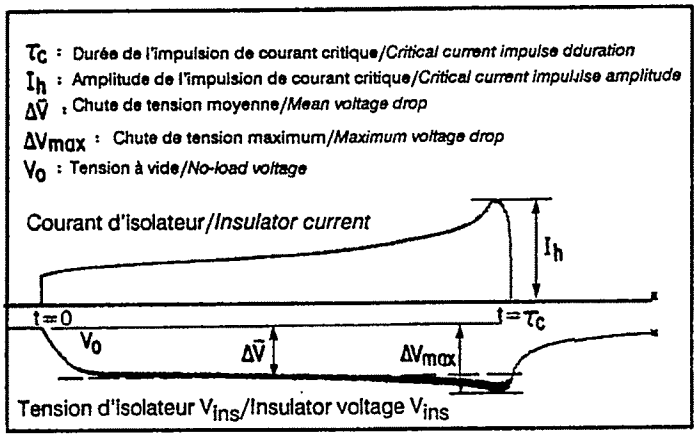

Figure 2.30[21]. Definitions of voltage drops associated with a critical current pulse.

V_o is the no load test voltage, τ_c is the duration of the critical current pulse. The following voltages drops are defined, definitions valid for the duration τ_c of the critical current pulse:

Maximum voltage drop, $\Delta V_{\max} = Max(Vo - V_{ins}(t))$

Mean voltage drop, $\Delta V_{av} = V_o - (\frac{1}{t_c}) . \int_o^{t_c} V_{ins}(t)\, dt.$

Figure 2.31[21] presents measured and simulated errors in the withstand voltage as a function of the maximum voltage drop. Figure 2.31 shows that the correlation between the error and the maximum voltage drop is very poor. A very conservative criterion should be to limit the maximum voltage drop to 5% in order that the error in the determination of the critical voltage should be always below 5%.

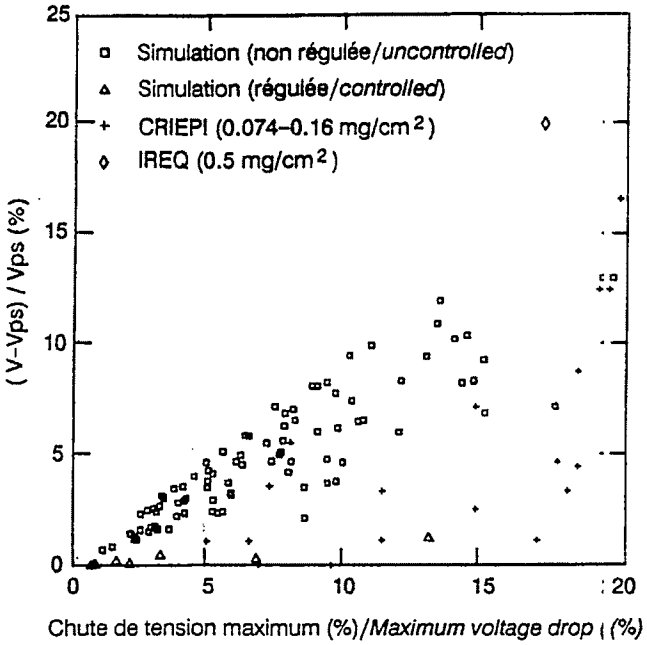

Figure 2.31[21]. Error in withstand voltage versus maximum voltage drop.

In reference 21 it is proposed that the average voltage drop shall be used to define a criterion. The physical significance of this proposal is that contrary to air insulation which responds to instantaneous voltage, the flashover along a polluted surface is a slow process which is influenced by the past arc motion and thermal phenomena on the contamination layer during the duration of the current. The same simulated results plotted on *Figure 2.31*[21] are now shown in *Figure 2.32*[21], but as a function of the mean voltage drop. The correlation appears to be much

better. It is reasonable to define as a criterion $\Delta V_{av} \leq 5\%$. This limits the error on the determination of the withstand voltage to 5%.

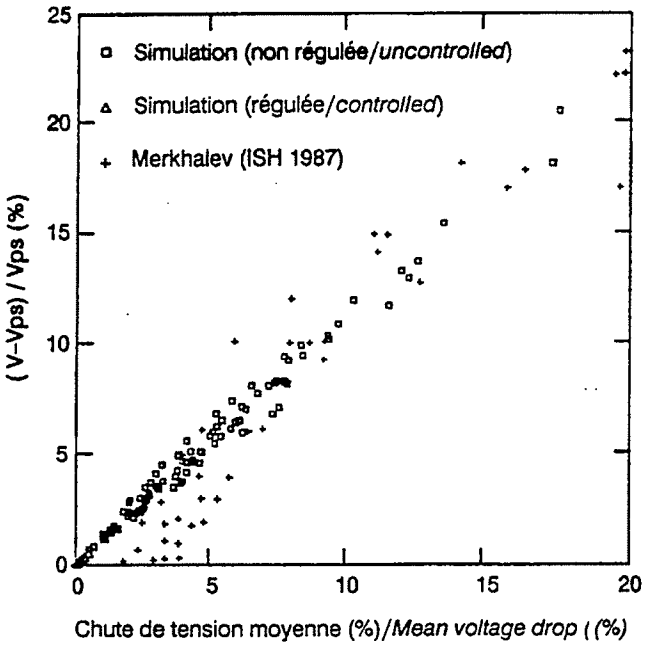

Figure 2.32[21]. Correlation between error in withstand voltage and mean voltage drop.

Based on these results, Rizk[21] proposes the following criteria to limit to 5% the error caused by the source on the flashover voltage determination of polluted insulators:

$\Delta V_{\max} \leq 10\%$;

$\Delta V_{av} \leq 5\%$;

Peak to peak voltage ripple ≤ 10%.

The problem with the criterion based on the mean voltage drop is that it has to be determined from a voltage oscillogram corresponding to a critical current pulse, this means that voltage and current oscillograms must be recorded during the voltage application and the above defined voltage drops calculated for that current pulse with highest amplitude at critical voltage level, the maximum voltage level which does not lead to flashover of the insulator.

The conclusions in this publication are mainly based on theoretical simulations of the test circuit, including a model for the insulator under test. Few results from real tests were presented.
In 1993 the International Electrotechnical Commission published Technical Report IEC 1245 - Type 2, Artificial pollution tests on high-voltage insulators to be used on dc systems[37].

Type 2 technical report of IEC is published when the subject is under technical development, which is the case for artificial testing of dc insulators under pollution, or when there is not immediate possibility of agreement on an international standard. It is intended for provisional application so that information and experience of its practical use may be accumulated. The dc test procedures specified in the report follow closely the ones specified for ac on the IEC Standard IEC 507: 1991, Artificial pollution tests on high-voltage insulators to be used on ac systems.

The requirements for the dc test source are not the same as those proposed by Rizk[21]. Table 2.5 presents a comparison of the requirements as proposed by Rizk[21] and on Technical Report IEC 1245.

Table 2.5. Comparison of criteria for dc voltage sources to be used for dc pollution testing

CRITERIA	Reference 21(1991)	IEC Technical Report(1993)
Main criterion for voltage drop	$\Delta V_{av} \leq 5\%$, during entire duration of critical current pulse	$\Delta V_{max} \leq 10\%$, during individual tests resulting in withstand
Additional criterion for voltage drop	$\Delta V_{max} \leq 10\%$, during entire duration of critical current pulse	$\Delta V_{av} \leq 5\%$, *if* $10\% \leq \Delta V_{max} \leq 15\%$, during individual tests resulting in withstand
Criterion for voltage ripple	Peak to peak ripple $\leq 10\%$, during entire duration of critical current pulse	Peak to peak ripple $\leq 6\%$, for a current of 100mA with a resistive load
Criterion for voltage overshoot	Not defined	Overshoot $\leq 10\%$, during individual tests resulting in withstand but test is not valid if flashover occurs during the time of overshoot with overshoot $\geq 5\%$
Criterion for short-circuit current	Not defined	Not defined

CHAPTER 3

DESCRIPTION OF EXPERIMENTS

3.1 - GENERAL CONSIDERATIONS

In order to study the effect of the voltage source during HVDC tests under pollution a series of experiments was planned and performed. The data from experiments were collected by a digital data acquisition system which enabled the collection of a large amount of information for different test conditions.

3.2 - EXPERIMENTAL WORK

This section describes the experimental work carried out together with the description of the test facilities used. It should be emphasized that as dielectric tests under pollution are very time consuming the number of tests was limited to those essential.

3.2.1 Test object

Vertical strings with 6 or 8 suspension, porcelain IEEE type insulators were tested. The IEEE insulator profile is shown in Figure 3.1. Also vertical strings with 4 suspension, glass ANTIFOG type insulators were tested. The ANTIFOG insulator profile is shown in Figure 3.2.

Table 3.1 presents the tested insulators main dimensions:

Table 3.1 - Tested insulators main nominal dimensions

	IEEE type	ANTIFOG type
Shed diameter(mm)	254	320
Unit spacing(mm)	146	170
Leakage distance(mm)	305	530
Top surface area(cm^2)	691	1297
Bottom surface area(cm^2)	908	2129
Total surface(cm^2)	1559	3426

As a high voltage conductor, a rigid hollow pipe 2.54 cm diameter and 2 m length terminated at both ends with anti corona electrodes was used.

The insulator string was suspended from the ceiling at the geometrical center of the test chamber.

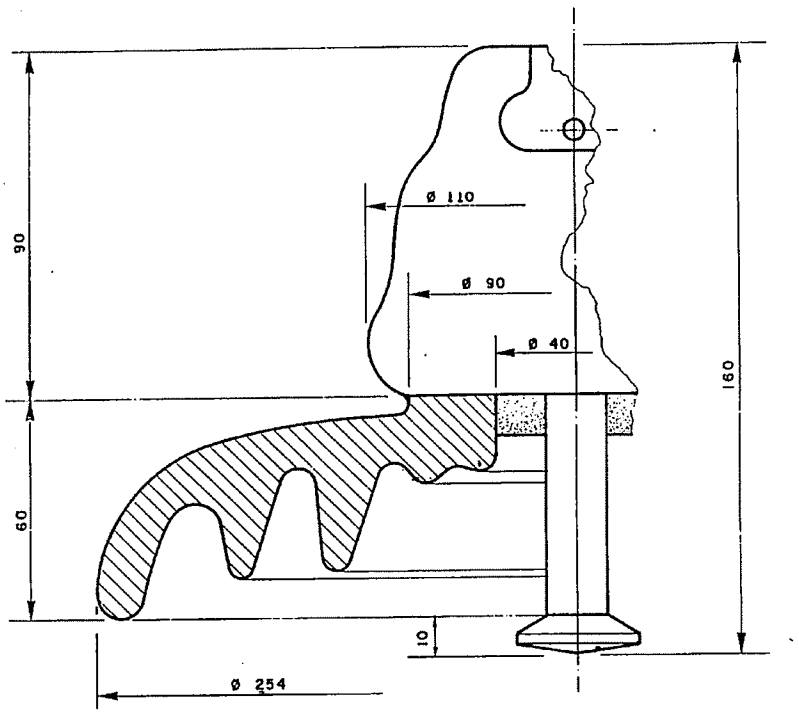

Figure 3.1: IEEE insulator profile. Dimensions in mm.

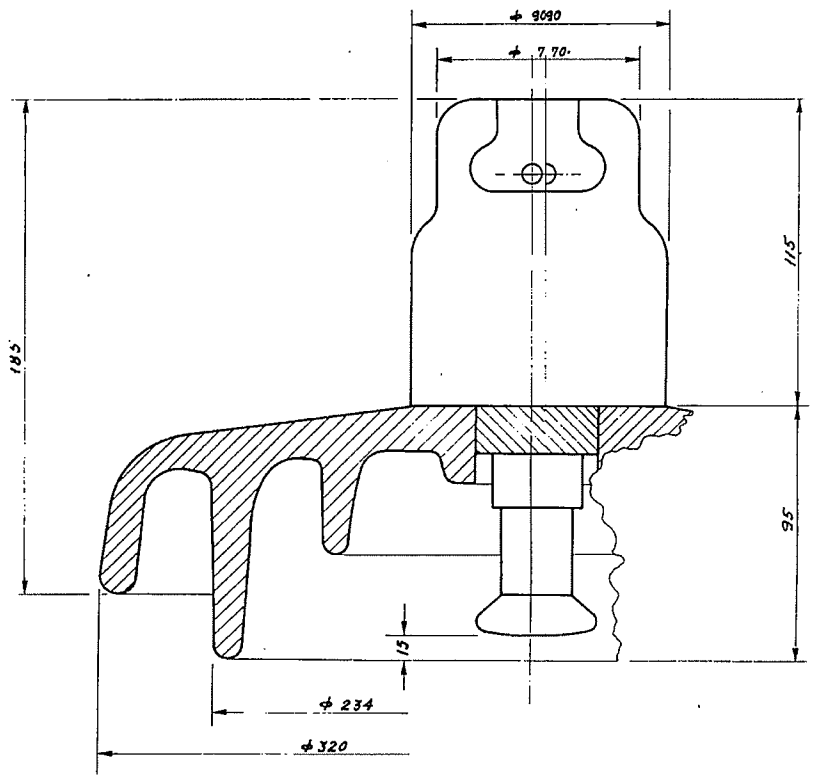

Figure 3.2: ANTIFOG insulator profile. Dimensions in mm.

3.2.2 Test chamber

The tests were performed in the small CEPEL's pollution test chamber with dimensions 5.2m x 4.6m x 4.6m (l, w, h). The high voltage was connected to the test object inside the chamber through a wall bushing. The maximum test voltage, limited by the bushing, was 140 kV. Figure 3.3 shows a cross-sectional view of the chamber.

3.2.3 Artificial pollution testing procedure

The solid layer method followed by steam fog for wetting the contamination layer was selected as the testing procedure. This procedure has proved to be reproducible and repetitive through a recent international intercomparison conducted by IEC and CIGRÉ.

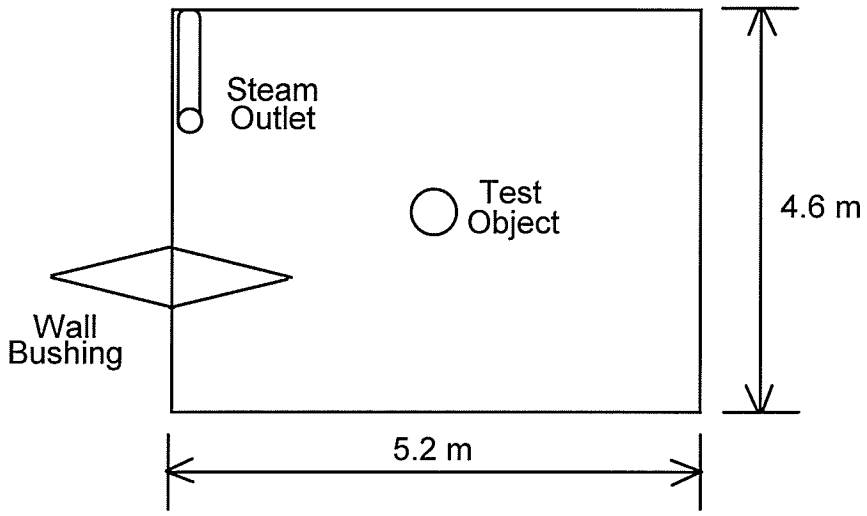

Figure 3.3: View of the pollution test chamber.

The contaminant consisted of a mixture of tap water, commercial sodium chloride (NaCl) and 40g/l of commercial kaolin from the Brazilian market as an inert material. The amount of NaCl depended on the SDD - Salt deposit density level specified.

Prior to the contamination, the insulators were carefully washed with detergent and thoroughly rinsed with tap water to remove any surface grease or impurity. Next, they were allowed to dry in ambient conditions and the contamination layer was applied by dipping the insulators inside a container with the previously prepared mixture. The insulators were then dried inside an oven at 60°C and afterwards were allowed to cool to room temperature inside a controlled low humidity room.

The wetting of the polluted insulator was performed using the steam fog method. Steam fog was produced outside the chamber, by a boiler, and was introduced at low velocity into it trough a 30 mm diameter pipe placed closed to the ground level. The steam input rate was measured during each individual voltage application and was proved to be around 0.06 $kg/m^3/hr$.

3.2.4 Salt deposit density levels tested

Three levels of contamination were used:

Light contamination level : SDD= 0.02mg/cm^2;

Medium contamination level : SDD= 0.07mg/cm^2;

Heavy contamination level : SDD= 0.20mg/cm^2.

In order to control the uniformity of the pollution process, SDD was measured on various samples. For each string prepared for testing, at least one additional insulator was polluted and selected at random.

SDD was measured for the top, bottom and total surface of the selected samples. SDD of each surface (top or bottom) of the insulator was measured according to the following procedure:

- the surface was cleaned completely, excluding metal parts, using a clean brush and a known volume of distilled water;
- the resulting suspension was stirred for at least 3 minutes and its volume conductivity σ_θ(S/m) and temperature θ(°C) were measured;
- the value σ_{20}(referred to standard temperature 20°C) was determined from σ_θ using equation $\sigma_{20=}\ \sigma_\theta[1\text{-}b(\theta\text{-}20)]$, where b is a factor depending on θ, given in IEC Technical Report 1245[27];
- the salinity S_a (kg/m^3) of the suspension was determined by the equation: $S_a = (5.7.\ \sigma_{20})^{1.03}$;
- the salt deposit density SDD(mg/cm^2) was then determined by the equation: SDD= $(V.S_a)/A$, where V is the volume of the suspension and A is the area of cleaned surface.

To measure SDD for the total surface, the two suspension obtained for top and bottom surfaces were mixed and the procedure above repeated. The results of these measurements are presented in Table 3.2.

Table 3.2: Measured SDD Values.

Insulator type	Nominal SDD (mg/cm^2)	Number of Samples	Measured SDD		Top/Bottom Ratio	
			Average (mg/cm^2)	Std. Dev. (%)	Average	Std. Dev. (%)
IEEE	0.02	14	0.0205	5.9	0.97	8.2
	0.07	55	0.0695	3.0	0.92	6.5
	0.20	91	0.2025	4.0	0.93	5.4
ANTIFOG	0.02	16	0.0207	4.4	1.03	8.7
	0.07	16	0.0710	4.2	1.00	13.0
	0.20	16	0.191	1.6	1.06	11.3

3.2.5 High voltage test sources

A voltage doubler circuit was used to generate the dc test voltage. One phase of the circuit consisted of one 8kV/180kV, 200kVA transformer, two high voltage diodes rated at 12A, 400kV with 1kΩ series protection resistor and one 220nF, 200kV, ac side capacitor. The basic configuration of the dc capacitor consisted of 110nF units 400kV capacitors. When higher output capacitance was needed to obtain a more powerful dc source, 36 units of 2μF, 40kV each were connected. Three branches of 12 parallel capacitors were connected in series to obtain a 8.000nF, 120kV dc capacitor.

The rectifier circuit was supplied from the laboratory 13.8kV network trough a 8kV/0 to 8kV, 3000kVA voltage regulator. The polarity of the generated dc voltage was changed manually by inverting the polarity of the high voltage diodes.

A protection resistor was placed between the dc capacitor and the test object to protect the high voltage diodes from high currents which flow when a flashover of the test object occurs during a voltage application. Two values of this resistor were used, R_p= 5kΩ and R_p= 1kΩ.

Five configurations of this basic circuit were used:

1- F1: Single phase voltage doubler circuit with 110nF dc capacitor(C_{dc}= 110nF), R_p= 5kΩ;

2- F2: Two phases doubler circuit connected in phase opposition, C_{dc}= 440nF, R_p= 5 kΩ;

3- F3: Same as 2 but with C_{dc}= 8000nF;

4- F4: Same as 2 but with R_p= 1kΩ;

5- F5 :Same as 3 but with R_p=1 kΩ. This voltage source is considered the strongest one.

Figure 3.4 presents the basic arrangement of the two phases doubler circuit. Photos 3.1 to 3.3 show the pollution chamber and the HVDC voltage test source.

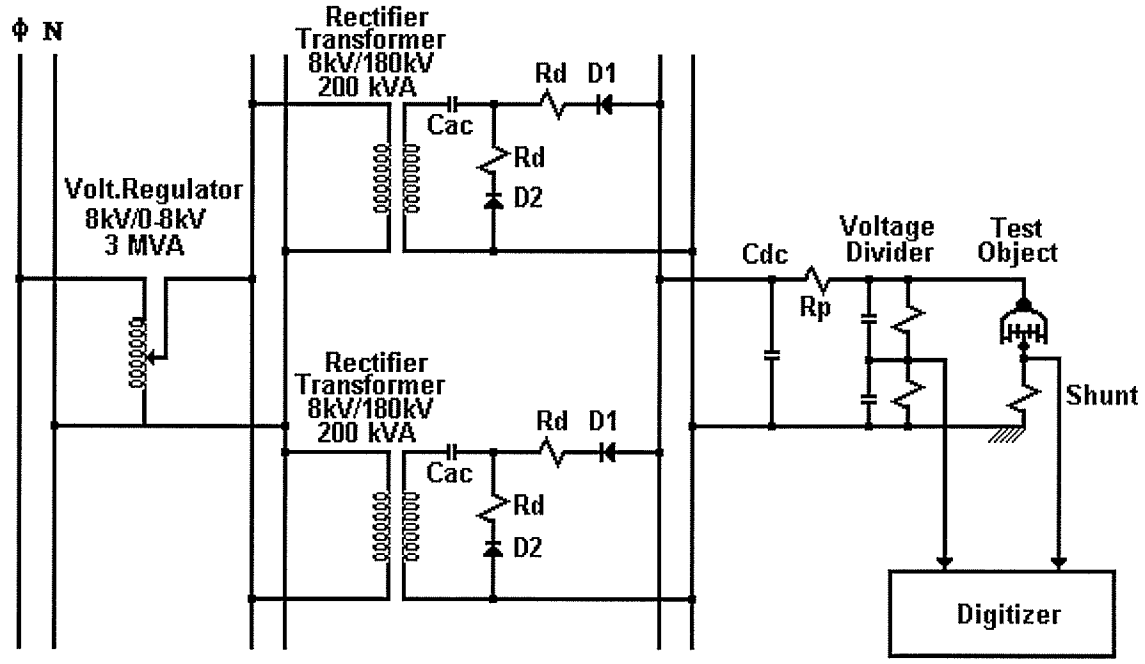

D1,D2 : HV Diodes; C_{ac} : ac Capacitors; C_{dc} : dc capacitor; R_d, R_p : Protection Resistors.
Figure 3.4: Doubler circuit.

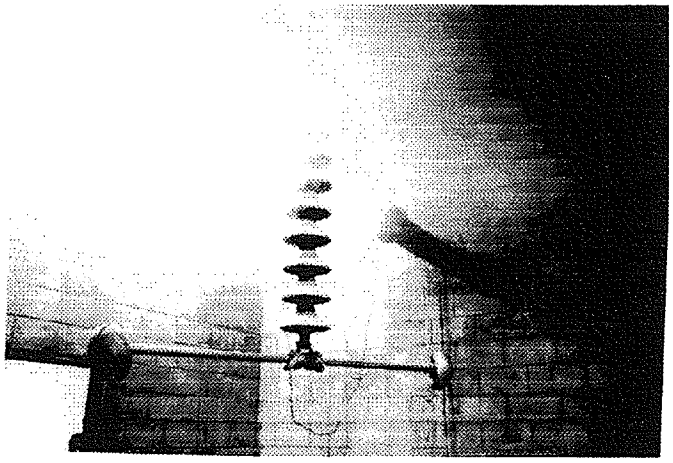

Photo 3.1
Test chamber with insulator string. Fog is filling the chamber from top.

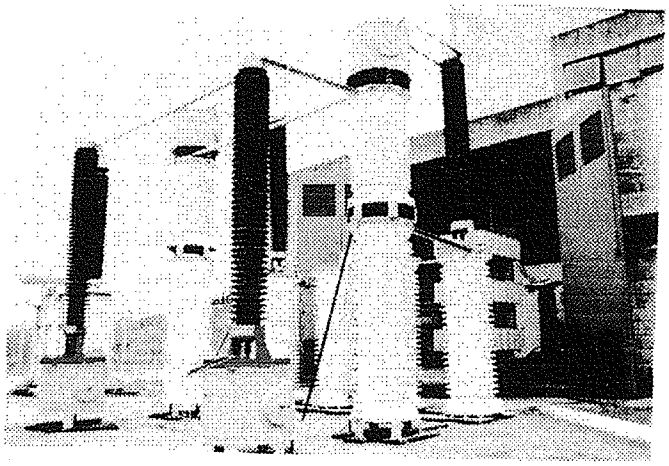

Photo 3.2
HVDC 2 phases doubler rectifier used as voltage source.

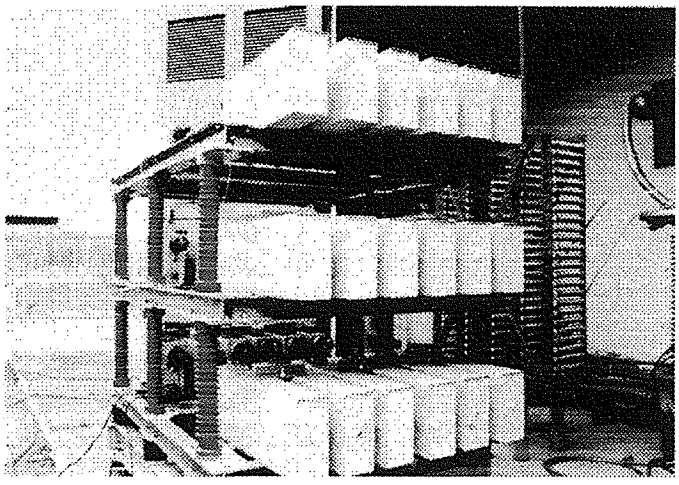

Photo 3.3
8μF, 120kV dc capacitor and protection resistor.

3.2.6 Measuring equipment

3.2.6.1 Voltage measuring system

Generally high dc voltages are measured using high ohmic voltage dividers. Many of these dividers, depending on their design, are not appropriate to measure the ac ripple superimposed to the dc voltage. The ripple frequency is dependent on the rectifier circuit used. In the present case two frequencies can occur, 60Hz for the 1 phase rectifier and 120Hz for the 2 phases one.

In order to measure the dc voltage and the superimposed ripple correctly, voltage measurement was performed using a mixed parallel RC type divider. This divider is adjusted to have approximately the same scale factor for dc and ac low frequencies voltages.

The divider comprised the following high voltage arm elements: resistance R_{HV}= 250MΩ and capacitance C_{HV}=2.375nF. The low voltage arm, also of the parallel RC type, was adjusted in order that both dc and low frequency ac 60Hz and 120Hz scale factors differ from the dc one by less than 5%. This guarantees a correct evaluation of the voltage ripple during tests using the weak sources. The measured values of the low voltage arm elements were: R_{LV}= 6.048kΩ and C_{LV}=97.4μF. These values include the effect of the measuring cable capacitance and also the input impedance of the two instruments used during the tests, a digitizer and a dc voltmeter.

The dc scale factor 41336:1 was measured at 1kV, using a dc Voltage Calibrator and the difference between the calculated and measured value was 0.3%.

A continuous check of the divider scale factor was made during the HVDC tests by monitoring the voltage at ac side of the rectifier and the dc voltage at the test object.

Figure 3.5 presents the measured frequency response of the voltage divider.

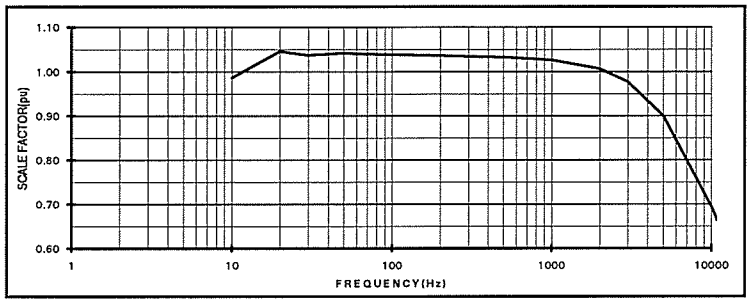

Figure 3.5. Voltage divider measured frequency response. 1pu= dc scale factor.

3.2.6.2 Current measuring system

The insulator current was measured through a shunt connected in series with the insulator string at the grounded side.

Figure 3.6 shows the circuit of the current shunt designed in order that protection of the measuring instrumentation is guaranteed in case of short circuit of the test object.

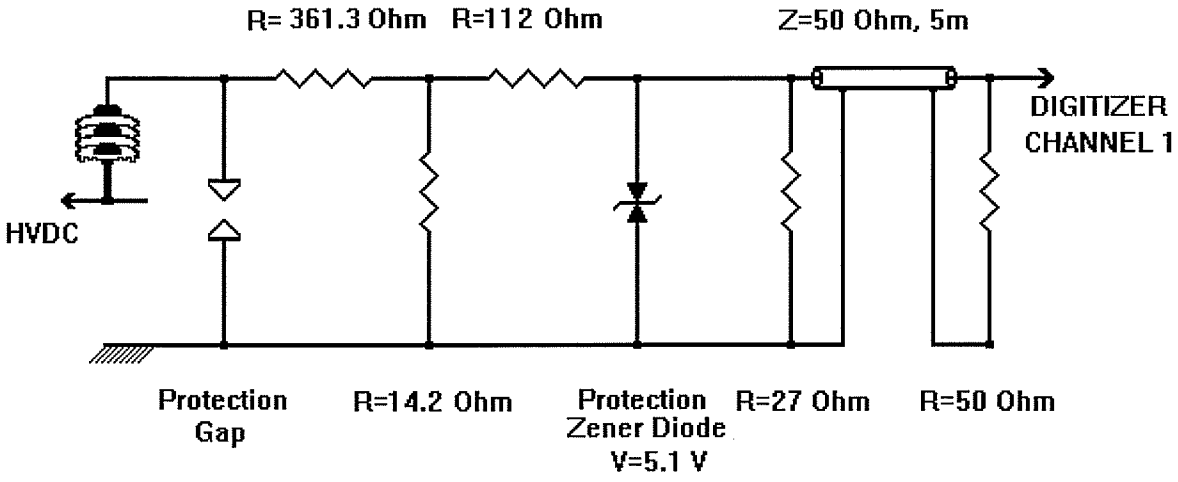

Figure 3.6. Current shunt circuit.

Figure 3.7 shows the frequency response of the current shunt.

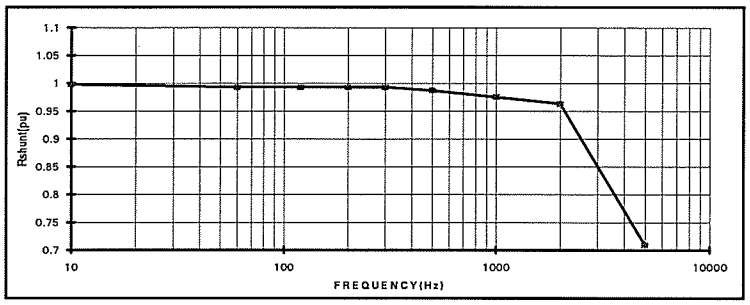

Figure 3.7. Measured current shunt frequency response. 1 pu= 1.692Ω.

The equivalent resistance, R= 1.692 Ω, of this shunt was measured by the application of a calibrated dc current, i = 70mA.

3.2.6.3 Data acquisition system

In order to record each individual current pulse and the corresponding simultaneous voltage evolution, during each voltage application, a data acquisition system was used. The main component of this system was a two channel digitizer model RTD2301 manufactured by Tektronix. Each channel had a 9 bit analog to digital converter and an input impedance of 1 MΩ.

The sampling rate used was 2000 samples per second (500μs sampling interval) which for 120Hz ripple guarantees the measurement with acceptable error.

Each channel is programmed to store 4096 data points, corresponding to a total record length of about 2 seconds.

The acquisition process is triggered by the current channel, with the trigger level adjusted in order that a current pulses with amplitude above a certain level, depending on the SDD used, are stored together with the simultaneous voltage evolution record.

The system was controlled by a 386 PC μcomputer and up to 128 files (64 per channel) could be stored during an individual voltage application.

When a trigger occurs the digitizer stores the two wave forms on its memory, the computer reads the digitizer memory, transfers the two wave forms to a hard disk, resets the digitizer to prepare it to store the next pulse. Due to the time needed to complete this full operation, if two pulses occur within an interval of less than 2 seconds, which was a seldom situation during the tests, the second pulse was not stored.

Software from Tektronix could be used to visualize the pulses and to calculate some of their desired characteristics. This has to be applied to each pulse individually, which is an extremely time consuming task. Although not all voltage applications had the individuals pulses stored, numerous wave forms were analyzed. A computer program was then developed which read the files related to each pulse and calculated those desired characteristics.

A paper oscillograph was used in parallel with the digitizer current channel in order to check if some important information is lost during tests. In fact, the digital system failed to store very few pulses during all tests performed.

3.2.7 Polarity of the applied voltage

The majority of tests were performed using negative polarity but some were performed with positive polarity.

3.2.8 Test procedure

The artificially polluted insulator at ambient temperature was mounted in the test chamber. The test voltage was applied and fog was introduced inside the chamber. The initial instant (t=0) of the test was considered as that moment when the fog was visually detected inside the chamber. The voltage was maintained constant until the insulator string flashed over or until a systematic reduction in the amplitude of current pulses was observed.

The up-and-down method with at least fifteen valid voltage applications was employed. Each voltage application was made on a new polluted test specimen. In this method, a number n of voltages levels spaced by a value ΔU is selected; a voltage is applied to the voltage level U, if a flashover occurs, the next application is made at the level $U-\Delta U$; if the test object withstands the voltage U, the next application is at voltage level $U+\Delta U$. This procedure is repeated until at least 15 valid voltage applications are obtained. The first valid voltage application is considered the one when the first change on the result of the voltage application occurs, withstand to flashover or flashover to withstand.

The results of the up-and-down test method, this means, voltage levels, $U_1, U_2, \ldots U_n$; number of voltage applications at each voltage level, NA_1, $NA_2, \ldots NA_n$; and the number of flashovers obtained at each voltage level, NF_1, $NF_2, \ldots NF_n$, are analyzed using the maximum likelihood method in order to obtain the values for the 50% disruptive discharge voltage U_{50} and the standard deviation σ of the disruptive discharge voltage of the insulator string under test. The maximum likelihood procedure is also used to determine the confidence limits of U_{50}.

The following parameters were determined from the individual recorded current pulses and corresponding voltage evolution:

- Time of pulse start. Time of occurrence of current pulse in relation to time t=0, time when the steam start to be introduced inside the test chamber;
- Peak value of current pulse and time of its occurrence, relative to the pulse duration;
- Energy dissipated over the insulator during the pulse;
- Charge content of the current pulse;
- Duration of current pulse;
- Maximum voltage drop and time of its occurrence. When ripple in the voltage is present, the maximum voltage drop is determined from a smoothed voltage curve;

- Average voltage drop, calculated for the duration of the current pulse;
- Voltage ripple, maximum peak to peak voltage ripple;
- Minimum insulator impedance during pulse duration;

This data was calculated automatically from the recorded current pulses and corresponding voltage by a specially developed digital program. A copy of this program is presented in Appendix I.

The data was used to analyze the effect of the voltage source on test results and also to clarify important aspects of the flashover evolution along polluted surfaces.

CHAPTER 4

TESTS RESULTS AND ANALYSIS

4.1 - U_{50} AND σ RESULTS

Tables 4.1, 4.2 and 4.3 present test results for the IEEE insulator and Tables 4.4, 4.5 and 4.6 for the ANTIFOG insulator.

Table 4.1 presents results obtained with 6 units IEEE insulator string for light contamination level, i.e. SDD=0.02 mg/cm^2. The tests were performed with voltage source F3. Table 4.2 presents similar results for the medium contamination level, i.e. SDD= 0.07 mg/cm^2; the tests were performed with voltage sources F1, F2 and F3 and the tested strings had 8 units IEEE insulator. In Table 4.3 results for the heavy contamination level, i.e. SDD= 0.20 mg/cm^2, are presented using 8 units IEEE insulator string. In this case the tests were performed with voltage sources F1, F2, F3, F4 (negative and positive polarity) and F5.

Tables 4.1 to 4.6 yield information about: U(kV), the voltage applied to the insulator during the test; NA, NF, number of voltage applications and number of flashovers obtained at the specific voltage level; U_{50}(kV), U_{50}(pu), 50% disruptive discharge voltage in kV and in pu, 1pu = U_{50} obtained with the strongest source used for that SDD level under study; σ(kV), σ(%), standard deviation in kV and as a percentage of the value of U_{50}; U_{mi}, U_{ma}, limits of the confidence interval for the value of U_{50}, calculated with a confidence level C.

Table 4.1 - IEEE Insulator - Results of high voltage tests, SDD=0.02mg/cm^2, 6 insulators string

Voltage Source	High Voltage Test Results		Maximum Likelihood Analysis Results			
F3	U(kV)	NF/NA	U_{50}	σ	U_{mi}	U_{ma}
2 Phases	-94.0	0/1				
C_{dc}= 8μF	-102.0	1/3	-110.2kV	18.4kV	-101.1kV	-118.7kV
R_p= 5kΩ	-110.0	2/7	1.00pu	16.7%	0.92pu	1.08pu
	-118.0	5/5	-18.4kV/unit		C= 0.90	

Table 4.2 - IEEE Insulator - Results of high voltage tests, SDD=0.07mg/cm^2, 8 insulators string

Voltage Source	High Voltage Test Results		Maximum Likelihood Analysis Results			
F1	U(kV)	NF/NA	U_{50}	σ	U_{mi}	U_{ma}
1 Phase	-90.0	0/1				
C_{dc}= 110nF	-95.0	1/5	-98.6kV	3.8kV	-93.7kV	-102.0kV
R_p= 5kΩ	-100.0	5/8	1.06pu	3.9%	1.01pu	1.10pu
	-105.0	1/3	-12.3kV/unit			
	-110.0	1/1			C= 0.90	
F2	U(kV)	NF/NA	U_{50}	σ	U_{mi}	U_{ma}
2 Phases	-85.0	0/2				
C_{dc}= 440nF	-90.0	2/6	-91.9kV	3.7kV	-86.6kV	-96.1kV
R_p= 5kΩ	-95.0	4/5	0.99pu	4.1%	0.93pu	1.03pu
	-100.0	2/2	-11.5kV/unit		C= 0.80	
F3	U(kV)	NF/NA	U_{50}	σ	U_{mi}	U_{ma}
2 Phases	-85.0	0/1				
C_{dc}= 8μF	-90.0	1/4	-92.9kV	5.8kV	-85.2kV	-98.1kV
R_p= 5kΩ	-95.0	4/8	1.00pu	6.3%	0.92pu	1.06pu
	-100.0	3/3	-11.6kV/unit		C= 0.90	

Table 4.3 - IEEE Insulator - Results of high voltage tests, SDD=0.20mg/cm^2, 8 insulators string

Voltage Source	High Voltage Test Results		Maximum Likelihood Analysis Results			
F1	U(kV)	NF/NA	U_{50}	σ	U_{mi}	U_{ma}
1 Phase	-90.0	0/6	-94.3kV	1.2kV	-91.9kV	-95.8kV
C_{dc}= 110nF	-95.0	6/8	1.48pu	1.3%	1.44pu	1.50pu
R_p= 5kΩ	-100.0	1/1	-11.8kV/unit		C= 0.90	
F2	U(kV)	NF/NA	U_{50}	σ	U_{mi}	U_{ma}
2 Phases	-59.5	0/4				
C_{dc}= 440nF	-63.0	4/7	-63.5kV	3.1kV	-59.3kV	-66.5kV
R_p= 5kΩ	-66.5	4/5	1.00pu	4.8%	0.93pu	1.04pu
	-70.0	1/1	-7.9kV/unit		C= 0.90	
F3	U(kV)	NF/NA	U_{50}	σ	U_{mi}	U_{ma}
2 Phases	-56.0	0/1				
C_{dc}= 8μF	-59.5	1/4	-62.5kV	3.0kV	-57.4kV	-67.2kV
R_p= 5kΩ	-63.0	4/8	0.98pu	4.9%	0.90pu	1.05pu
	-66.5	3/3	-7.8kV/unit		C= 0.90	
F4	U(kV)	NF/NA	U_{50}	σ	U_{mi}	U_{ma}
2 Phases	-56.0	0/2				
C_{dc}= 440nF	-59.5	2/5	-61.1kV	3.4kV	-53.7kV	-65.7kV
R_p= 1kΩ	-63.0	4/6	0.96pu	5.5%	0.84pu	1.03pu
	-66.5	2/2	-7.6kV/unit		C= 0.90	
F5	U(kV)	NF/NA	U_{50}	σ	U_{mi}	U_{ma}
2 Phases	-59.5	0/3				
C_{dc}= 8μF	-63.0	3/6	-63.7kV	3.0kV	-58.6kV	-67.2kV
R_p= 1kΩ	-66.5	4/5	1.00pu	4.7%	0.92pu	1.05pu
	-70.0	1/1	-8.0kV/unit		C= 0.90	
F4+	U(kV)	NF/NA	U_{50}	σ	U_{mi}	U_{ma}
2 Phases	+66.0	0/2	+70.5kV	0.9kV	+70.0kV	+72.8kV
C_{dc}= 440nF	+70.0	2/7	1.11pu	1.3%	1.08pu	1.14pu
R_p= 1kΩ	+74.0	5/5	+8.8kV/unit		C= 0.90	

Tables 4.4 to 4.6 present the results for tests performed on strings of 4 units ANTIFOG Insulator using voltage source F5. Results for light contamination level, i.e. SDD=0.02 mg/cm^2, are presented in Table 4.4. Table 4.5 presents the test results for the medium contamination level, i.e. SDD= 0.07 mg/cm^2 and Table 4.6 presents the test results for the heavy contamination level, i.e. SDD= 0.20 mg/cm^2.

Table 4.4 - ANTIFOG Insulator - Results of high voltage tests, SDD=0.02mg/cm^2, 4 insulators string

Voltage Source	High Voltage Test Results		Maximum Likelihood Analysis Results			
F5	U(kV)	NF/NA	U_{50}	σ	U_{mi}	U_{ma}
2 Phases	-94.0	0/2				
C_{dc}= 8μF	-102.0	2/4	-109.2	9.7kV	-100.6kV	-120.3kV
R_p= 1kΩ	-110.0	2/7	1.00pu	8.9%	0.92pu	1.10pu
	-118.0	4/4	-27.3kV/unit		C= 0.80	

Table 4.5 - ANTIFOG Insulator - Results of high voltage tests, SDD=0.07mg/cm^2, 4 insulators string

Voltage Source	High Voltage Test Results		Maximum Likelihood Analysis Results			
F5	U(kV)	NF/NA	U_{50}	σ	U_{mi}	U_{ma}
2 Phases	-65.0	0/1				
C_{dc}= 8μF	-70.0	1/3	-74.7kV	4.3kV	-68.3kV	-79.3kV
R_p= 1kΩ	-75.0	3/8	1.00pu	5.7%	0.91pu	1.06pu
	-80.0	5/5	-18.7kV/unit		C= 0.90	

Table 4.6 - ANTIFOG Insulator - Results of high voltage tests, SDD=0.20mg/cm^2, 4 insulators string

Voltage Source	High Voltage Test Results		Maximum Likelihood Analysis Results			
F5	U(kV)	NF/NA	U_{50}	σ	U_{mi}	U_{ma}
2 Phases	-46.0	0/2				
C_{dc}= 8μF	-49.0	2/6	-51.3kV	4.9kV	-47.5kV	-56.8kV
R_p= 1kΩ	-52.0	4/6	1.00pu	9.6%	0.93pu	1.11pu
	-55.0	2/3	-12.8kV/unit		C= 0.70	

Figure 4.1 presents the relationship between U_{50}, with confidence limits, and Salt Deposit Density, obtained for the IEEE and ANTIFOG insulators. In the Figure, the values of U_{50} obtained in tests with the strongest sources are plotted.

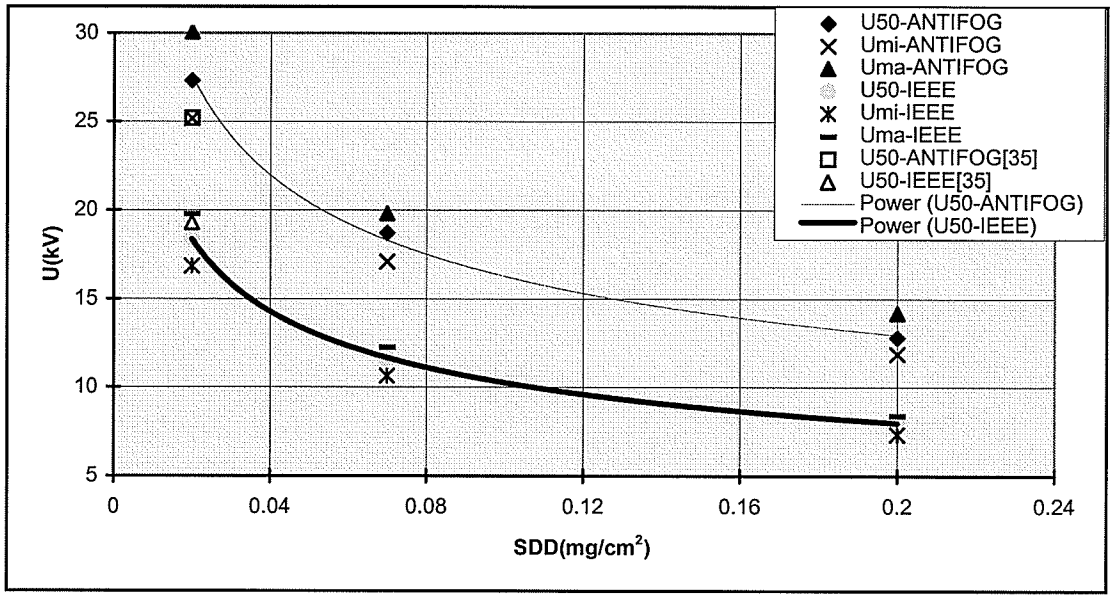

Figure 4.1. Values of U_{50} and confidence limits versus SDD.

In Figure 4.1 are also plotted the regression trendlines of the form $U_{50}= A.SDD^{K}$ for both insulators. The following trendline regression equations were obtained(SDD in mg/ cm^2 and U_{50} in kV):

- IEEE insulator: $U_{50}= -4.46.SDD^{-0.36}$, $R^2= 0.9999$; (1)

- ANTIFOG insulator: $U_{50}= -7.64.SDD^{-0.33}$, $R^2=0.9974$. (2)

The exponent K which here was determined as -0.36(IEEE insulator) and -0.33(ANTIFOG insulator) was determined in Reference 36, for different designs of HVDC station post insulators tested using the solid layer method, with SDD values between 0.005mg/cm^2 and 0.05mg/cm^2,

and steam fog for humidification of the layer, as having values between -0.32 to -0.41 with average value of -0.36.

If, instead of U_{50}, the relation U_{50}/LL, where LL is the leakage length, 305mm for the IEEE insulator and 530mm for the ANTIFOG insulator, is related to the contamination level, the following regression equations are obtained, for U_{50}/LL in V/mm and SDD in mg/cm^2:

- IEEE insulator: $U_{50}/LL = -14.61.SDD^{-0.36}$ (3)

- ANTIFOG insulator: $U_{50}/LL = -14.46.SDD^{-0.33}$ (4)

These two equations are similar and if only one regression equation is determined for both insulators one obtains:

$$U_{50}/LL = -14.53.SDD^{-0.35},\ R^2 = 0.9712 \quad (5)$$

This equation was used to determine the U_{50} values for both insulators and Table 4.7 shows the values calculated and errors when compared with the experimental results.

Table 4.7 - Estimation of U_{50} from Equation 5 and comparison with tests results

INSULATOR	SDD (mg/cm^2)	U_{50}(kV)		Error(%)
		Equation 5	Tests	
IEEE	0.02	-17.4	-18.4	-5.4
	0.07	-11.2	-11.6	-3.5
	0.20	-7.8	-8.0	-2.5
ANTIFOG	0.02	-30.3	-27.3	+11.0
	0.07	-19.5	-18.7	+4.3
	0.20	-13.5	-12.8	+5.5

Figure 4.2 presents U_{50} values for the IEEE insulator together with the confidence limits for the heavy pollution level tested.

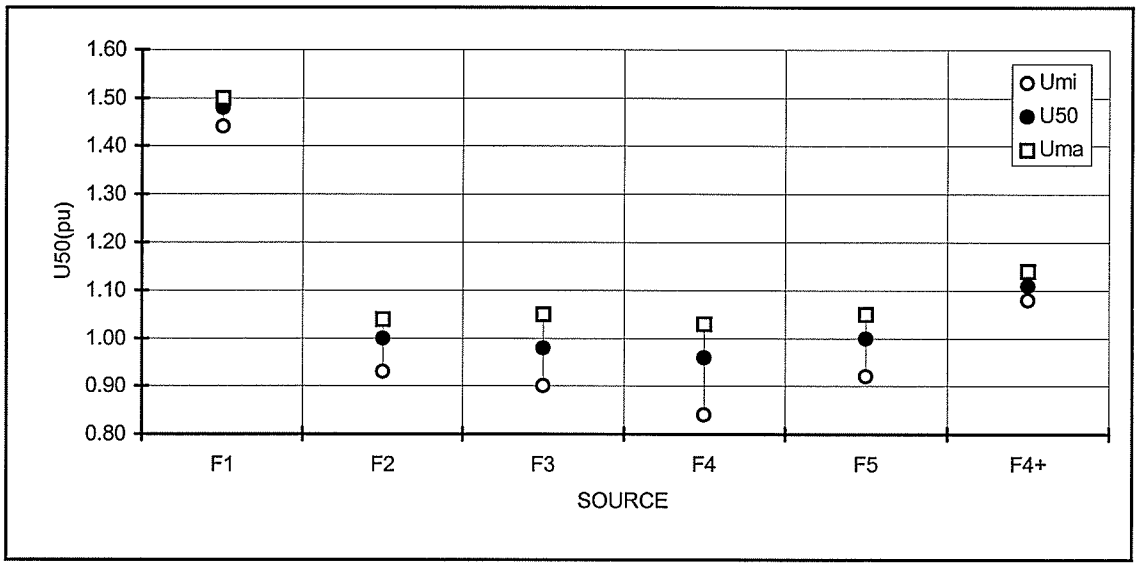

Figure 4.2 - Results of high voltage tests, IEEE Insulator with 8 units, SDD=0.20 mg/cm^2. 1pu=-63.7kV

The following main conclusions can be drawn from the above Figure:

- Tests with HVDC sources F2, F3, F4 and F5 gave practically the same U_{50} values even for the heavy contamination level SDD=0.20 mg/cm^2 tested, in spite of the different values for the dc capacitance and protection resistor of these sources. Source F1, the weakest one gave 48% higher value for U_{50};

- Test with positive polarity gave 11% higher value for U_{50}, when compared with the negative polarity result.

Figure 4.3 presents the U_{50} values for the IEEE insulator together with the confidence limits for the medium pollution level tested. For this contamination level, even the weakest source F1 resulted in a value for U_{50} close to the results obtained with the stronger sources.

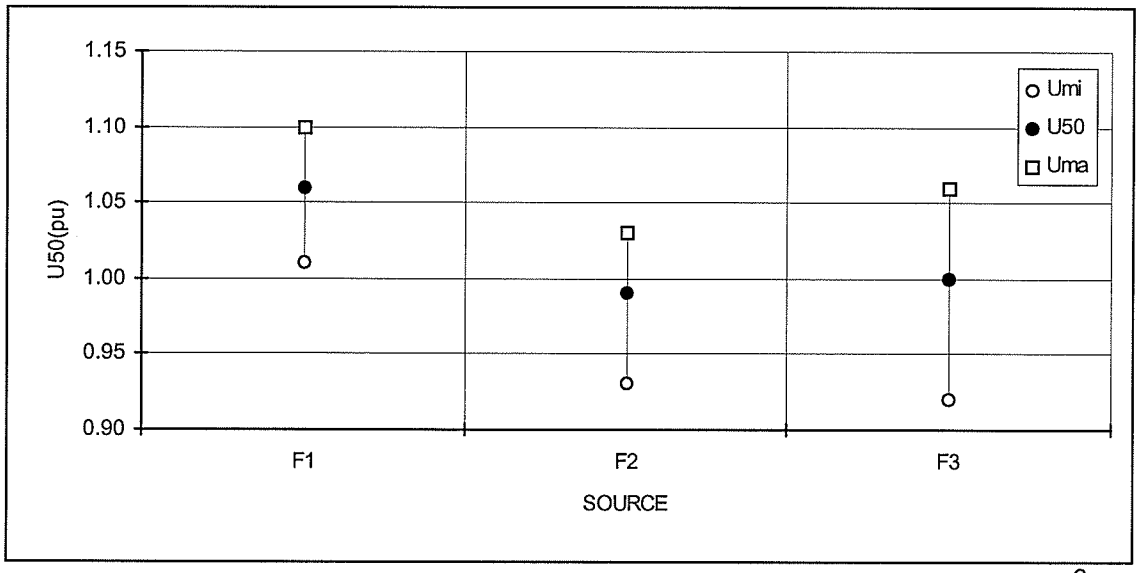

Figure 4.3 - Results of high voltage tests, IEEE Insulator with 8 units, SDD=0.07 mg/cm^2. 1pu=-92.9kV

4.2 - CRITICAL CURRENT PULSES, VOLTAGE DROPS AND U_{50}

An analysis according to Risk[21] and IEC Technical Report 1245[37] was performed to relate the error caused by the source in the determination of U_{50} to the average and maximum voltage drops during a critical current pulse I_H, which is the current pulse with highest amplitude at critical voltage level, the maximum voltage level which does not lead to flashover of the insulator

Table 4.8 presents the values for voltage drops obtained for critical current pulses(I_H) during tests on both insulators.

Table 4.8 - Critical current pulses and corresponding voltage drops

Insulator	SDD (mg/cm^2)	Source	Peak of I_H(ma)	Avg.Volt. Drop (%)	Max.Volt. Drop (%)	U_{50} (kV/unit)
IEEE	0.02	F3	-39.0	1.4	2.0	-18.4
	0.07	F1	-237.6	11.0	18.0	-12.3
		F2	-264.9	10.2	14.4	-11.5
		F3	-209.8	4.5	7.8	-11.6
	0.20	F1	-1526.0	26.8	55.1	-11.8
		F2	-310.9	13.1	17.1	-7.9
		F4	-402.7	10.7	16.9	-7.6
		F5	-255.1	5.5	8.6	-8.0
ANTIFOG	0.02	F5	-38.1	0.3	0.3	-27.3
	0.07		-239.5	3.5	6.0	-18.7
	0.20		-485.0	8.9	13.7	-12.8

Table 4.9 presents the values of U_w/LL and the peak values of I_H, measured during tests on both insulators, where:

- U_w - critical voltage - maximum voltage withstood by the insulator tested on all voltage applications for the same SDD, in kV/unit. The critical voltages are obtained from Tables 4.1 to 4.6. When tests with different voltage sources are performed, those obtained with the strongest source are considered

- LL - leakage length for the insulator under test, in mm;

- I_H - critical current pulses, from Table 4.8.

Table 4.9 - U_w/LL and I_H for the insulators and SDD tested.

Insulator	SDD(mg/cm^2)	U_w(kV)	U_w/LL(V/mm)	I_H(mA)
IEEE	0.02	-15.7	-51.5	-39.0
	0.07	-10.6	-34.8	-209.8
	0.20	-7.4	-24.3	-255.1
ANTIFOG	0.02	-23.5	-44.3	-38.1
	0.07	-16.3	-30.8	-239.5
	0.20	-11.5	--21.7	-485.0

Figure 4.4 presents the relation between U_w/LL and I_H. The regression line was obtained for the 6 points considered with a regression index R^2=0.88.

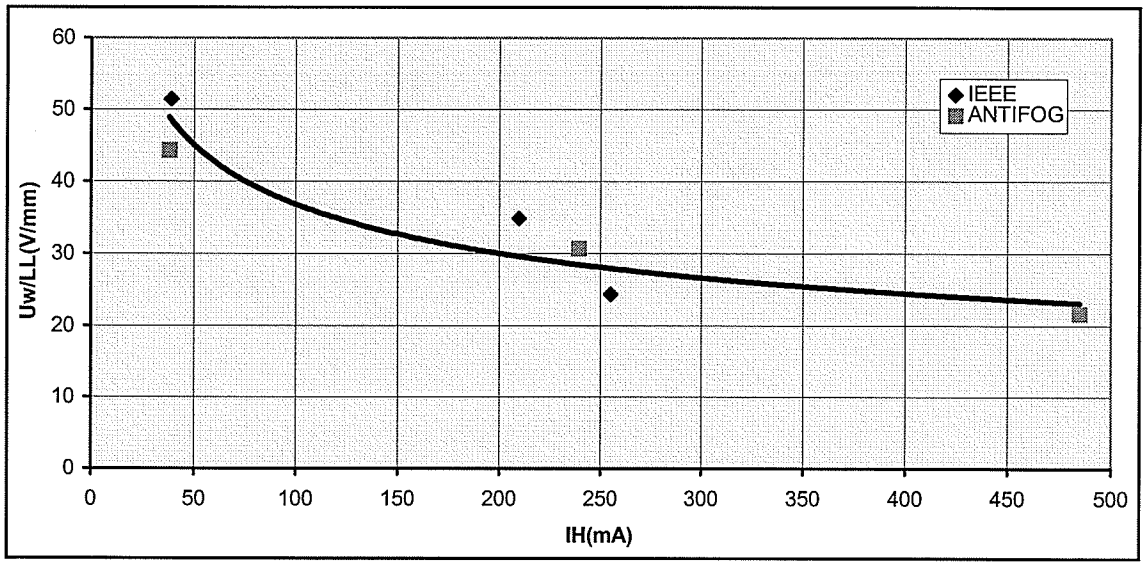

Figure 4.4 - U_w/LL versus I_H

The curve in Figure 4.4, although obtained with a few number of points, and for only two types of insulators, can have an important meaning, to prove the validity of the critical current concept and its use as a control characteristic for diagnosis of contaminated insulators in service. More tests with other types of insulators and with non uniform pollution distribution as observed in service are necessary to prove if such a characteristic has general validity.

Figure 4.5 presents the average voltage drop characteristic, obtained from measured data, of two test sources when all highest current pulses are considered, even at those voltage levels where flashover occurred.

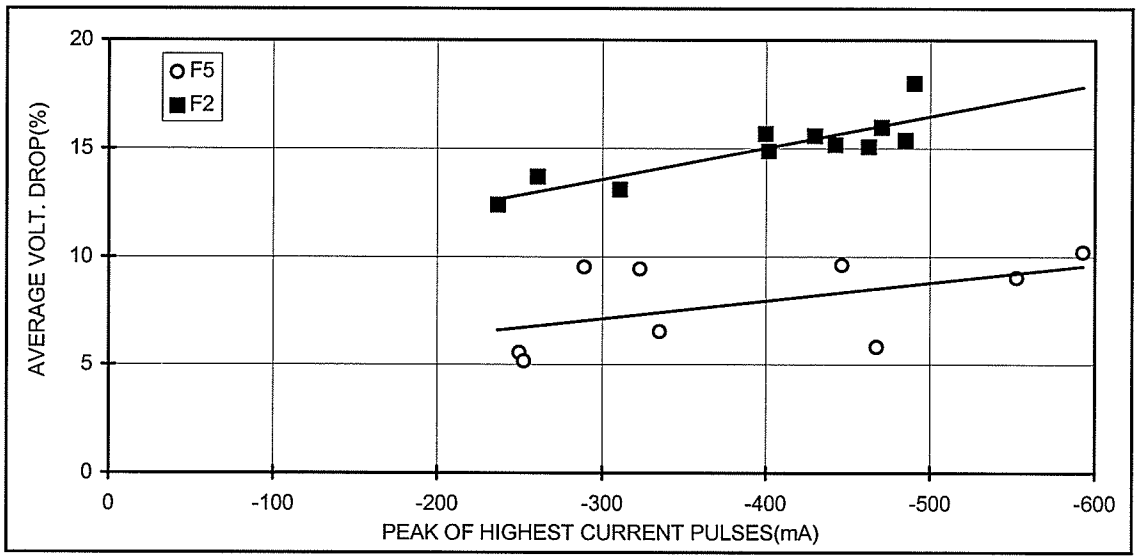

Figure 4.5 - Average voltage drop for highest current pulses. Tests with sources F2 and F5, SDD=0.20 mg/cm^2.

Although source F5 presents a lower voltage drop x current characteristic when compared to source F2, it presents a higher dispersion for voltage drop values for similar amplitude of current pulses.

In order to find the reason for this higher dispersion, let us analyze, for example, two current pulses obtained during tests with voltage source F5, the one with peak equal to -466.7 mA(average voltage drop 7.2%) and the other with lower peak value, -316.7mA, but higher corresponding average voltage drop, 9.9%. These two pulses were measured as those with highest amplitude during two different voltage applications 01 and 04 during the up-and-down test procedure with SDD=0.20 mg/cm^2 on the IEEE insulator string.

Table 4.10 presents the measured characteristics of these two pulses.

Table 4.10- Characteristics of two highest current pulses, SDD=0.20 mg/cm^2, source F5

Measured Characteristics	Current Pulse 01	Current Pulse 02
Voltage application Nr.:	-63.0	-66.5
Time of pulse start(min.)	37.7	55.8
Current pulse duration(msec.)	407.0	1010.0
Current peak(mA)	-466.7	-316.7
Time of occurrence of peak(msec)	222.5	92.5
Average voltage drop, ΔU_{av}(%)	7.2	9.9
Maximum voltage drop, ΔU_{max}(%)	13.2	11.8
Time of occurrence of ΔU_{max}(msec.)	355.0	551.0
Charge content of current pulse(mC)	95.1	-195.0

Figure 4.6 show these two current pulses and Figure 4.7 the corresponding voltage evolution.

The pulse with lower amplitude, -316.7mA, has longer duration and presents higher average voltage drop, although similar maximum voltage drop when compared with the current pulse with -466.7mA amplitude.

These curves and the corresponding pulse data show that not always the highest voltage drop(average or maximum) corresponds to the current peak with highest amplitude. This is frequently the case for test sources with high output capacitance, for example source F5. In these cases the voltage changes slowly due to the long time constant output capacitor-insulator and the duration of the current pulse has an important influence on the maximum voltage drop obtained.

Also for these types of voltage sources the maximum voltage drop does not occur simultaneously with the current maximum. In general, the voltage minimum occurs much later, specially when the current peak occurs at the beginning of the pulse, as is usually the case, or when the current pulse passes through a maximum value and decreases rapidly.

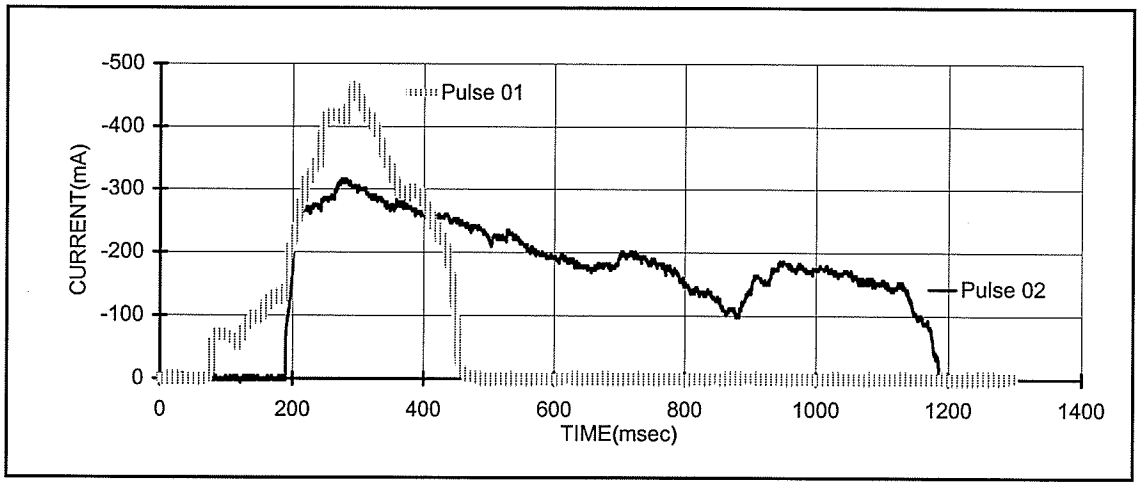

Figure 4.6 - Two highest current pulses for voltage applications 1 and 4 with SDD=0.20 mg/cm^2, Voltage Source F5.

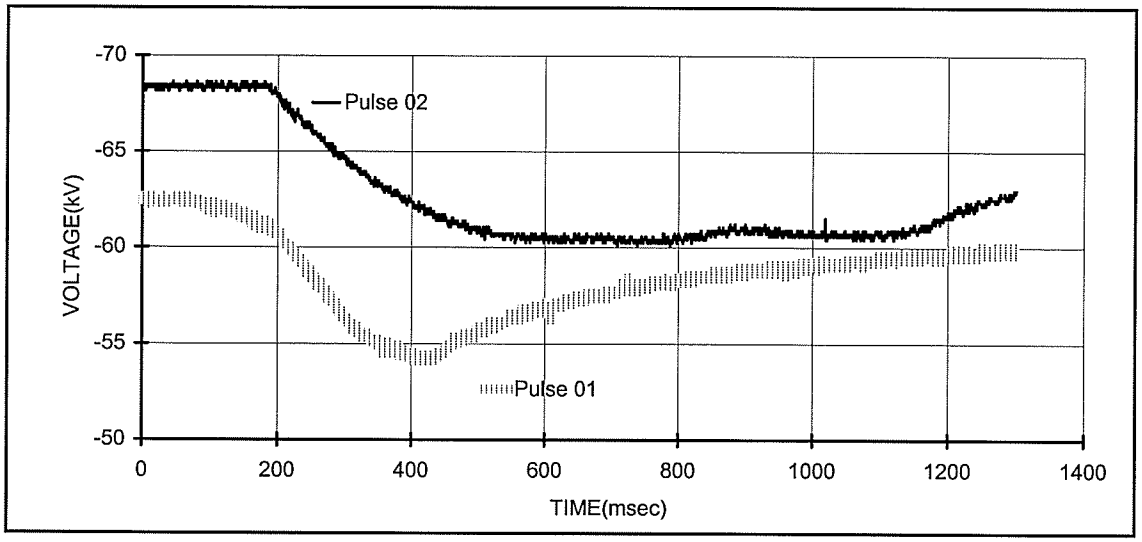

Figure 4.7 - Voltage evolution for current pulses of Figure 4.6.

These results suggest that it is more appropriate to consider as the maximum voltage drop that drop which occurs at the moment the current is maximum.

Similar conclusion can be made with reference to the average voltage drop, which is calculated as the difference between the no load voltage and the integral of the voltage during the entire duration of the current pulse. This calculation should not cover the entire current pulse duration but only the time period when current is increasing due to the arc advance along the insulator surface, that is, until current peak is reached.

If the average and maximum voltage drops are calculated from beginning of the pulse till current maximum the following values, presented in Table 4.11, are obtained for these two pulses under analysis.

Table 4.11 - Comparison of voltage drops values

		Current Pulse 01 Peak Value -466.7mA	Current Pulse 02 Peak Value -316.7mA
ΔU_{max}	Calculation for the total pulse duration[21]	13.2%	11.8%
	Calculation until pulse current maximum	9.4%	4.7%
ΔU_{av}	Calculation for the total pulse duration[21]	7.2%	9.9%
	Calculation until pulse current maximum	3.0%	2.0%

The values for voltages drops calculated from pulse start to maximum are considerably lower than those calculated previously for the entire pulse duration.

The curves in Figures 4.6 and 4.7 shall be compared to those shown in figures 4.8 and 4.9. These are highest current pulses obtained during two different voltage applications, numbers 8 and 14, on the string constituted by IEEE insulators, at heavy contamination level, with voltage source F2, at -59.5 kV.

As this voltage source has an output capacitance, C_{dc}= 440nF, 18.2 times smaller than source F5, C_{dc}= 8000nF the voltage follows almost immediately variations in the current. So in this case, generally the instant of maximum voltage drop coincides with that of current maximum.

These two current pulses were selected because they present practically the same peak value, -413.1mA and -411.7 mA, respectively. Although the pulse duration are different(597.5 msec and 981.0 msec),the maximum voltage drops(18.5% and 18.6%)and also the average voltage drops(13.5% and 15.2%) have practically the same values.

For sources with medium and low dc capacitance (F1, F2 and F4), the dc capacitor-insulator time constant is smaller than the pulse front, the voltage follows the current pulse shape, the instant of maximum voltage drop coincides with instant of current peak and the voltage drops are the same, whether calculated over the entire pulse duration or until current maximum.

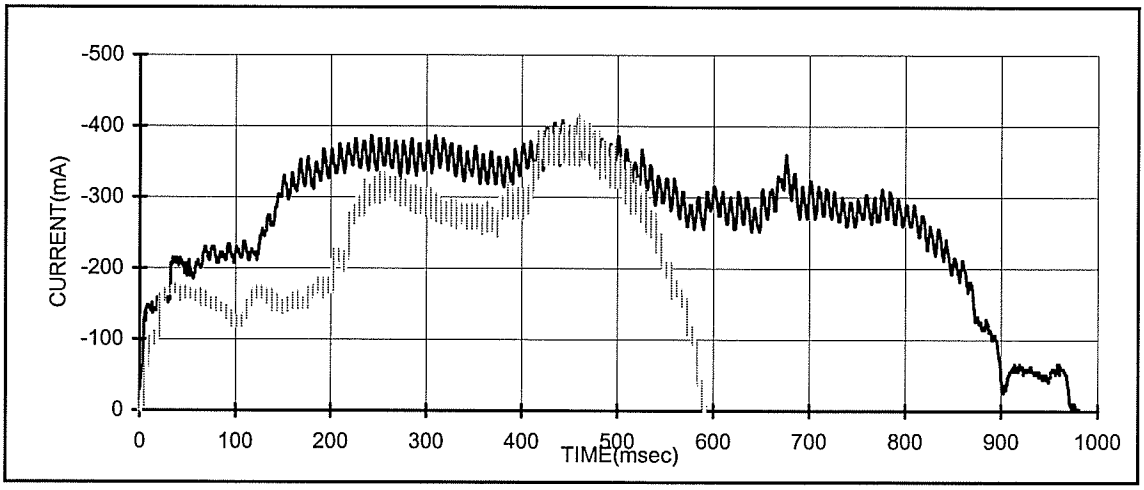

Figure 4.8 - Highest current pulses for voltage applications 08 and 14, SDD=0.20 mg/cm^2. Voltage Source: F4, IEEE insulator.

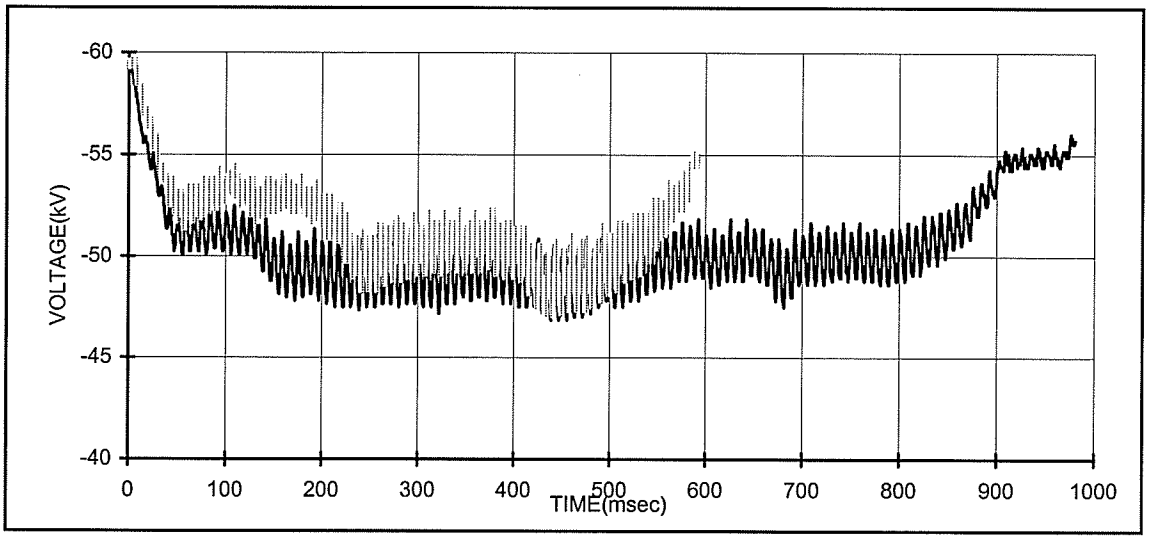

Figure 4.9 - Voltage evolution for current pulses of Figure 4.8.

4.3 - ANALYSIS OF HIGHEST CURRENT PULSES

During each voltage application a series of current pulses occurs, starting from low amplitudes, 10 mA or lower, when the humidification process is at initial stage, has an increasing tendency with time and consequent reduction of surface resistivity, and afterwards, if no disruptive discharge occurs, their amplitudes reduce due to the increase of surface resistivity caused by the washing process.

Figure 4.10 shows a typical evolution of current pulse peaks during voltage application 04, with test source F3, U= -63 kV, when testing the IEEE insulator.

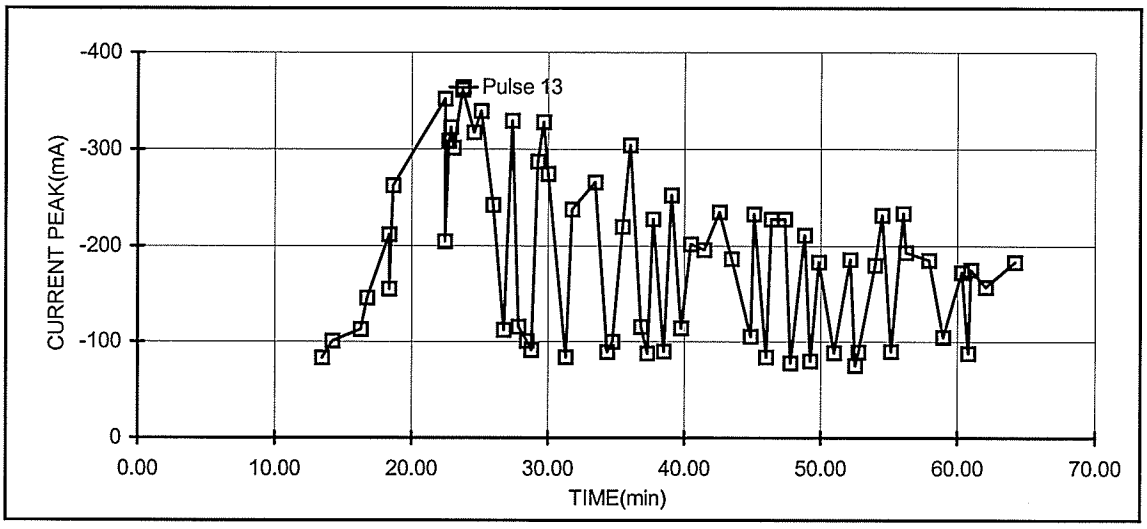

Figure 4.10 - Evolution of current peaks, voltage application 04, SDD=0.2 mg/cm^2, source F3, IEEE insulator.

All those pulses above a certain level (-20 mA for SDD= 0.02mg/cm^2, -70 mA for SDD= 0.07mg/cm^2 and -200 mA for SDD= 0.20mg/cm^2) were recorded and in the following a complete analysis was performed for those of highest amplitude such is the case of pulse Number 13 in Figure 4.10. In the next section the results of the analysis of these pulses are presented for the cases studied for the IEEE and ANTIFOG insulators. As only the highest current pulses for those recorded voltage levels withstood by the insulator are considered, the number of pulses analyzed for each pollution level and test source studied is limited, from 5 to 8 pulses. The average, the minimum and the maximum values for different characteristics analyzed are presented for comparison purposes.

4.3.1 - Time of occurrence.

Figures 4.11 and 4.12 present, for the IEEE insulator, the time of occurrence of the highest current pulses, counted from t=0, instant when steam fog starts inside the test chamber, at those voltage applications with no flashover, using the indicated voltage sources, SDD= 0.07mg/cm^2 and SDD= 0.20mg/cm^2

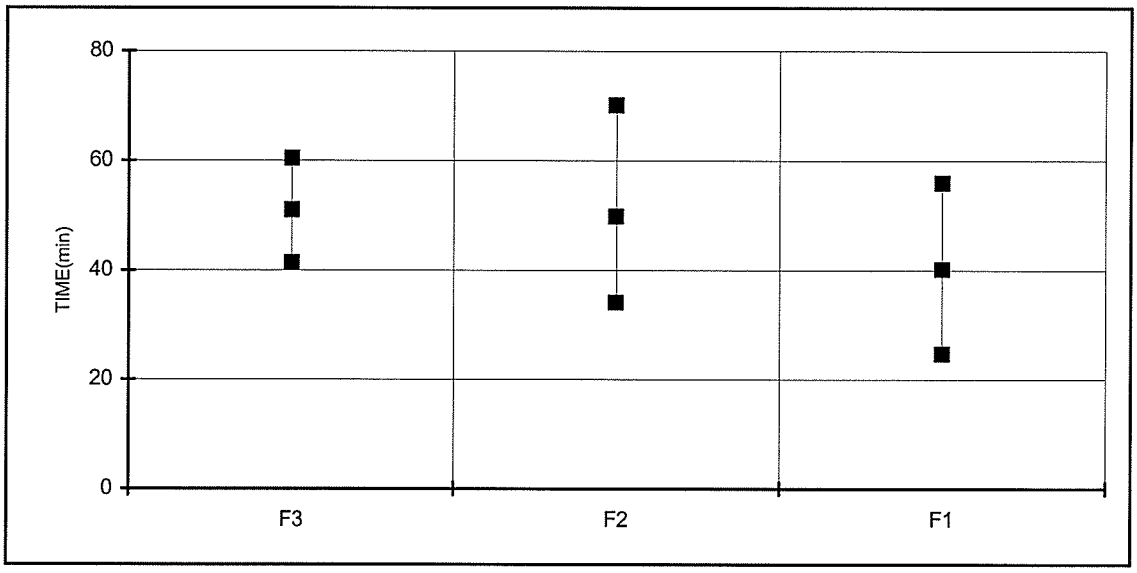

Figure 4.11 - Time of occurrence of highest current pulses. SDD=0.07 mg/cm^2. IEEE Insulator.

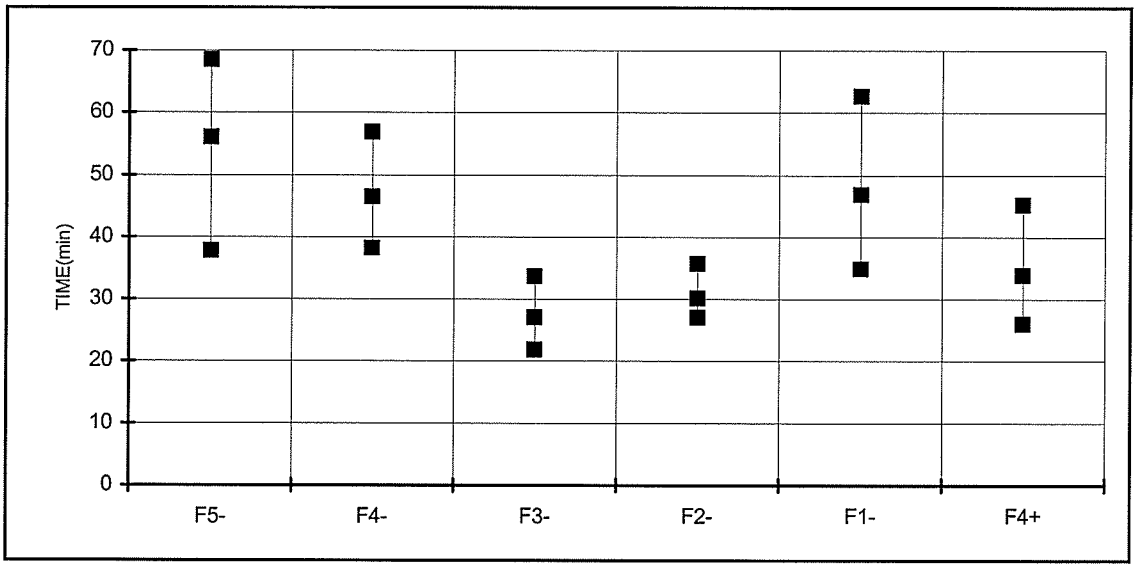

Figure 4.12 - Time of occurrence of highest current pulses. SDD=0.20 mg/cm^2. IEEE Insulator.

It can be seen that, for SDD=0.07 mg/cm^2 no significant difference in the time of occurrence of highest current pulses can be observed. For SDD=0.20 mg/cm^2, apparently a reduction of the protection resistor R_p from 5kΩ to 1 kΩ resulted in an increase of the time. Also with the very

weak voltage source F1, at the heavy pollution level, the occurrence of the highest current pulses is delayed.

Figure 4.13 presents the same information for the ANTIFOG insulator, all tests performed with the strongest source F5.

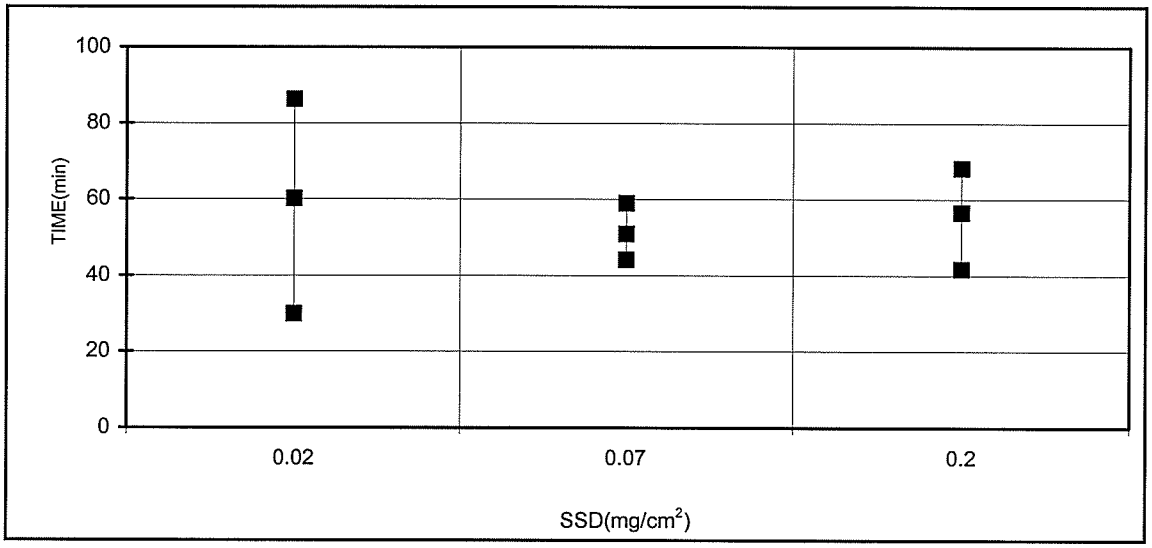

Figure 4.13 - Time of occurrence of highest current pulses. Test source F5, ANTIFOG Insulator.

The information obtained here show that in some cases the highest current pulses can occur after more than one hour of fog application. This reinforces the need of monitoring the current pulses during the test in order to certify that the risk of flashover is negligible before reducing the voltage. This information is not in agreement with recommendation of IEC Technical Report 1245-1993[37], where the risk of flashover was said to be negligible if 30 min had passed from the start of discharge activity, indicated by the leakage flashover measurements. A conservative procedure is to maintain the voltage for at least 100 min, if no monitoring of current pulses is performed during tests.

4.3.2 - Peak values of current pulses

Figures 4.14 and 4.15, for the IEEE insulator, present the peak value of the analyzed pulses for both SDD levels tested.

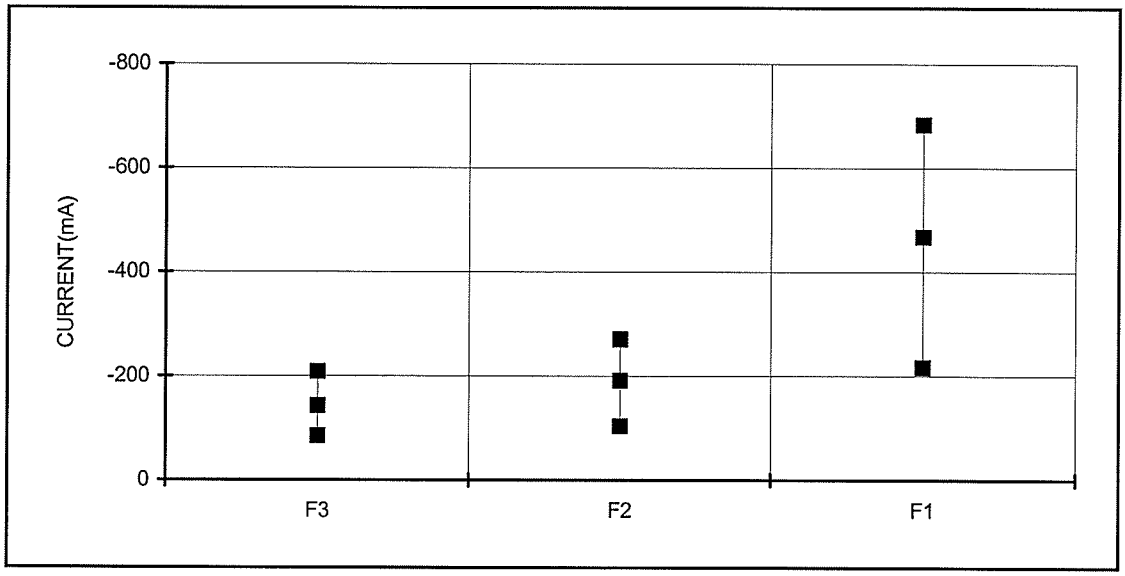

Figure 4.14 - Peak values of highest current pulses. SDD=0.07 mg/cm^2. IEEE insulator.

No significant difference in the peak values is observed when testing with voltage source F2 and F3, for the medium contamination level or F2,F3,F4 and F5, at negative polarity for the heavy contamination level.

During tests with source F1, significantly higher current pulses are observed, even if the considerable superimposed ripple is eliminated from the current wave shape.

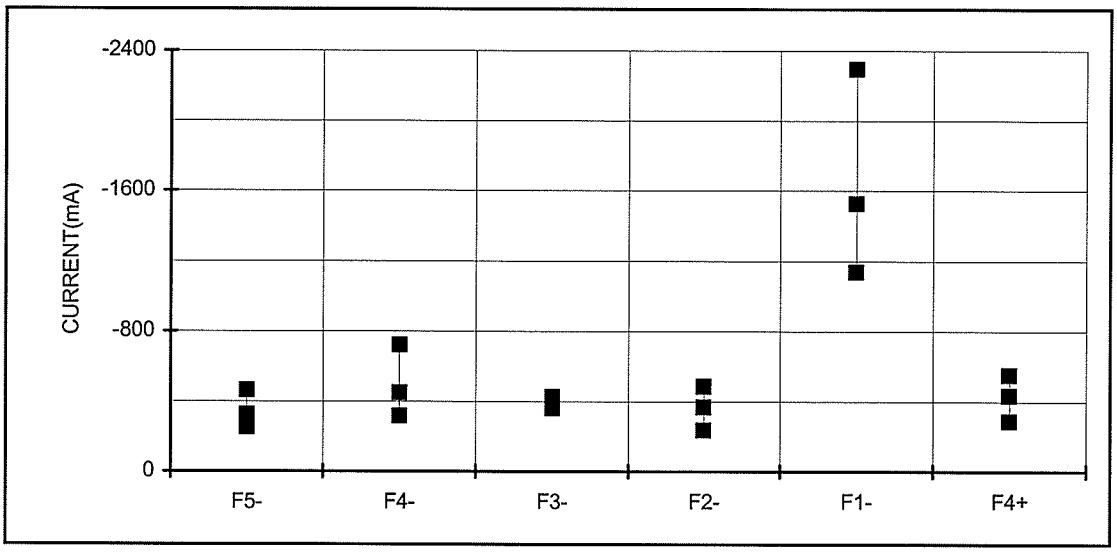

Figure 4.15 - Peak values of highest current pulses. SDD=0.20 mg/cm^2. IEEE insulator.

The above results confirm the information found in the literature, the strong effect of type of voltage source on the amplitude of highest current pulses during pollution tests. Much higher current pulses are obtained when performing tests with weak sources.

Figure 4.16 presents the peak values of highest current pulses recorded during tests on the ANTIFOG insulator.

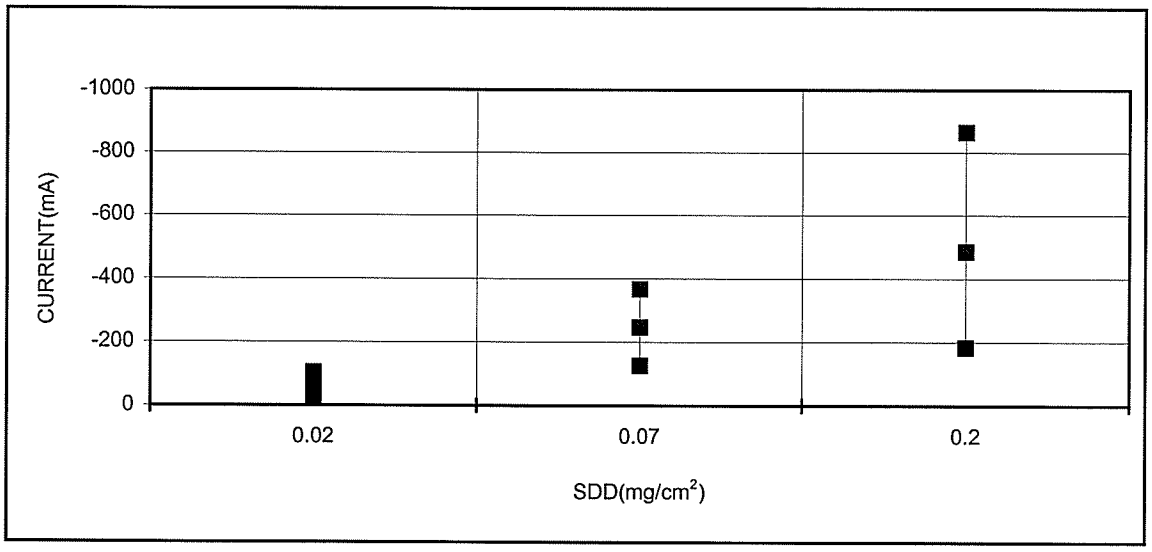

Figure 4.16 - Peak values of highest current pulses. Source F5. ANTIFOG insulator.

4.3.3 - Voltage drops and voltage ripple

Maximum and average voltage drops measured for highest current pulses are presented in Figures 4.17 to 4.22. These voltage drops were calculated from pulse start to current peak.

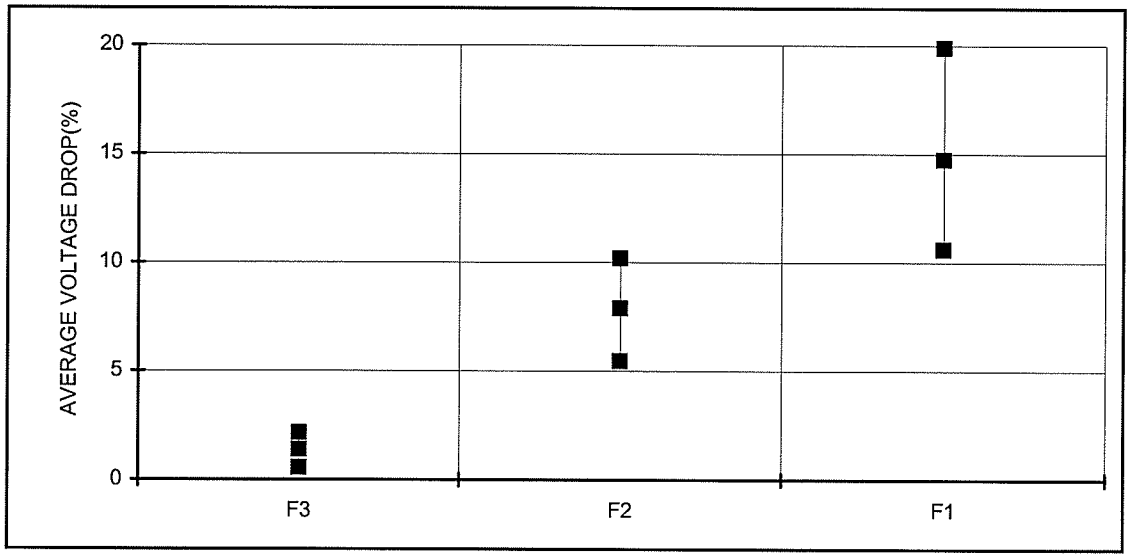

Figure 4.17 - Average voltage drops. SDD=0.07 mg/cm^2. IEEE insulator.

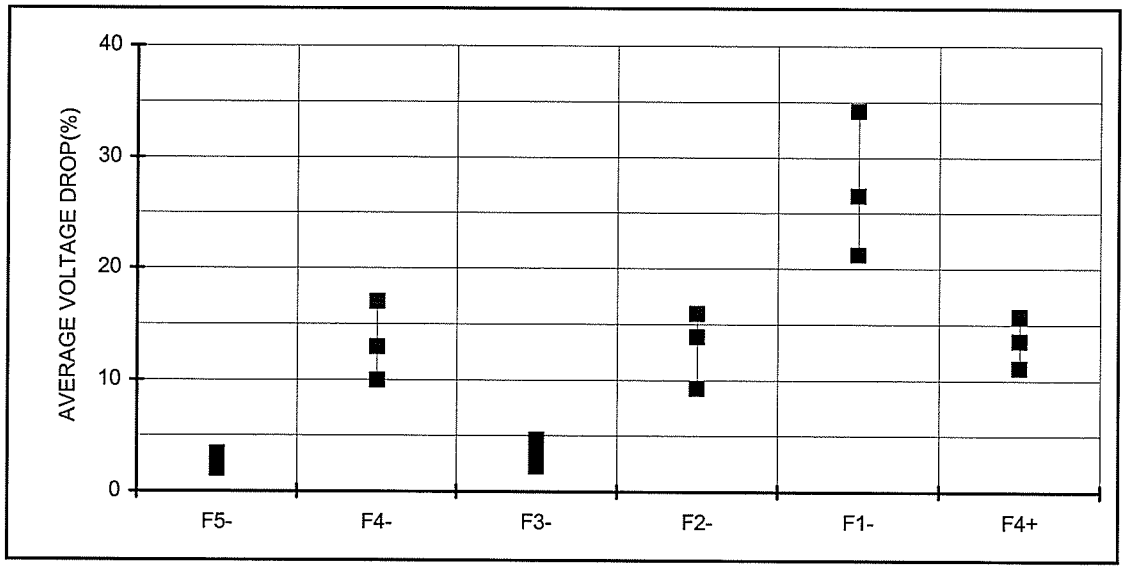

Figure 4.18 - Average voltage drops. SDD=0.20 mg/cm^2. IEEE insulator.

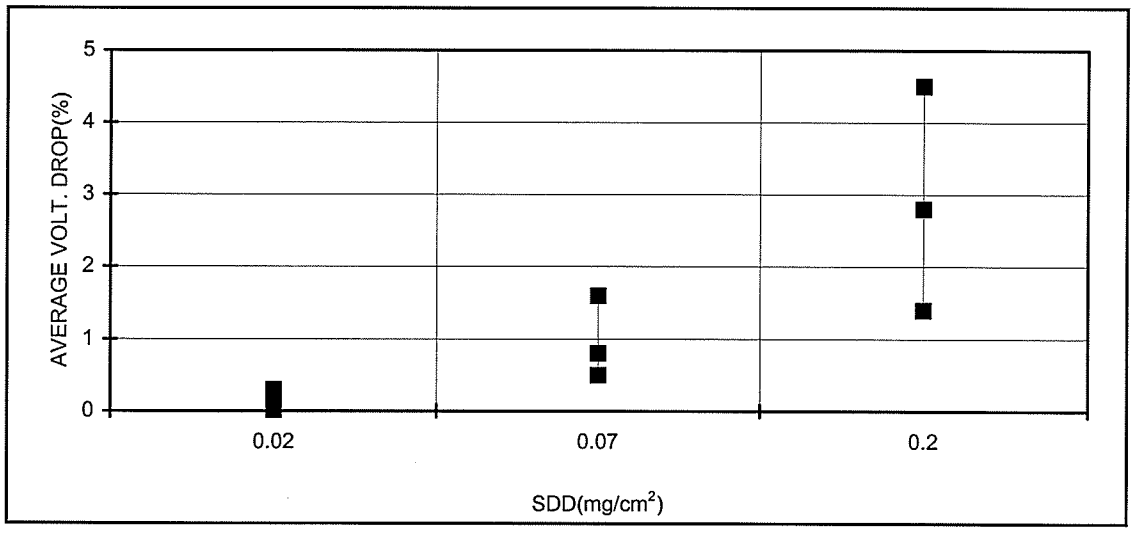

Figure 4.19 - Average voltage drops. Source F5. ANTIFOG insulator.

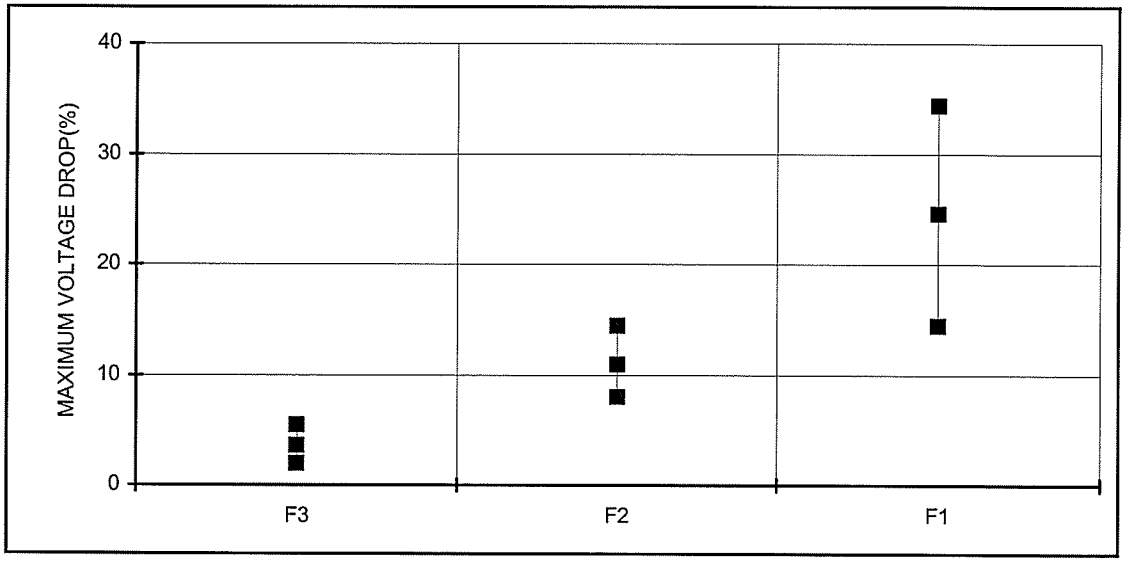

Figure 4.20 - Maximum voltage drops. SDD=0.07 mg/cm^2. IEEE insulator.

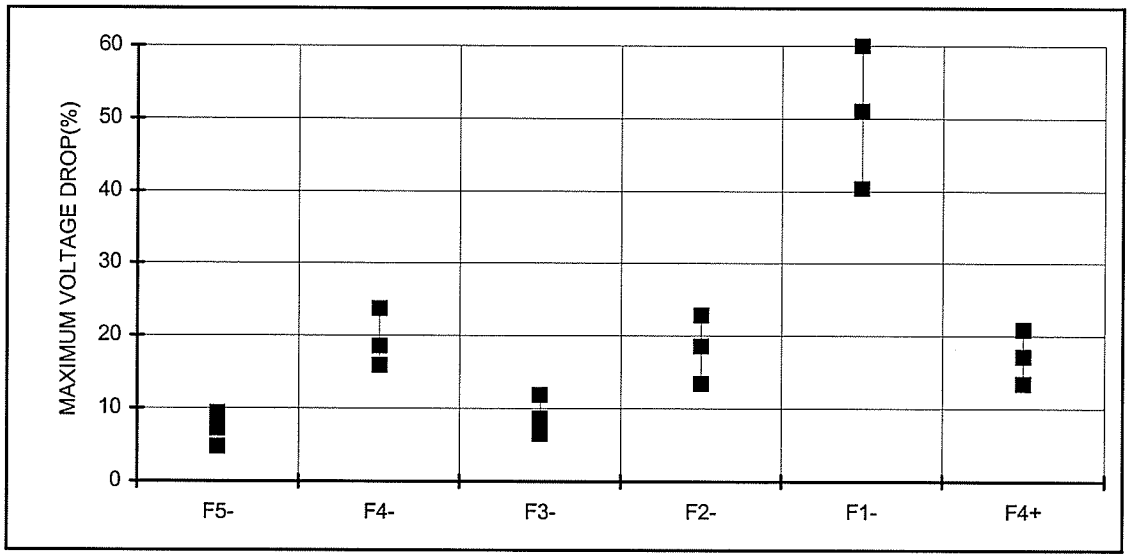

Figure 4.21 - Maximum voltage drops. SDD=0.20 mg/cm^2. IEEE insulator.

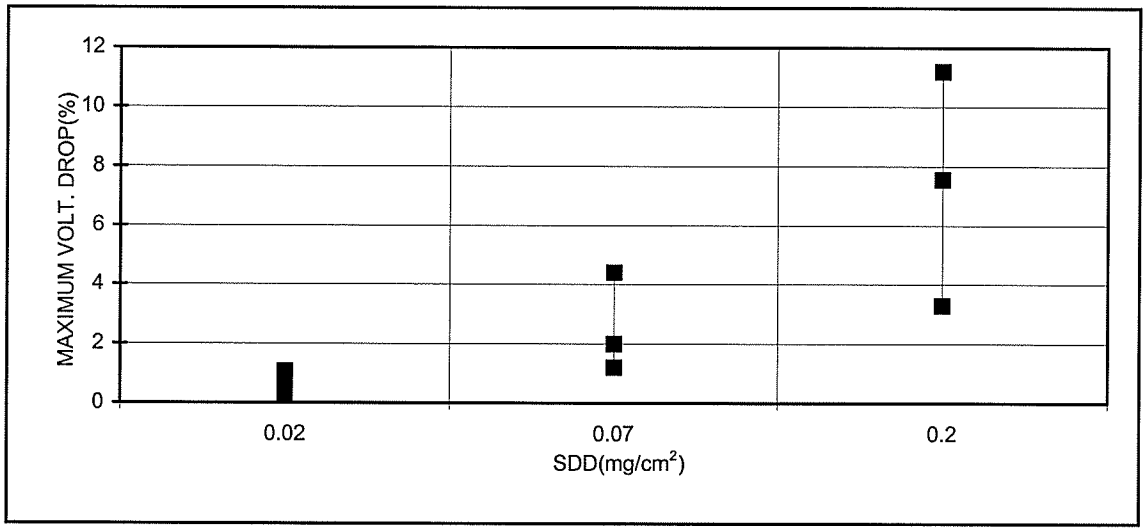

Figure 4.22 - Maximum voltage drops. Source F5. ANTIFOG insulator.

Tests results from IEEE insulator show that Sources F3 and F5 produce similar voltage drop values, lower than those for sources F2 and F4. Source F1 gave much higher voltage drops for both SDD levels tested.

Peak to peak ripple values for highest current pulses are presented in Figures 4.23 to 4.26 for tests on both insulators.

Figure 4.23 - Peak to peak ripple. SDD=0.07 mg/cm^2. IEEE insulator.

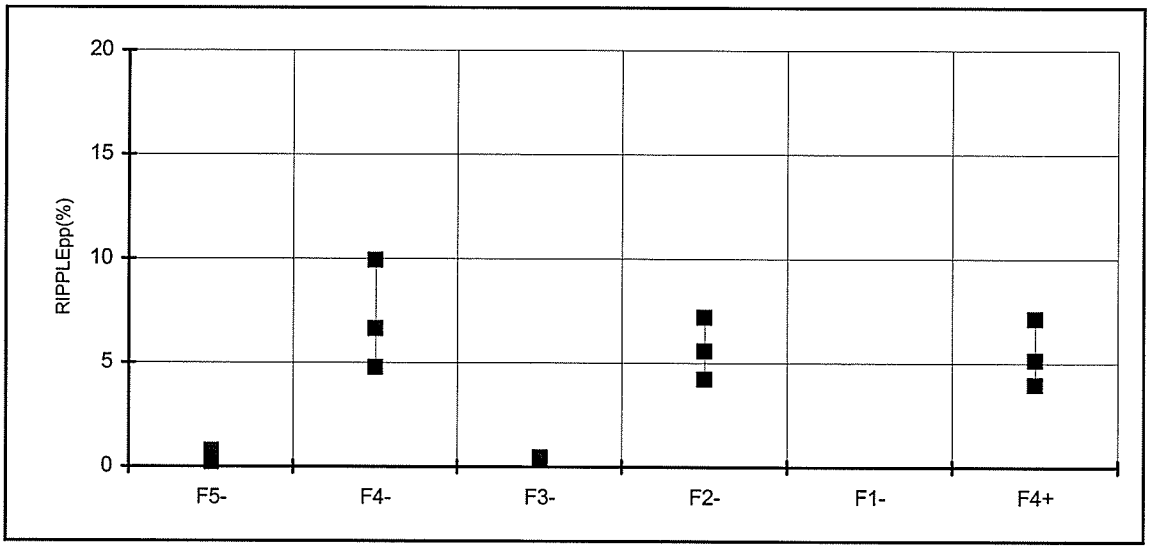

Figure 4.24 - Peak to peak ripple. SDD=0.20 mg/cm^2. IEEE insulator.

Ripple values for test source F1, SDD=0.20 mg/cm^2 are between 59% and 100%, and are not shown in Figure 4.24.

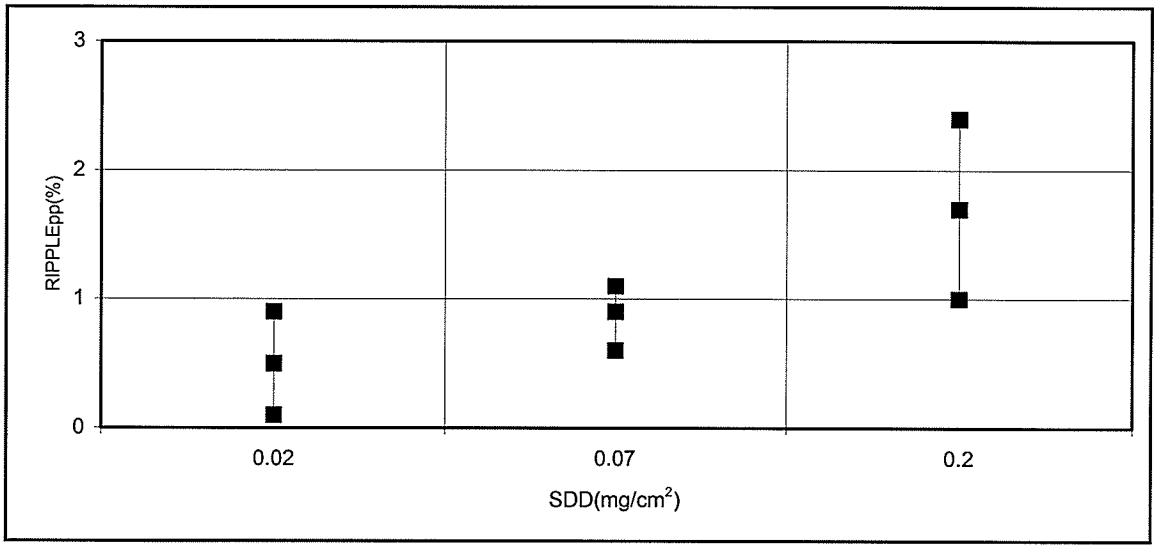

Figure 4.25 - Peak to peak ripple. Source F5. ANTIFOG insulator.

Sources F3 and F5, with 8000nF dc capacitor presented very low voltage ripple, less than 2.5%, during tests with all pollution levels on both insulators types. Sources F2 and F4 presented voltage ripple between 4.3% and 10% during tests with heavy contamination and between 2% and 5.3% during tests with medium contamination level. Source F1 had measured ripple between 60% and 100% during tests with SDD=0.20 mg/cm^2 and between 21% and 48% during tests with SDD=0.07 mg/cm^2.

Table 4.12 presents an analysis, from IEEE insulator pollution tests results, of the voltage sources according to the two criteria shown in Table 1.5.

It should be emphasized that Rizk's criteria[21] are based on the critical current pulse(I_H), while IEC Technical Report's criteria are based on highest voltage drops recorded on all voltage levels without flashover, which in general corresponds to those voltage drops measured during highest current pulses. The measured characteristics for critical current pulses(I_H), are included in Table

4.12 and corresponds to the lower values in the ranges of characteristics presented for the highest current pulses.

Table 4.12 - Analysis of voltage sources according to Reference 21 and IEC Test Report 1245.

SDD	U_{50} (pu)	Test Sources and characteristics measured for highest current pulses	Reference 21, 1991 $\Delta U_{av} \leq 5\%$; $\Delta U_{max} \leq 10\%$ and Ripple $\leq 10\%$	IEC Report 1245, 1993 $\Delta U_{max} \leq 10\%$ or $10\% \leq \Delta U_{max} \leq 15\%$ and $\Delta U_{av} \leq 5\%$
0.07 mg/cm^2	1.06	F1 $14.5\% \leq \Delta U_{max} \leq 34.4\%$ $10.5\% \leq \Delta U_{av} \leq 20.0\%$ $21\% \leq$ Ripple $\leq 48\%$	Criteria are not satisfied	Criteria are not satisfied
	0.99	F2 $8.0\% \leq \Delta U_{max} \leq 14.4\%$ $5.5\% \leq \Delta U_{av} \leq 10.2\%$ $2.0 \leq$ Ripple $\leq 5.3\%$	Criteria are not satisfied	Criteria are not satisfied
	1.00	F3 $2.0\% \leq \Delta U_{max} \leq 5.5\%$ $0.5\% \leq \Delta U_{av} \leq 2.2\%$ Ripple $\leq 1.0\%$	Criteria are satisfied	Criteria are satisfied
0.20 mg/cm^2	1.48	F1 $40\% \leq \Delta U_{max} \leq 60\%$ $21.2\% \leq \Delta U_{av} \leq 34.1\%$ $60\% \leq$ Ripple $\leq 100\%$	Criteria are not satisfied	Criteria are not satisfied
	1.00	F2 $13.4\% \leq \Delta U_{max} \leq 22.8\%$ $9.3\% \leq \Delta U_{av} \leq 16.0\%$ $4.3\% \leq$ Ripple $\leq 7.2\%$	Criteria are not satisfied	Criteria are not satisfied
	0.98	F3 $6.5\% \leq \Delta U_{max} \leq 11.8\%$ $2.2\% \leq \Delta U_{av} \leq 4.7\%$ Ripple $\leq 1\%$	Criteria are satisfied	Criteria are satisfied
	0.96	F4 $16.0\% \leq \Delta U_{max} \leq 23.8\%$ $9.9\% \leq \Delta U_{av} \leq 17.0\%$ $4.8\% \leq$ Ripple $\leq 9.9\%$	Criteria are not satisfied	Criteria are not satisfied
	1.00	F5 $4.7\% \leq \Delta U_{max} \leq 9.4\%$ $2\% \leq \Delta U_{av} \leq 3.4\%$ Ripple $\leq 1\%$	Criteria are satisfied	Criteria are satisfied

It is clear from Table 4.12 that only tests sources F3 and F5 satisfy the criteria from IEC and Reference 21. Although tests performed with sources F2 and F4 yield the same U_{50} as sources F3 and F5, these two sources are excluded by criteria established by IEC and Reference 21.

Source F1 is also excluded, but only for the heavy contamination level, the U_{50} value is significantly higher(48%) than that obtained from tests with the strongest sources F5 or F3. For the medium contamination level, the difference obtained for U_{50}, was only 6%.

These results strongly suggest that the source requirements recommended in the present guidelines can probably be relaxed.

4.3.4 - Energy.

Figures 4.26 to 4.28 show the energy dissipated in the surface of the insulator string for the pulses under consideration.

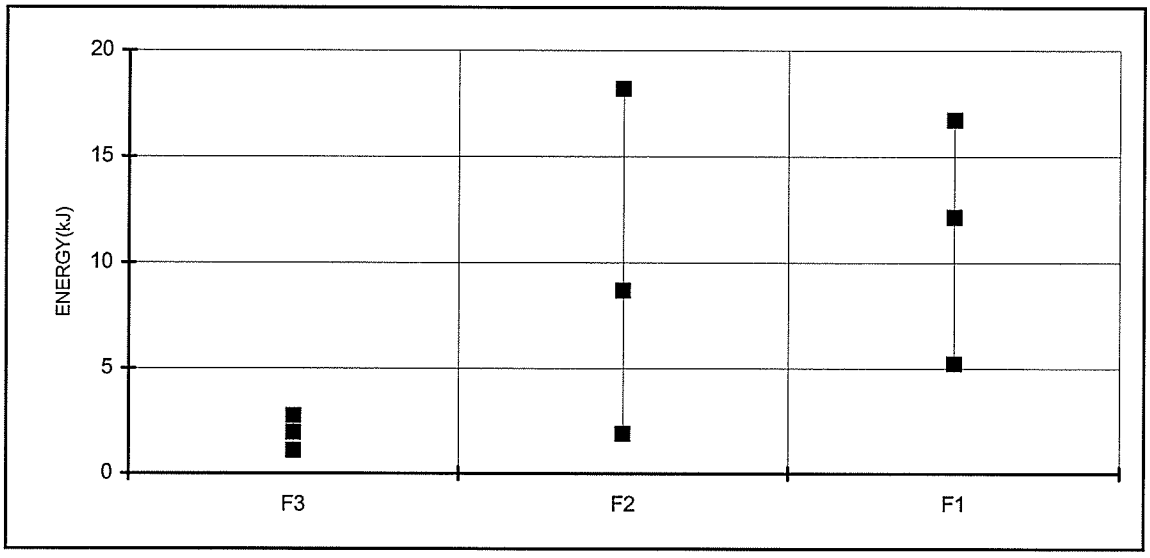

Figure 4.26 - Energy. SDD=0.07 mg/cm^2. String with 8 IEEE insulators.

These Figures show that tests with high output dc capacitor yield lower energy current pulses. The dispersion of energy values is also smaller. As expected, the reduction of the protection resistor from 5 kΩ to 1 kΩ has only a small influence on the pulse energy.

Tests performed with voltage source F4 under positive polarity yielded pulses with lower energy when compared to tests with the same source at negative polarity, although higher voltages were applied

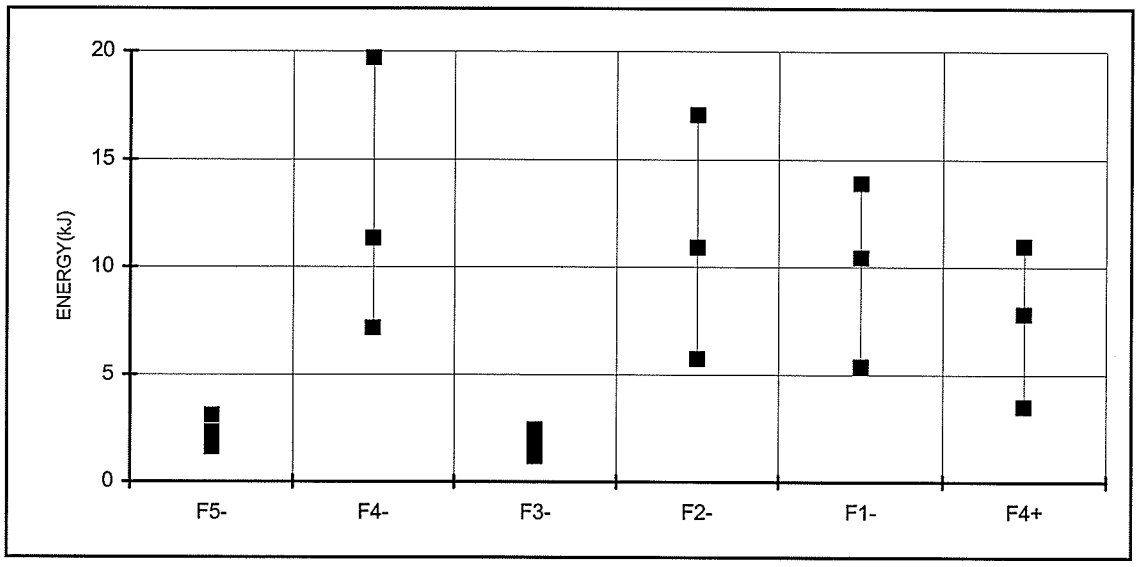

Figure 4.27 - Energy. SDD=0.20 mg/cm^2. String with 8 IEEE insulators.

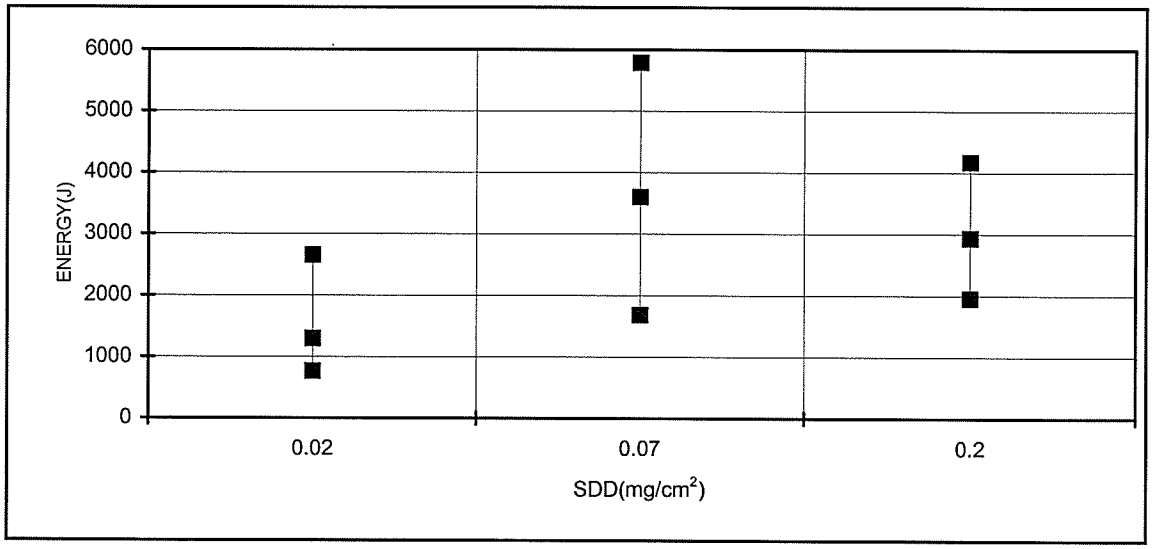

Figure 4.28 - Energy. Source F5. ANTIFOG insulator, string with 4 units.

4.3.5 - Charge and Pulse duration.

The same pattern as for the energy can be observed for the charge content and duration of the pulses as can be seen from Figures 4.29 to 4.34.

It is also interesting to note that pulse duration appears to be constant for both pollution levels studied for tests with the same voltage source, and that sources F2 and F4 give longer duration pulses than sources F3 and F5

Considering tests performed with strongest sources, all highest current present duration below 1 second.

Positive current pulses have longer duration than negative ones for tests with same SDD and same voltage source.

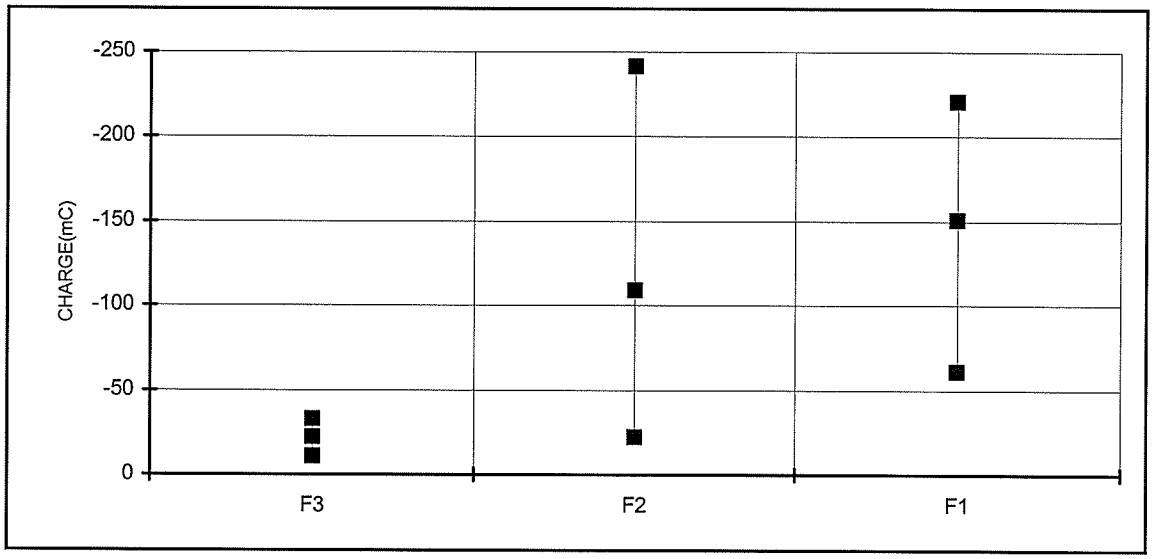

Figure 4.29 - Charge content of current pulses. SDD=0.07 mg/cm^2. String with 8 IEEE insulators.

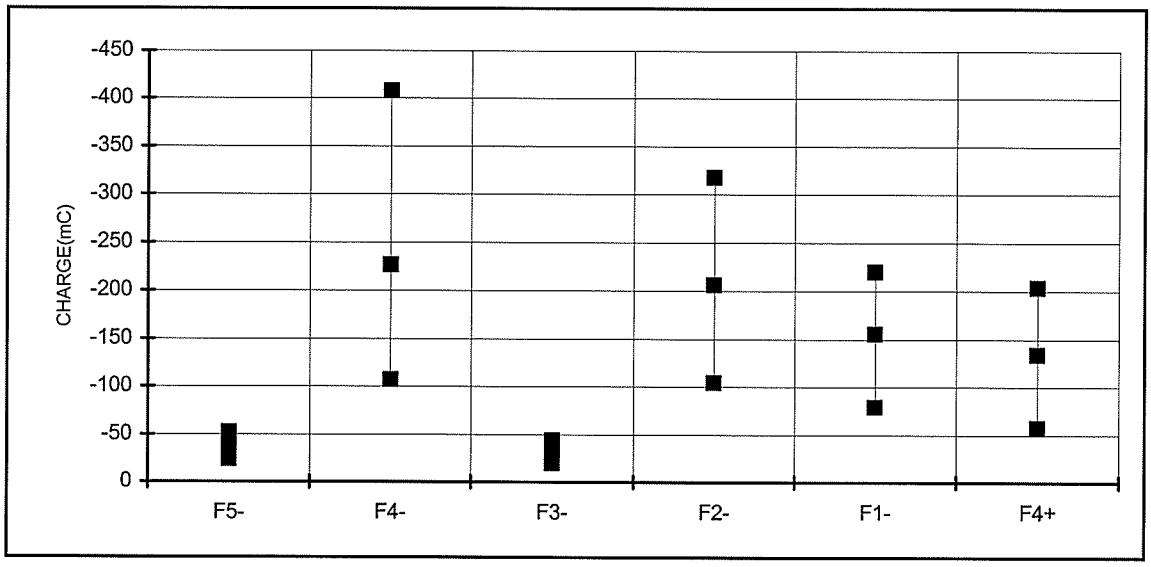

Figure 4.30 - Charge content of current pulses. SDD=0.20 mg/cm^2. String with 8 IEEE insulators.

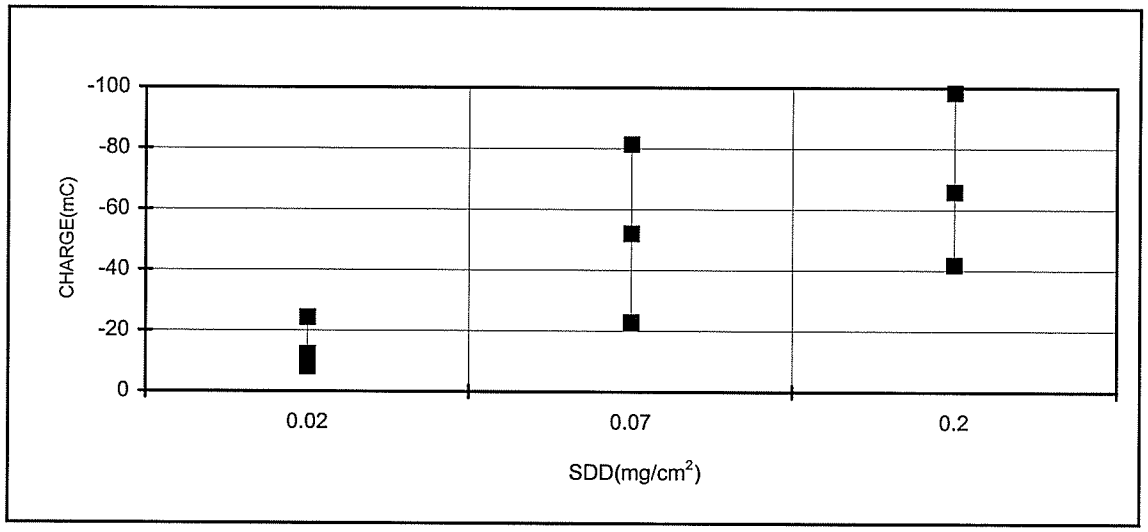

Figure 4.31 - Charge content of current pulses. Source F5. ANTIFOG insulator, string with 4 units.

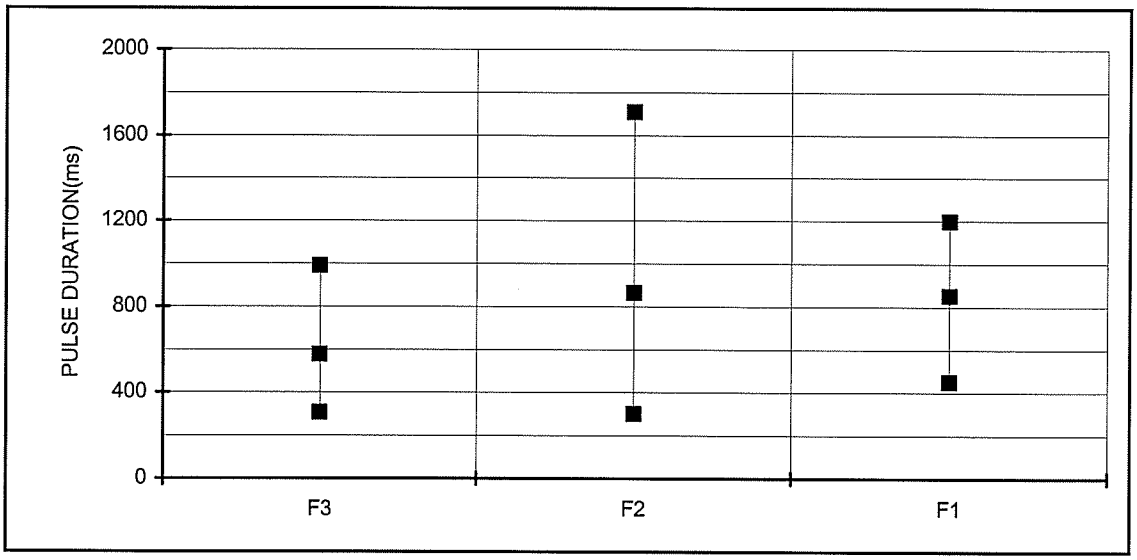

Figure 4.32 - Current pulses duration. SDD=0.07 mg/cm^2. String with 8 IEEE insulators.

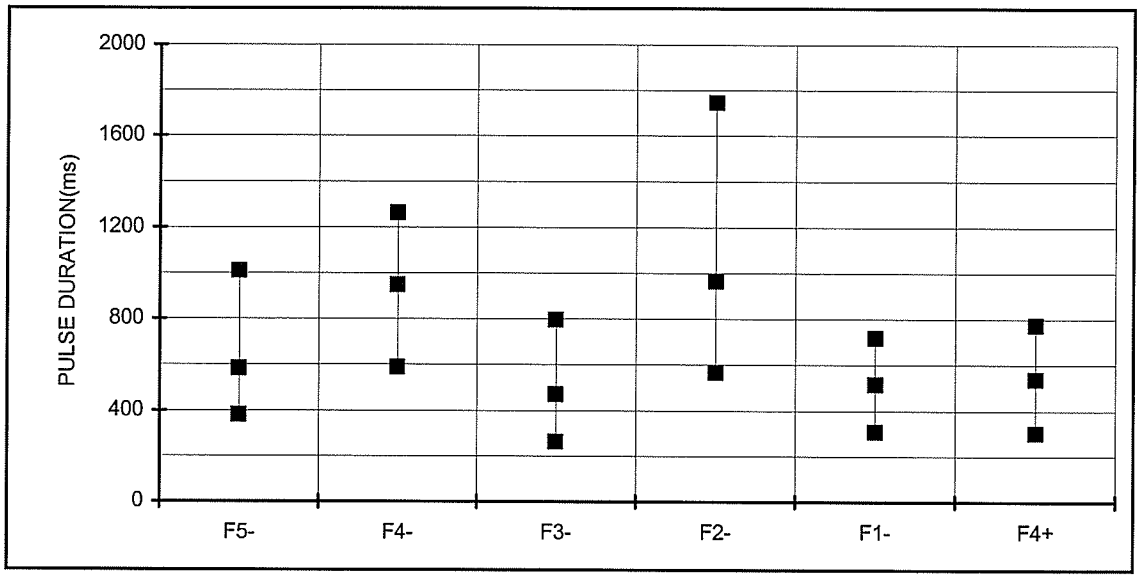

Figure 4.33 - Current pulses duration. SDD=0.20 mg/cm^2. String with 8 IEEE insulators.

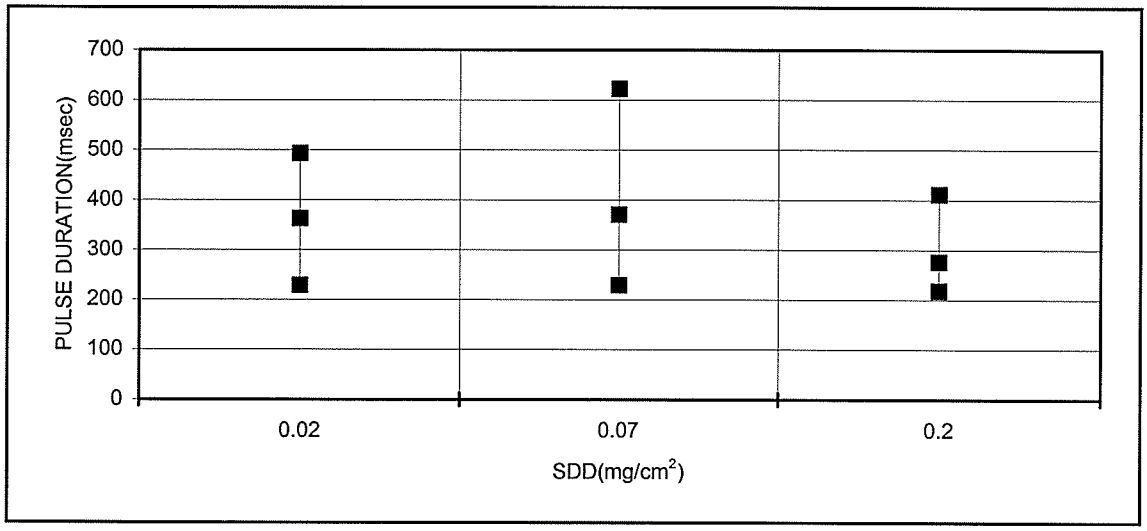

Figure 4.34 - Current pulses duration. Source F5. ANTIFOG insulator, string with 4 units.

4.3.6 - Time to peak of highest current pulses.

Figures 4.35 to 4.37 present information about the time to peak of highest current pulses. The values are in percent of the total pulse duration in order that an idea of the position of the peak related to the total pulse duration can be given.

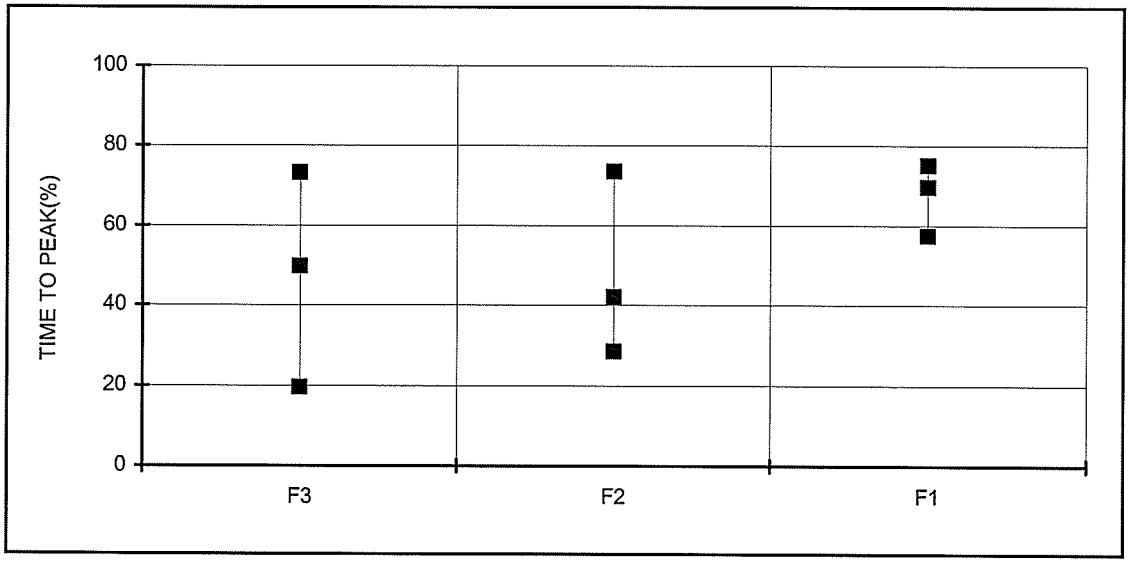

Figure 4.35 - Time to peak of highest current pulses. SDD=0.07mg/cm². IEEE insulator.

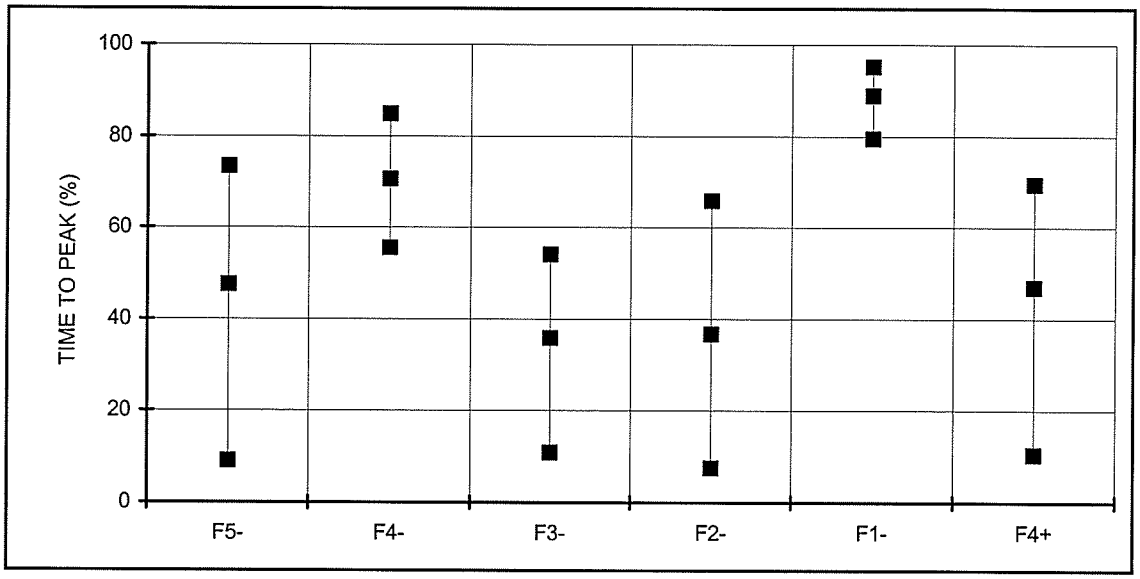

Figure 4.36 - Time to peak of highest current pulses. SDD=0.20mg/cm^2. IEEE insulator.

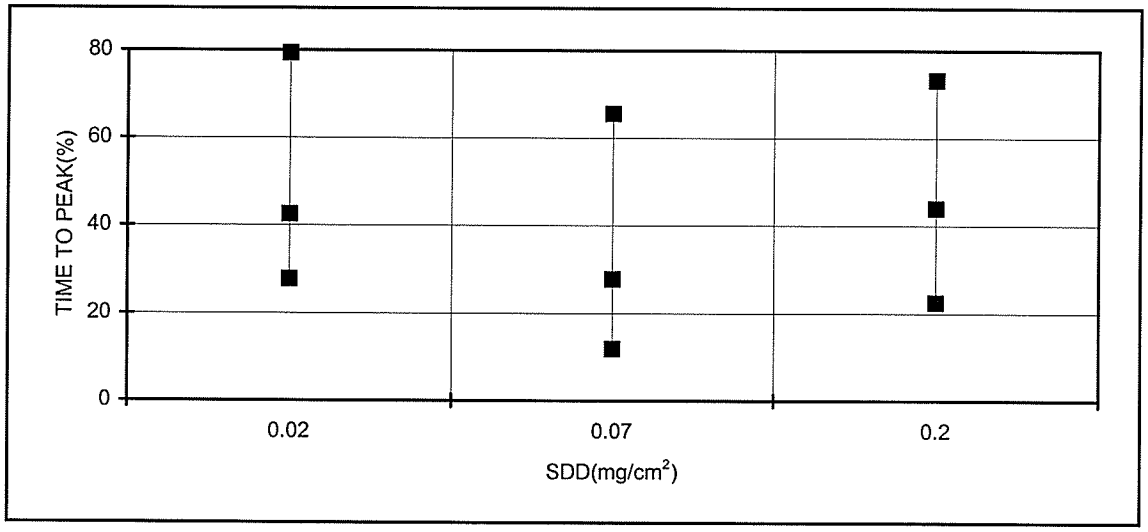

Figure 4.37 - Time to peak of highest current pulses. Source F5. ANTIFOG insulator, string with 4 units.

It can be seen from these figures that the time to peak of the highest current pulses occurs in average close to the middle of the pulse. Exception is made to pulses obtained during tests with the weak source F1.

Table 4.13 summarizes the different characteristics of the highest current pulses recorded during tests on the IEEE and ANTIFOG insulator strings for the light, medium and heavy pollution level, with the strongest test sources, F3 or F5.

Table 4.13 - Average values for highest current pulses characteristics. IEEE insulator string with 8 units, ANTIFOG insulator string with 4 units

Pulse characteristic	SDD=0.02mg/cm^2		SDD=0.07mg/cm^2		SDD=0.20mg/cm^2	
	IEEE	ANTIFOG	IEEE	ANTIFOG	IEEE	ANTIFOG
	F3	F5	F3	F5	F5	F5
Time of occurrence from fog start (min)	33.1	60.2	51.1	51.0	56.1	56.6
Peak Value (mA)	-68.3	-60.1	-141.1	-246.2	-317.1	-485.9
Energy/unit (J)	405.0	325.0	238.8	900	286.3	734
Charge/unit (mC)	-3.9	-3.1	-2.7	-13.0	-4.7	-16.5
Pulse duration (msec)	676	364	578	371	583	276
Time to peak (in % of pulse duration)	35.5	42.6	49.6	27.8	47.6	44.0

4.4 - SHAPE OF CURRENT PULSES DURING FLASHOVER

In this section some considerations are made about the wave shape and values of current pulses along the test duration.

Figures 4.38 and 4.39 show three typical current pulses and corresponding voltage evolution observed during voltage application 03, U= -66.5 kV, voltage source F3, SDD= 0.20 mg/cm^2, when testing the insulator string with 8 IEEE units.

Pulse 1 was the first one recorded, after 14 minutes of steam and voltage application.

Pulse 13, after 26 minutes of wetting, is the highest current pulse obtained before flashover. The current peak reaches -400 mA.

Pulse 21, after 35 minutes of steam, the last one recorded, is the one which led to the flashover of the insulator.

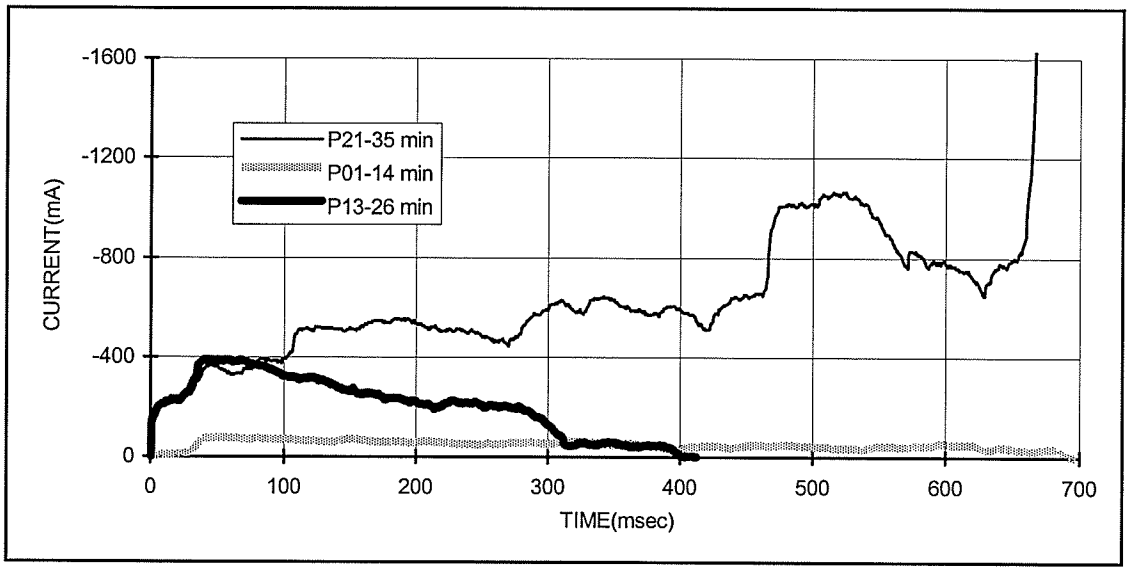

Figure 4.38 - 3 pulses during voltage application W03. SDD= 0.20 mg/cm^2, U=-66.5 kV. Source F3, at different times of wetting.

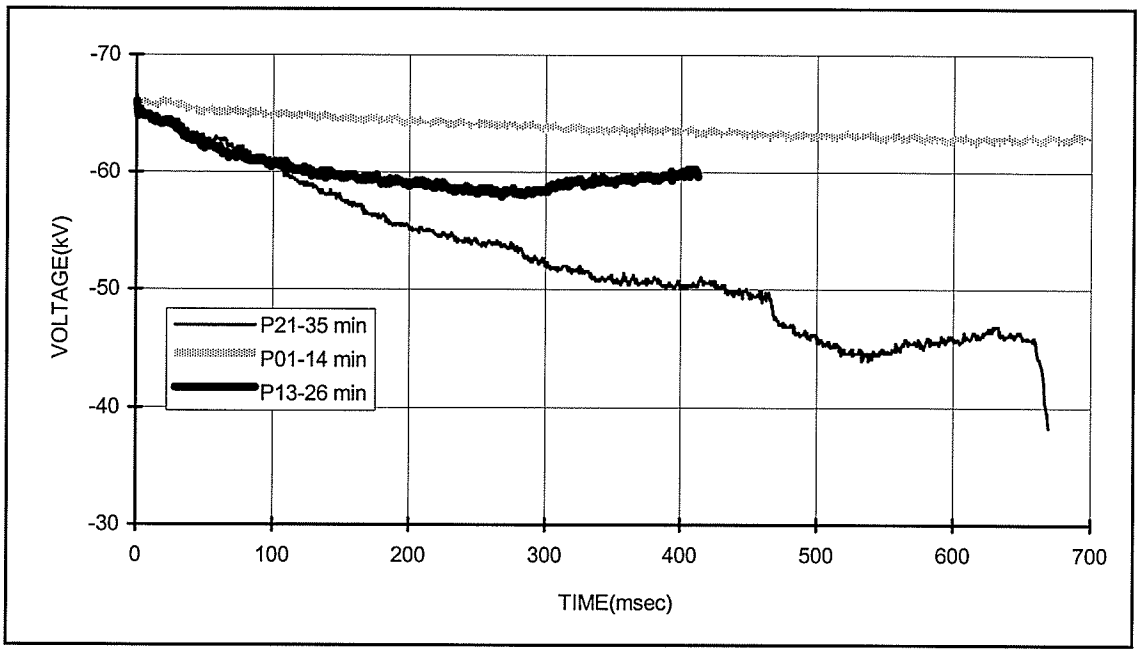

Figure 4.39 - Voltage evolution for current pulses of Figure 4.38.

These curves show the typical current pulses and corresponding voltages during a dc test which results in flashover. At the beginning of the test the current pulses are of small amplitude and longer duration. As the humidification process proceeds with consequent reduction of insulator surface resistivity the pulses increase in amplitude. A reduction in the pulse duration is also observed as shown by Pulse 13, the one with highest peak.

In general, the current increase during the arc propagation along the polluted surface is quite slow. Only at the beginning of the pulse, when the dry band is short-circuited there is a rapid current variation. Afterwards, the current increases slowly till maximum or until conditions leading to flashover are reached and the current increases then rapidly to full short circuit current. The current reduction is also slow, if the pulse does not progress to a flashover.

Pulse 21, before flashover, although initially similar to pulse 13, shows much higher current values and consequently a much higher voltage drop is presented by the corresponding voltage curve.

Before flashover a maximum peak of about -1100 mA is observed. The current then decreases to about -700 mA and afterwards increases to the short-circuit value. The voltage at this last current minimum is about -46 kV, which means an instantaneous voltage drop of 31%.

Another point to observe is that this voltage level, -66.5 kV, was applied three times during the up-and-down procedure to determine the 50% flashover voltage with source F3, SDD=0.20 mg/cm^2 and all three applications resulted in flashover.

Similar patterns were observed during tests using voltage sources F1, F2 and F3, SDD= 0.07 mg/cm^2, or using the voltage sources F2, F3, F4 and F5 , SDD=0.20 mg/cm^2. The final evolution of the arc to complete flashover, in general, does not start from those current levels defined by the highest current pulses, but rather from higher current levels as shown by Figure 4.38.

From the data recorded during tests the insulator impedance can be calculated. Figure 4.40 shows the temporal variation of insulator impedance for the three current pulses shown in Figure 4.38.

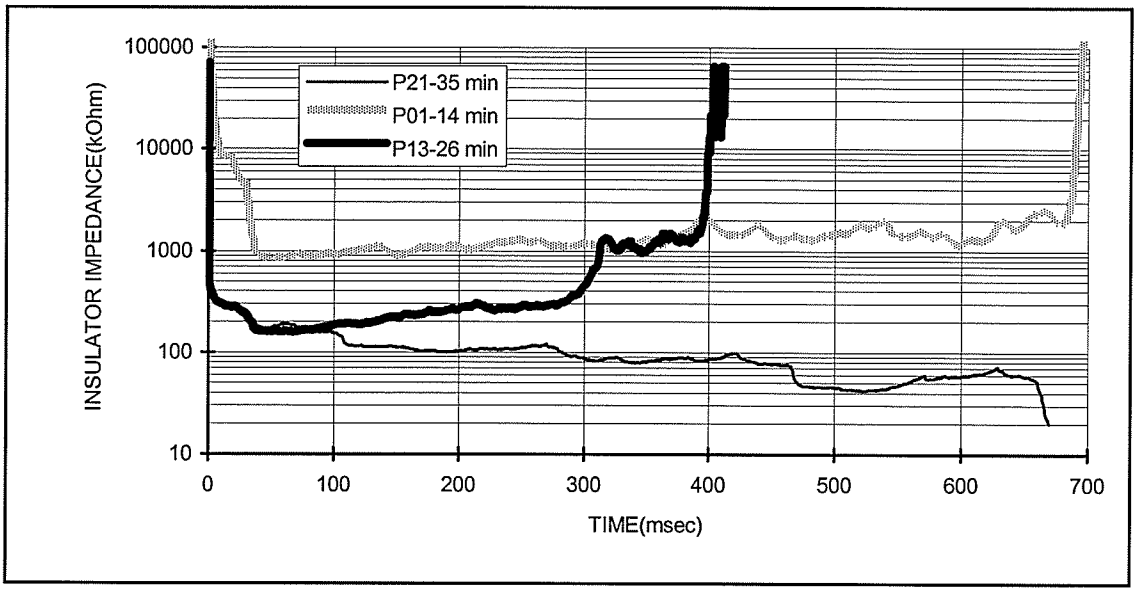

Figure 4.40 - Insulator impedance during pulses of Figure 4.37.

4.5 - SIMULATION OF INSULATOR FLASHOVER

Based on the paper " Dynamic Arc Modeling of Pollution Flashover of Insulators under dc Voltage", by R. Sundararajan and R. S. Gorur(Reference 33), a program was developed to calculate the flashover voltage of the two insulators tested.

4.5.1 Digital model

The flashover process under pollution is simulated using a dynamic model. This model takes into account the instantaneous changes in arc parameters as the arc progresses along the insulator surface. It also takes into account the actual geometry of the insulators.

The simulation starts considering that after formation of a dry band around the insulator pin an arc is formed across the dry band in series with the polluted surface.

The simulation considers that, due to the wetting process, the highest conductivity for the pollution layer is obtained.

Considering:

- **x** - the arc length, in cm;
- **i** - the current, in A;
- $\mathbf{r_{arc}}$ - arc resistance per unit length, Ω/cm;
- **LL** - insulator leakage length, cm;
- **r** - insulator external radius, variable along the insulator surface, cm;
- $\mathbf{V_s}$, $\mathbf{V_c}$ **and** $\mathbf{V_a}$ - applied voltage, cathode and anode voltage drops, V.
  $\mathbf{V_c}$ and $\mathbf{V_a}$ are constants and equal to 700V and 200V respectively;
- $\mathbf{R_p}$ - pollution layer resistance, Ω;
- $\mathbf{r_p}$ - pollution layer resistance per unit leakage path, Ω/cm;
- **N, n** - constants for the static arc characteristic in air, **N**=63 and **n**=0.5;
- σ - pollution layer conductivity, μS;
- **f** - form factor calculated for each position of arc along the insulator surface:

$$f = \int_{x}^{LL} dl/2\pi r \qquad (1)$$

- E_a - arc voltage gradient, V/cm;
- E_p - pollution layer voltage gradient, V/cm;
- τ - arc time constant, μs;
- **v** - arc velocity in cm/s, calculated from: $v = m.E_a$, being m the arc mobility in cm^2/ V.s,

The calculation starts by giving an initial value for the arc length **x**(LL/100) and for the arc resistance per unit length r_{arc}(10 to 3000. Ω/cm). For the applied voltage V_s an initial estimate for the flashover voltage is considered.

R_p is calculated from:

$$R_p = f/\sigma \qquad (2)$$

where the form factor f is calculated integrating (1) from the arc length to LL, leakage length, or from the point on the surface where the arc current is injected(x), to the insulator cap(LL).

This equation introduces the geometry of the insulator, at each time step, in the model.

For t=0, the current **i** is then calculated from:

$$i = (V_s - V_a - V_c)/(r_{arc}.x + R_p) \quad (3)$$

From the instantaneous current, E_a is computed:

$$E_a = N.i^{-n} \quad (4)$$

The critical condition of arc propagation, as stated by Hampton is $E_p > E_a$[12]. The calculation of the voltage gradient along the pollution layer, deduced for this critical condition, see section 1.3.4, Equations 11(from Alston-Zoledziowski[16]) or equation 20(from Hesketh[17]), is given by Equation 5:

$$E_p = N^{(1/n+1)}.r_p^{(n/n+1)} \quad (5)$$

E_a and E_p are then compared.

If $E_p < E_a$ the arc extinguishes. The procedure is restarted from t=0, increasing the applied voltage V_s.

If $E_p > E_a$, the arc will propagate and a procedure is implemented in order to simulate the propagation along the polluted surface. This procedure consists of comparing the arc length **x** with the insulator leakage length **LL**. If **x > LL** flashover is obtained and the applied voltage V_s is the flashover voltage. If **x < LL**, the new arc position and arc resistance per unit length is calculated using the equation for the dynamic change in arc resistance given by Equation 6:

$$dr_{arc}/dt = r_{arc}/\tau - (r_{arc}^2.i^{(n+1)})/(\tau.N) \quad (6)$$

Calculation is performed for the new r_{arc}, $r_{arc}(new) = r_{arc}(old) + dr_{arc}$, the arc velocity, $v = m.E_a$, and for the new arc position, $x(new) = x(old) + dt.v$. The time is also increased by one time step.

Now the current **i** is computed again using Equation 3, with new values for the arc length **x,** for the arc resistance per unit length $\mathbf{r_{arc}}$, for pollution layer resistance $\mathbf{R_p}$, calculated for the new arc position in Equations 1 and 2, and for the same applied voltage $\mathbf{V_s}$.

The procedure is repeated until a flashover is obtained.

A digital program, presented in Appendix II, was developed. It was used to simulated the flashover voltage for the two insulators tested.

4.5.2 Simulation results

First of all, the form factor **f** as a function of arc position was calculated for the two insulators tested. Figure 4.41 presents the form factor for the IEEE insulator and Figure 4.42 for the ANTIFOG insulator. x=0 corresponds to the insulator pin.

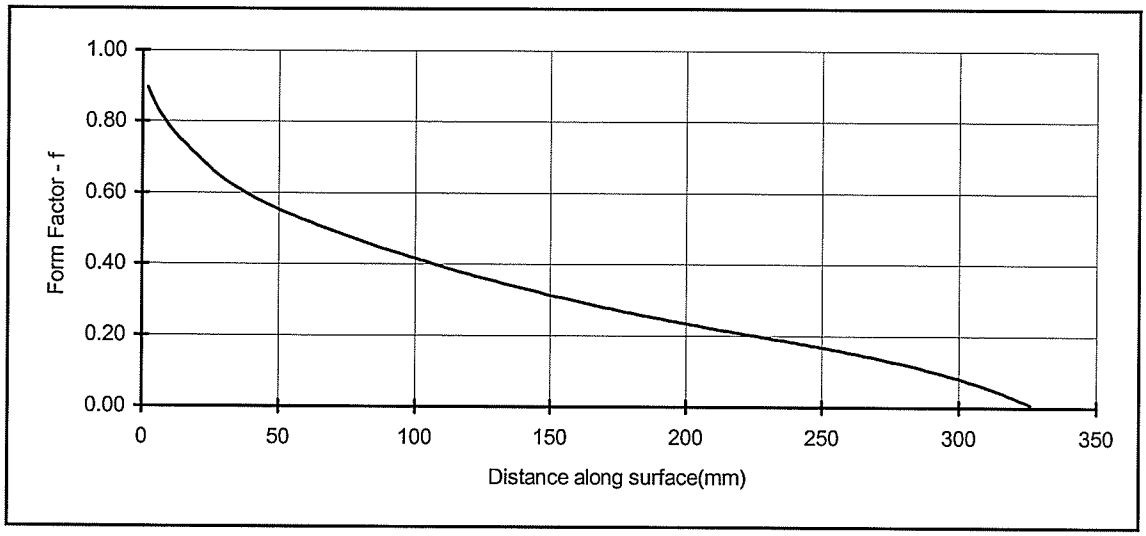

Figure 4.41 - Form factor for the IEEE insulator

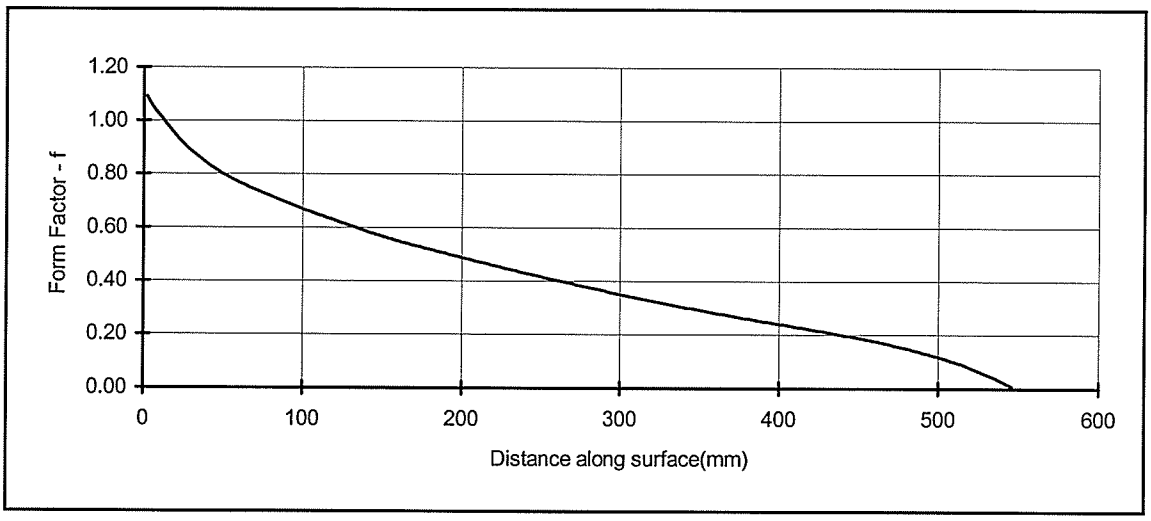

Figure 4.42 - Form factor for the ANTIFOG insulator

Figures 4.43 and 4.44 present the results of simulation for both insulators. The U_{50} values obtained experimentally and the corresponding regression lines are also plotted.

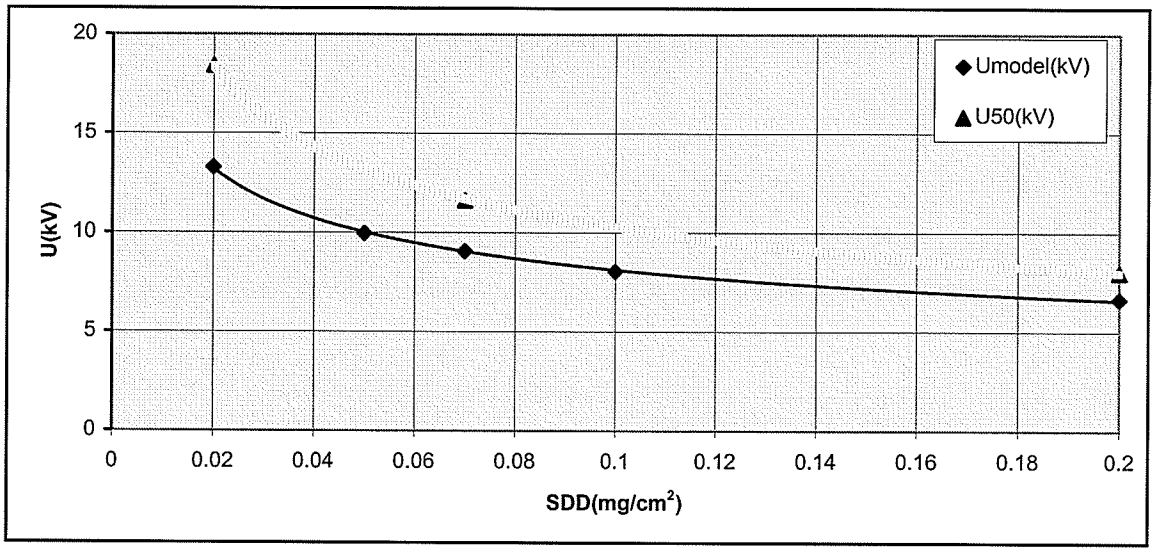

Figure 4.43 - Comparison of simulation and experimental results. IEEE insulator.

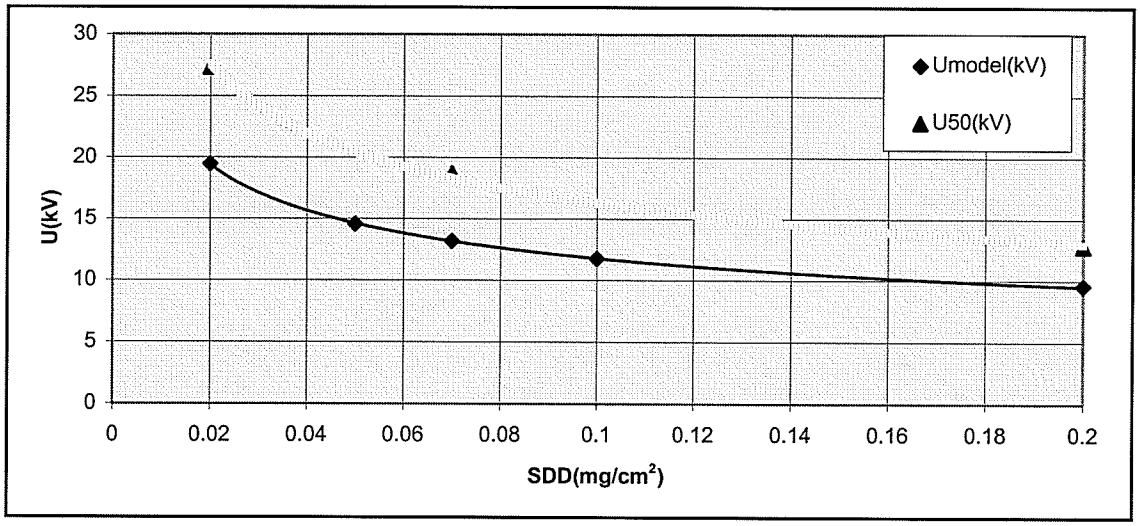

Figure 4.44 - Comparison of simulation and experimental results. ANTIFOG insulator.

The results obtained from simulation are 30% to 17% lower than the values obtained experimentally. The results are closer when higher SDD are considered. These results are reasonable as differences of up to 13% from tests are considered satisfactory[35], and prove that the model can be used to rank different types of insulators for an specific application, reducing the need of extensive testing.

An attempt was made to improve the model. Previously, other researchers[38,39], when modeling the flashover mechanism of polluted insulators under ac, instead of using the form factor to calculate the pollution layer resistance, used a resistance function, $R_p(x)$, obtained experimentally.

In fact the use of the form factor implies that the arc current is injected along all the insulator circumference at point of injection, and that no current flows along the insulator surface between the point of current injection and the pin. This is equivalent to have a dry band stretching from the pin to the current injection point.

In practice the arc is injected in a small area on the insulator surface and from that point to the insulator cap the current distributes along all the surface. Only the dry band, a small area around the pin, is not covered by the current.

If the surface conductivity is constant, the current distribution and the corresponding resistance value between the arc injection point and insulator cap is defined by the insulator geometry.

Various attempts were made to find the R(x) curve for the two insulators tested.

- 3D modelling using a digital electromagnetic program was tried with no success because two dimensions of the insulator, diameter and leakage length, are much higher than the third dimension, the thickness of the surface pollution layer.

- an attempt was made to measure the function R(x) in the fog chamber. The insulator was polluted as for the high voltage tests and wetted using steam fog. An special set up was constructed with insulating material to maintain metallic probes on different points of the surface of the insulator. The measuring probes were pressed against the insulator surface by springs. Photo 4.1 shows the set up for this measurement. The resistance between the pin or 6 points along the insulator surface to the cap were measured applying low dc voltage between the point and the cap. The current was measured, through a shunt in series with the insulator at ground side. Ten units of the IEEE insulator were measured. The results were erratic and not repetitive. Resistance values were dependent on local contamination distribution on the surface area were the probe was installed. The resistance of some points presented abrupt changes with time of exposure to the fog, due to concentration of salt around the metallic electrode.

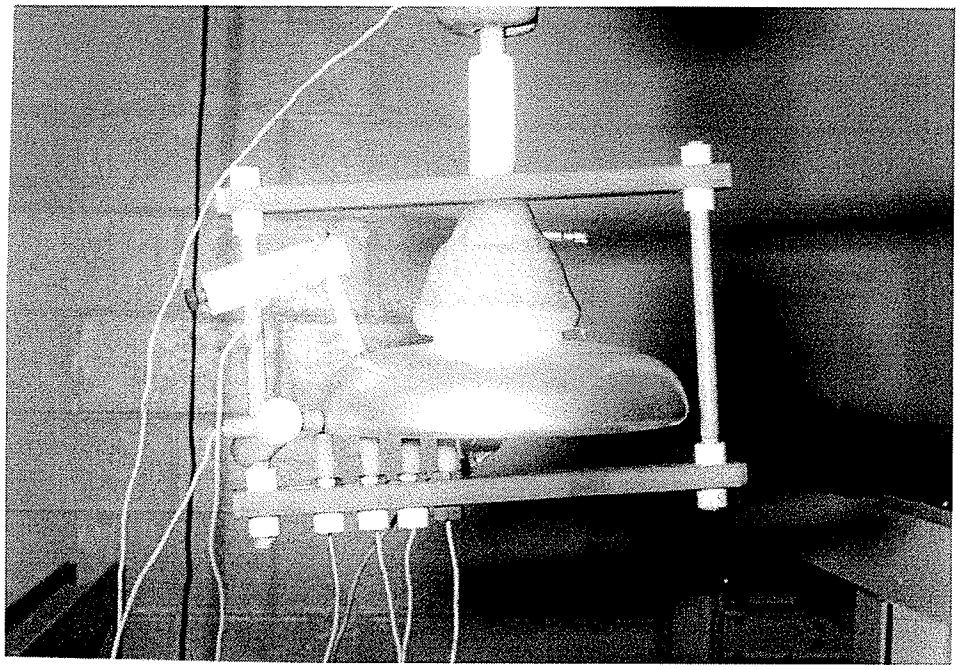

Photo 4.1 - Set up for R(x) measurement in the fog chamber

- a third attempt was made, painting the insulator surface with silver paint diluted in solvent. Before applying the silver paint 3 mm diameter and 3 mm deep holes were carefully drilled on the porcelain IEEE insulator surface. 3 mm diameter pieces of copper conductor, the measuring probes, were glued with cement in the holes. The insulator was washed with detergent and rinsed with tap water, and after a drying period, painted carefully spraying silver paint, as uniform as possible, over the surface. Afterwards, with a fine brush, silver paint was applied around the copper conductors in order to maintain a good contact between the conductor and surface. In order to verify the uniformity of the layer, three sets of 7 probes were installed along the insulator surface, each set 120° apart from the other two. The probes positions are shown numbered from 2 to 8 in Figure 4.45. Point number 1 corresponds to the pin.

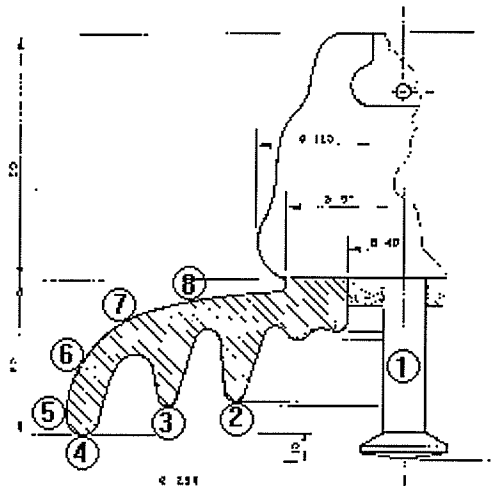

Figure 4.45 - Points for measurement of R(x). IEEE insulator.

Solvent to silver paint ratios(volume) of 8/1, 4/1 and 2/1, were tried. The most uniform condition was obtained with the 2/1 solvent/silver paint mixture.

The resistance between each point on the surface and the cap was measured by injecting in the surface a dc current of the order of 250 mA and measuring the voltage drop between the injection point and the cap. Table 4.14 show the resistance values when the 2/1 solvent/silver paint mixture was used to paint the IEEE insulator.

As seen from Table 4.14, reasonable differences are observed between the 3 points, at the same relative position over the surface, for distance x= 209 mm and x= 234 mm. This can be attributed to local differences of surface paint thickness. However, when average values are considered the maximum difference between the average value and any individual resistance value is reduced to 31%.

Table 4.14 - Measured values for resistance R(x)

Measuring point	R(x) (mΩ)			
	α=0	α=120°	α=240°	Average
1 - Pin, x=0	198	200	199	199
2, x= 80 mm	213	226	230	223
3, x= 144 mm	162	154	193	170
4, x=209 mm	138	180	236	185
5, x= 234 mm	121	173	231	175
6, x= 254 mm	131	155	171	152
7, x= 274 mm	171	165	183	173
8, x= 294 mm	107	105	115	109

The average value of the function R(x) was used to simulate the IEEE insulator. An equivalent form factor f was determined from measured function R(x).

Figure 4.46 presents the two form factors, based on equation 1 and based on the measured values of Table 4.14.

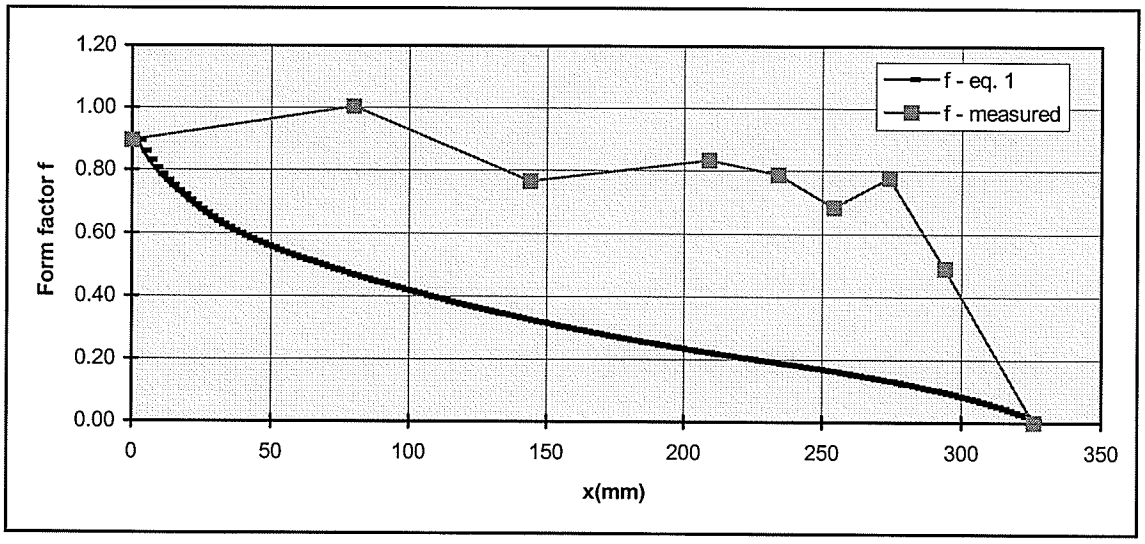

Figure 4.46 - Comparison of form factors. IEEE insulator.

Using the digital program the IEEE insulator was simulated to determine the flashover voltage. The results of the flashover voltage calculated for different pollution levels are shown in Figure 4.47 together with the U_{50} values obtained experimentally.

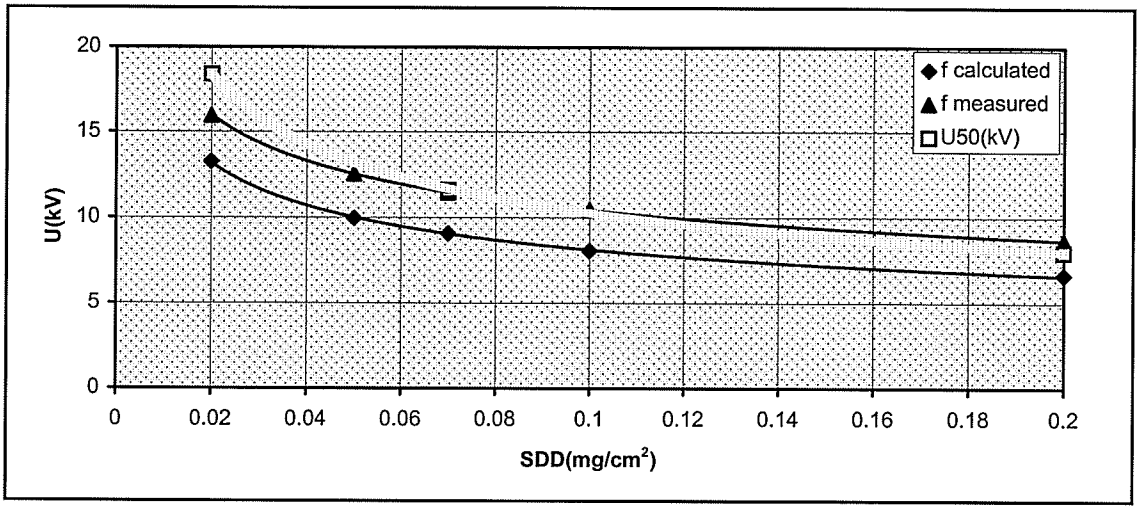

*Figure 4.47 - Simulation of IEEE insulator, using as form factor **f:** values calculated from Equation 1 and measured on the painted insulator. Experimental U_{50} values are also plotted.*

As seen from Figure 4.47, the simulated results using the form factor values obtained from measured resistance values over the insulator surface are much closer to the U_{50} values obtained from tests. The maximum difference obtained was -13.3% for the light pollution level. These results encourage the research for an easier experimental or analytical method to determine R(x) for the various insulators designs used in HVDC transmission.

CHAPTER 5

CONCLUSIONS

Extensive laboratory flashover tests of on high voltage dc polluted insulators have been performed.

The conclusions in this study are derived from the analysis of the extensive experimental data obtained during the described tests and also some simulations performed using mathematical modeling of the flashover process under pollution.

The main conclusions are:

1 - The use of an analog to digital data acquisition system during tests has made it possible to gather a considerable amount of fundamental information on the development of the flashover process under dc voltages.

2 - New information about the current pulses characteristics during arc activity has been obtained. Also the effect of the voltage source on the characteristics of highest current pulses has been studied.

All these information obtained provides a better understanding of the flashover process of dc insulators under pollution and can be used to verify and improve existing theoretical models.

3 - The results obtained strongly suggest that the present restrictions on voltage drops imposed on the tests sources can probably be relaxed. Although the present requirements exclude sources which influence the test results, they exclude also sources which determine flashover

voltages with negligible error when compared to results obtained with powerful sources. Tests carried out with different voltage sources that yielded different voltage drops characteristics gave approximately the same U_{50} values.

4 - The present definition for the calculation of maximum and average voltage drops, parameters which are used to define the voltage source requirements such that it will not influence test results, was found to be not of general application. Voltage sources with high output capacitance, in general, gave maximum voltage drops which did not occur simultaneously with the current maximum, as is the case for voltage sources with low output capacitance.

5 - The average and maximum voltage drops shall be calculated not for the entire duration of the critical current pulse, but from the instant of pulse start to the instant of current maximum.

6 - An analysis of the time of occurrence of highest current pulses show that some of these pulses can occur more than one hour from the start of wetting. A duration of 100 minutes is suggested for the voltage applications, if the current pulses are not monitored during tests.

7 - The results obtained can contribute to the normalization of procedures for artificial pollution tests on HVDC insulators.

8 - For both types of insulators tested, an equation of the form $U_{50}= A.SDD^{K}$ relating U_{50} to SDD(Salt deposit density) was calculated from the experimental data. Exponent K was determined to be -0.36 for the IEEE insulator and -0.33 for the ANTIFOG insulator. These values are in accordance with solid layer tests on HVDC post insulators reported in the literature, where an average value of -0.36 was determined for the exponent K. For a given insulator design, if K is known for the solid layer test procedure under dc, and a value of U_{50} is determined experimentally for a certain pollution level, U_{50} can be estimated for any other pollution severity. The values of A were -4.46 and -7.64 for the IEEE and ANTIFOG insulators, respectively.

9 - A relation between U_w/LL(critical voltage gradient) and the critical current pulse I_H amplitude was determined from results for both insulators tested. If this relation can be generalized for other insulators designs, and for natural polluted insulators, it can be used as control characteristic for diagnosis of polluted insulators in service.

10 - A model proposed in the literature was used to estimate the flashover voltage for both insulators tested with reasonable results. However, for one insulator tested, the model was improved when a measured R(x) characteristic was used to calculate the pollution layer resistance for each arc position along the surface. This result encourages the research for an easier experimental or analytical method to determine R(x) for the various insulator designs used in HVDC transmission. The measured R(x) characteristic represents the current distribution between the point of current injection and the insulator cap.

REFERENCES

1 - S. S. Low, G. R. Elder, "Experience dictates future HVDC insulator requirements", IEEE Trans. on Electrical Insulation, Vol. EI - 16, No. 3, June 1981, Pages 263-266.

2 - W. Lampe, K. A. Eriksson, C. A. O. Peixoto, "Operating experience of HVDC stations with regard to natural pollution", CIGRE 1984, Paper 33-01.

3 - H. M. Schneider, J. F. Hall, C. L. Nellis, S. S. Low, D. J. Lorden, "Rain and contamination tests on HVDC bushings", IEEE Transactions on Power Delivery, Vol. 6, No. 3, July 1991, Pages 1289,1300.

4 - T. C. Cheng, C. T. Wu, J. N. Rippey, F. M. Zedan, "Pollution performance of DC insulators under operating conditions", IEEE Trans. on Electrical Insulation, Vol. EI - 16, No. 3, June 1981, Pages 154-164.

5 - H. M. Schneider, "Measurements of contamination on post insulators in HVDC converter stations", IEEE Trans. on Power Delivery, Vol. 3, No. 1, January 1988, Pages 398-404.

6 - T. Kawamura, T. Seta, K. Nagai, K. Naito, "DC pollution performance of insulators", CIGRE 1984, Paper 33-10.

7 - K. Takasu, T. Shindo, N. Arai, "Natural contamination test of insulators with DC voltage energization at inland areas", IEEE Transactions on Power Delivery, Vol. 3, No. 4, October 1988, Pages 1847-1853.

8 - W. Lampe, T. Hoglund, C. Nellis, P. Renner, R. Stearns, "Long-term tests on HVDC insulators under natural pollution conditions at Big Eddy Test Center, IEEE Trans. on Power Delivery, Vol. 4, No. 1, January 1989.

9 - EPRI HVAC Transmission Line Reference Book.

10 - K. Chrzan, Z. Pohl, T.Kawalak, "Hygroscopic properties of pollutants on HV insulators", IEEE Trans. on Electrical Insulation, Vol. EI - 24, No. 1, February 1989, Pages 107-112.

11 - G. Karady, "The effect of fog chamber parameters on the testing of artificially contamined insulators in a fog chamber", IEEE Trans. on Power apparatus and Systems, Vol. 94, No. 2, March-April 1975, Pages 378-387.

12 - B. F. Hampton, "Flashover Mechanism of polluted insulation", Proc. IEE, Vol. 111, No. 5, May 1964, Pages 985-990.

13 - M. R. Raghuveer, E. Kuffel, "Experimental and analytical studies of factors which affect flashover voltage on polluted insulators surfaces", IEEE Trans. on Power Apparatus and Systems, Vol.74, Jan-Feb 1974, Pages 312-320.

14 - F. A. M. Risk, "Mathematical models for pollution flashover", Elektra, Vol.78, Pages 71-103, 1981.

15 - Report prepared by the IEEE Group on Insulator Contamination, Lightning and Insulator Subcommittee, "Application of insulators in a contamined environment", IEEE Trans. on Power Apparatus and Systems, Vol.98, No. 5, Sept-Octb 1979, Pages 1676-1695.

16 - L. L. Alston, S. Zoledziowski, "Growth of discharges on pollutes insulation", Proc. IEE, Vol. 110, No. 7, July 1963, Pages 1260-1266.

17 - S. Hesketh, "General criterion for the prediction of pollution insulation"' Proc. IEE, Vol. 114, No. 4, April 1967, Pages 531-532.

18 - R. Wilkins, A. A. J. Al-Baghdadi, "Arc propagation along an electrolyte surface", Proc. IEE, Vol. 118, No. 12, December 1971, Pages 1886-1892.

19 - R. Wilkins, "Flashover voltage of high voltage insulators with uniform surface pollution films", Proc. IEE, Vol. 116, No. 3, March 1969, Pages 457-465.

20 - F. A. M. Rizk, "Application of dimensional analysis to flashover characteristics of polluted insulators", Proc. IEE, Vol. 117, No. 12, December 1970, Pages 2257-2260.

21 - F. A. M. Rizk, "HVDC source requirements in polluted insulator test", Elektra, Vol.136, June 1991, Pages 97-111.

22 - F. A. Chagas, J. G. C. Barros, J. A. M. Duque, R. M. Maia, "Design of a +/- 1000 kV testing equipment for tests on polluted external insulation", 5 th. ISH, Braunschweig, 1987, Paper 62.07.

23 - W. Mosca, P. Murgia, R. Nicolini, A. Spinelli, "HVDC 700 kV generator for pollution testing", 6 th. ISH, New Orleans, 1989, Paper 47.34.

24 - Y. Hasegawa, K. Naito, K. Arakawa, H. M. Schneider, L. E. Zaffanella, "A comparative program on HVDC contamination tests", IEEE Trans. on Power Delivery, Vol. 3, No. 4, October 1988, Pages 1986-1995.

25 - T. Seta, K. Nagai, K. Naito, Y. Hasegawa, "Studies on the performance of contamined insulators energized with DC voltage", IEEE Trans. on Power Apparatus and Systems, Vol. 100, No. 2, February 1981, Pages 518-527.

26 - L. Pargamin, J. Huc, S. Tartier, "Considerations on the choice of insulators for HVDC overhead lines", CIGRE 1984, Paper 33-11.

27 - K. Naito, CIGRE 1984, Special Report to Group 33-03, Contribution to Question #2, Pages 53-54.

28 - K. Naito, R. Matsuoka, S. Ito, S. Morikawa, "An investigation of the horizontally mounted insulator for HVDC Station", IEEE Trans. on Power Delivery, Vol. 4, No. 1, January 1989, Pages 653-662.

29 - Task Force 04.04 of Study Committee 33, "Artificial pollution testing of HVDC insulators: analysis of factors influencing performance", Elektra, Vol. 140, February 1992, Pages 99-113.

30 - W. Koehler, K. Feser, "Test source for HVDC pollution tests", 5 th. ISH, Braunschweig, 1987, Paper 62.08.

31 - S. D. Merkhalev, L. L. Vladimirsky, "Requirements and design of rectifiers for HVDC Pollution tests", 5 th. ISH, Braunschweig, 1987, Paper 63.18.

32 - H. M. Schneider, "Specifications for a comparative evaluation of the clean fog test for HVDC insulators", CIGRE 34-90(WG-04).

33 - R. Sundararajan, R. S. Gorur, "Dynamic arc modeling of pollution flashover of insulators under DC voltage", IEEE Trans. on Electrical Insulation, Vol. 28, No.2, April 1993.

34 - R. Sundararajan, R. S. Gorur, "Effect of insulators profiles on dc flashover voltage under polluted conditions - A study using dynamic arc model", IEEE Trans. on Electrical Insulation, Vol. 1, No. 1, February 1994.

35 - K. Naito, H. M. Schneider, "Round robin artificial contamination test on high voltage dc insulators", IEEE Trans. on Power Delivery, Vol.10, No.3, July 1995.

36 - A. C. Baker, L. E. Zaffanella, L. D. Anzivino, H. M. Schneider, J. H. Moran, "Contamination performance of HVDC station post insulators", IEEE Trans. on Power Delivery, Vol. 3, No. 4, October, 1988.

37 - IEC Technical Report 1245, "Artificial pollution tests on high-voltage insulators to be used on dc systems", first edition, 1993-10.

38 - P. Claverie, "Predetermination of the behavior of polluted insulators", IEEE Trans. on Power Apparatus and systems, Vol. 90, No. 4, July-August, 1971.

39 - P. Claverie, Y. Porcheron, " How to choose insulators for polluted areas", IEEE/PES Summer Meeting, San Francisco, CA, July 9-14, 1972.

40 - F. A. Chagas, E. Kuffel, "Experimental verification of HVDC test source requirements for pollution tests", IEEE /PES 1994 Summer Meeting, San Francisco, CA, July 24-28, 1994.

APPENDIX I

CURRENT PULSES AND VOLTAGE ANALYSIS

```
CLS
REM CURRENT & VOLTAGE ANALYSIS
REM
PRINT "**********        ANALYSIS OF PULSES DATA        **********"
PRINT
REM INPUT DATA ABOUT VOLTAGE APPLICATION
REM
REM ESDD
PRINT"INFORM ESDD(mg/cm^2)"
INPUT ESD$
PRINT"INFORM APPLIED VOLTAGE(kV or V)"
INPUT APV
IF ABS(APV)>1000 THEN AV=APV/1000 ELSE AV=APV
F$="#####.###":IZ=1
PRINT"VOLTAGE APPLICATION Nr":INPUT AA$
PRINT"TIME OF INITIATION OF STEAM IN TEST CHAMBER : HH/MM/SS"
INPUT H$
XHI=VAL(MID$(H$,1,2)):XMI=VAL(MID$(H$,4,2)):XSI=VAL(MID$(H$,7,2))
XMI=XMI+4:XHI=XHI+1
IF XMI>=60 THEN XMI=XMI-60:XHI=XHI+1
H$=STR$(XHI)+":"+STR$(XMI)+":"+STR$(XSI)
PRINT"TYPE OF SOURCE: 1 = 1 PHASE,  C=.11 microF"
PRINT"                2 = 2 PHASES, C=.44 microF"
PRINT"                3 = 2 PHASES, C= 8  microF"
TY$(1)="1p,110nF":TY$(2)="2p,440nF":TY$(3)="2p,8000nF"
PRINT"TYPE=":INPUT ITY:IF ITY=1 THEN NP=16 ELSE NP=8
PRINT"NUMBER OF FIRST AND LAST FILES TO BE ANALYSED"
INPUT NF0,NF1
```

```
      PRINT"WANT TO STORE FILES  FOR CUR & VOLT PLOTING?
      1=YES  : 2=NO"
      INPUT KY
      PRINT"WANT TO GENERATE FILES FOR EXCEL ANALYSIS?
      1=YES  : 2=NO"
      INPUT MC
      IF MC<>1 THEN 5
      DIM Z9$(228),Z10(228),Z11(228),Z12(228),Z13(228),Z14(228),Z15(228)
      DIM Z16(228),Z17(228),Z18(228),Z19(228),Z20(228),Z21(228),Z22(228)
      DIM,Z23(228),Z24(228),Z25(228),Z26(228)
5     FOR I1=NF0 TO NF1 STEP 2
      IF I1<=9 THEN A1$=RIGHT$(STR$(I1),1):B1$=RIGHT$(STR$(I1+1),1):GOTO 10
      IF I1<=99 THEN A1$=RIGHT$(STR$(I1),2):B1$=RIGHT$(STR$(I1+1),2):GOTO 10
      A1$=RIGHT$(STR$(I1),3):B1$=RIGHT$(STR$(I1+1),3)
10    A$="WFM"+A1$+".AD0"
      B$="WFM"+B1$+".AD0"
      Y$="W"+AA$+"-"+A1$+","+B1$
      PRINT A$:PRINT B$
      OPEN "I",1,A$:OPEN "I",2,B$
      FOR I2=1 TO 23
      INPUT#1,C$:INPUT#2,D$
      IF I2<>7 THEN GOTO 50
      DAT$=MID$(C$,22,8):XHO=VAL(MID$(C$,31,2))
      XMN=VAL(MID$(C$,34,2)):SEC=VAL(MID$(C$,37,2))
      PULT$=MID$(C$,31,8):GOTO 100
50    IF I2<>8 THEN GOTO 60
      DELT=VAL(MID$(C$,49,12)):PRINT "DELT=";DELT:GOTO 100
60    IF I2<>10 THEN GOTO 100
```

```
      NPOI=VAL(MID$(C$,8,4)):PRINT "NPOI=";NPOI
100   NEXT I2
110   PRINT "DATA=";DAT$,"PULSE TIME= ";PULT$
      PRINT "XHO=";XHO," XMN=";XMN," SEC=";SEC
      REM
      REM PRINTING GENERAL INFORMATION
      REM
      IF I1>NF0+1 THEN 120
      DIM CUR(NPOI),VOL(NPOI),CNEW(NPOI),VNEW(NPOI)
      PRINT"TEST DATE        =";:PRINT DAT$
      PRINT"ESDD             =";:PRINT ESD$+" mg/cm^2"
      PRINT"VOLT APPLIC Nr   =";:PRINT AA$
      PRINT"APPLIED VOLTAGE  =";:PRINT USING F$;AV;:PRINT" kV"
      PRINT"TYPE OF SOURCE   ="+TY$(ITY)
      PRINT"TIME OF STEAM INIT =";:PRINT H$
120   PRINT
      PRINT"FILES            ="+A$+" , "+B$
      PRINT"PULSE TIME       =";:PRINT PULT$
      PRINT"DELTA T          =";:PRINT USING F$;DELT*1E6;:PRINT" microsec"
      PRINT"Nr OF DATA POINTS  =";:PRINT USING F$;NPOI
      PRINT
      REM CALCULATION OF TIME OF PULSE OCCURENCE FROM STEAM
      REM INITIATION(SECONDS)
      TPUL=(XHO-XHI)*3600+(XMN-XMI)*60+(SEC-XSI)
      REM READING OF DATA OF CURRENT AND VOLTAGE PULSES
      REM CALCULATION OF MIN & MAX VALUES
      CMAX=-100000:VMIN=100000
      FOR I3=1 TO NPOI
```

```
      INPUT#1,CUR(I3),X:INPUT#2,V,X:IF ABS(APV)>1000 THEN VOL(I3)=V*.001 ELSE
      VOL(I3)=V
      IF CUR(I3)>CMAX THEN CMAX=CUR(I3):IIMAX=I3
      IF VOL(I3)<VMIN THEN VMIN=VOL(I3):IVMIN=I3
      NEXT I3
      CLOSE 1:CLOSE 2
      PRINT"VMIN =";VMIN;" TVMIN=";IVMIN*DELT
      PRINT "CMAX =";CMAX;" TCMAX=";IIMAX*DELT
      REM HISTOGRAM TO FIND ZERO CURRENT AND APPLIED VOLTAGE LEVEL
      DIM HC(10),HV(10),V1(10),V2(10),C1(10),C2(10)
      DV=.0025*VMIN:V1(1)=VMIN:V2(1)=VMIN-DV
      FOR J=1 TO 10:HC(J)=0:HV(J)=0:NEXT J
      IF CMAX>0 THEN DC=.2*CMAX ELSE DC=-.01*CMAX
      C1(1)=CMAX:C2(1)=CMAX-DC
      FOR I=2 TO 10
      V1(I)=V1(I-1)-DV:V2(I)=V2(I-1)-DV
      C1(I)=C1(I-1)-DC:C2(I)=C2(I-1)-DC
      NEXT I
      REM FOR I=1 TO 10:PRINT V1(I),V2(I),C1(I),C2(I):NEXT I
      REM PRINT CMAX,VMIN
      FOR I=1 TO NPOI
      IF CUR(I)<C2(10) THEN 150
      FOR K=1 TO 10
      IF CUR(I)>C1(K) OR CUR(I)<C2(K) THEN 140 ELSE HC(K)=HC(K)+1
140   NEXT K
150   IF VOL(I)>V2(10) THEN 170
      FOR K=1 TO 10
      IF VOL(I)<V1(K) OR VOL(I)>V2(K) THEN 160 ELSE HV(K)=HV(K)+1
```

```
160     NEXT K
170     NEXT I
        REM FOR I=1 TO 10:PRINT HC(I),C1(I),C2(I):NEXT I
        REM FOR I=1 TO 10:PRINT HV(I),V1(I),V2(I):NEXT I
        REM HISTOGRAM MEANS
        C50=0:V50=0:HCS=0:HVS=0
        FOR I=1 TO 10
        C50=C50+C1(I)*HC(I):V50=V50+(V1(I)+V2(I))*.5*HV(I)
        HCS=HCS+HC(I):HVS=HVS+HV(I)
        NEXT I
        C50=C50/HCS:V50=V50/HVS
        PRINT "C50=",C50," V50=",V50
        REM ADJUSTING CURRENT POINTS
        FOR I=1 TO NPOI:CUR(I)=CUR(I)-C50:NEXT I
        REM CALCULATION OF CURVES WITHOUT RIPPLE
        FOR I4=1 TO NPOI
        VNEW(I4)=0:CNEW(I4)=0
        FOR I5=I4-NP TO I4+NP
        IF I5<=0 OR I5>NPOI THEN CAUX=0:VAUX=AV ELSE
        CAUX=CUR(I5):VAUX=VOL(I5)
        CNEW(I4)=CNEW(I4)+CAUX/(2*NP+1):VNEW(I4)=VNEW(I4)+VAUX/(2*NP+1)
        NEXT I5
        NEXT I4
        REM RECORDING OF VOLTAGE AND CURRENT CURVES
        IF KY<>1 THEN GOTO 200
        O1$="CO"+A1$+".DAT":O2$="CN"+A1$+".DAT":O3$="VO"+A1$+".DAT"
        O4$="VN"+A1$+".DAT"
        OPEN "O",1,O1$:OPEN "O",2,O2$:OPEN "O",3,O3$:OPEN "O",4,O4$
```

```
        FOR I=1 TO NPOI
        WRITE#1,CUR(I):WRITE#2,CNEW(I):WRITE#3,VOL(I):WRITE#4,VNEW(I):NEXT I
        CLOSE
200     REM FINDING NUMBER OF CURRENT PULSES IN THE FILE WITH
        AMPLITUDE> 50 mA
        IK=1:KC(IK)=1
220     FOR I=KC(IK) TO NPOI
        IF CUR(I)>-200 THEN GOTO 250
        FOR K=I TO KC(IK) STEP -1
        IF CUR(K)>=0 THEN KC(IK)=K:IK=IK+1:GOTO 260
        IF K=1 THEN KC(IK)=K:IK=IK+1:GOTO 260
        NEXT K
250     NEXT I
        GOTO 270
260     FOR K=I TO NPOI
        IF CUR(K)>=0 THEN KC(IK)=K:IK=IK+1:KC(IK)=KC(IK-1):GOTO 220
        NEXT K
270     IF KC(IK)=0 THEN NPUL=(IK-2)/2 ELSE NPUL=(IK-1)/2
        PRINT "NUMBER OF PULSES=";NPUL
        REM CALCULATION OF PARAMETERS FOR ALL PULSES
        IF NPUL=0 THEN 900
        FOR I=1 TO NPUL
        I5=(I*2-1):I6=I*2:T1=KC(I5)*DELT:T2=KC(I6)*DELT:QC=0:SV=0:SJ=0
        CMI=1000:VMA=-1000:CMIN=100000:VMAX=-100000:ZMIN=1E12:ZMIA=1E12
        REM CALCULATION OF PULSE DURATION(s)
        TAL=T2-T1:TPI=TPUL+T1
        REM CALCULATION OF PULSE CHARGE AND AVERAGE VOLTAGE DROP
        REM CALCULATION OF MAXIMUM VOLTAGE DROP AND RIPPLE
```

```
        REM CALCULATIOM OF MAXIMUM CURRENT AND RIPPLE
        FOR K=KC(I5) TO KC(I6)-1
        QC=QC+.5*(CUR(K)+CUR(K+1))*DELT:SV=SV+.5*(VOL(K)+VOL(K+1))*DELT
        IF CMI>CNEW(K) THEN CMI=CNEW(K):TCMI=K*DELT
        IF CUR(K)<CMIN THEN CMIN=CUR(K):TCMIN=K*DELT
        IF VMA<VNEW(K) THEN VMA=VNEW(K):TVMA=K*DELT
        IF VOL(K)>VMAX THEN VMAX=VOL(K):TVMAX=K*DELT
        SJ=SJ+.5*(CUR(K)*VOL(K)+CUR(K+1)*VOL(K+1))*DELT
        IF CUR(K)>=0 GOTO 300
        ZAUX1=VOL(K)/CUR(K):IF ZAUX1<ZMIN THEN ZMIN=ZAUX1:TZMIN=K*DELT
300     IF CNEW(K)>=0 GOTO 400
        ZAUX2=VNEW(K)/CNEW(K):IF ZAUX2<ZMIA THEN ZMIA=ZAUX2:TZMIA=K*DELT
400     NEXT K
        VAV=SV/TAL:DELVA=(VAV-V50)/V50:DVMAX=(VMA-V50)/V50
        RIPV=2*(VMAX-VMA)/VMA:RIPC=2*(CMIN-CMI)/CMI
        PRINT"PULSE NUMBER=";I
        PRINT "APPLIED VOLTAGE(kV) =",:PRINT USING F$;V50
        PRINT"PULSE CHARGE(mC)   =",:PRINT USING F$;QC
        PRINT "PULSE START(s)     =",:PRINT USING F$;TPI
        PRINT "PULSE DURATION(ms)  =",:PRINT USING F$;TAL*1E3
        PRINT "AVER VOLT DROP(%)   =",:PRINT USING F$;ABS(DELVA*100)
        PRINT"RIPPLE pp(%)       =",:PRINT USING F$;ABS(100*RIPV)
        PRINT "MAX CURRENT(mA)     =",:PRINT USING F$;CMIN
        PRINT"TIME OF OCCUR(ms)   =",:PRINT USING F$;(TCMIN-T1)*1000
        PRINT "TIME OF OCCUR(%)    =",:PRINT USING F$;100*(TCMIN-T1)/TAL
        PRINT "SMOOTH CUR MAX(mA)  =",:PRINT USING F$;CMI
        PRINT "TIME OF OCCUR(ms)   =",:PRINT USING F$;(TCMI-T1)*1000
        PRINT "TIME OF OCCUR(%)    =",:PRINT USING F$;100*(TCMI-T1)/TAL
```

```
        PRINT "MAX VOL DROP(%)    =",:PRINT USING F$;ABS(DVMAX*100)
        PRINT"TIME OF OCCUR(ms)   =",:PRINT USING F$;(TVMA-T1)*1000
        PRINT "ZMIN(kohm)         =",:PRINT USING F$;ZMIN*1E3
        PRINT "TIME OF OCCUR(ms)  =",:PRINT USING F$;(TZMIN-T1)*1000
        PRINT "ZMIN SMOOT V/I(kohm)=",:PRINT USING F$;ZMIA*1E3
        PRINT "TIME OF OCCUR(ms)  =",:PRINT USING F$;(TZMIA-T1)*1000
        PRINT "PULSE ENERGY(J)    =",:PRINT USING F$;SJ
        PRINT "AVERAGE CURRENT(mA) =",:PRINT USING F$;QC/TAL
        IF MC<>1 THEN 800
        Z9$(IZ)=Y$
        Z10(IZ)=V50:Z19(IZ)=QC
        Z11(IZ)=TPI:Z20(IZ)=TAL*1E3
        Z12(IZ)=ABS(DELVA*100):Z21(IZ)=ABS(100*RIPV)
        Z13(IZ)=CMIN:Z22(IZ)=(TCMIN-T1)*1000
        Z14(IZ)=CMI:Z23(IZ)=(TCMI-T1)*1000
        Z15(IZ)=ABS(DVMAX*100):Z24(IZ)=(TVMA-T1)*1000
        Z16(IZ)=ZMIN*1E3:Z25(IZ)=(TZMIN-T1)*1000
        Z17(IZ)=ZMIA*1E3:Z26(IZ)=(TZMIA-T1)*1000
        Z18(IZ)=SJ
        IZ=IZ+1
800     NEXT I
900     NEXT I1
        IF MC<>1 THEN 1000
        OPEN"O",10,"OUT.DAT"
        WRITE#10," "
        WRITE#10,"  ESDD "," ","DATE"," ","VOLTAGE"," ","V AP Nr"," ","SOURCE"
        WRITE#10,"mg/cm^2"," ","    "," ","  kV   "," ","       "," "," TYPE "
        WRITE#10,ESD$," ",DAT$," ",AV," ",AA$," ",TY$(ITY)
```

```
        WRITE#10," "
        WRITE#10,"Files","Time","","Vapp","","DVav","","Imax","","Ismx","","DVmx","","Zmin,
        "","Zsmi","","Ener","","Char","","PuDu","","Ripp","","Timx","","Tism","","Tdvm","",
        "Tzmi","","Tzsm","","Imed","","Timx","","Tism"
        WRITE#10,"","  sec","","  kV ","","  % ","","  mA ","","  mA ","","  % ","","kohm","","kohm"
        ,"","  J ","","  mC ","","  ms ","","  % ","","  ms ","","  ms ","","  ms ","","  ms ","","  mA
        ","","  % ","","  % "
        WRITE#10," "
        FOR I=1 TO IZ-1
        Y$=Z9$(I)
        WRITE#10,Y$,Z11(I),"",Z10(I),"",Z12(I),"",Z13(I),"",Z14(I),"",Z15(I),"",Z16(I),"",Z17(I),
        "",Z18(I),"",Z19(I),"",Z20(I),"",Z21(I),"",Z22(I),"",Z23(I),"",Z24(I),"",Z25(I),"",Z26(I),"",
        1000*Z19(I)/Z20(I),"",100*Z22(I)/Z20(I),"",100*Z23(I)/Z20(I)
        NEXT I
        CLOSE
1000    STOP
        END
```

APPENDIX II

DYNAMIC ARC MODEL ACCORDING TO SUNDARARAJAN/GORUR

(TRANSACTIONS ON ELECTRICAL INSULATION, APRIL/93)

```
CLS
REM DYNAMIC ARC MODEL - Sundararajan-Gorur, TEI April/93
REM
REM DIMENSIONING VECTORS FOR STORING RESULTS
DIM T(10000),C(10000)
K=1:TIME=0
REM READING VECTOR WITH FORM FACTOR, ARC LENGTH IN mm
DIM XL(300),XF(300)
nponto=9
OPEN "I",1,"Rxieee.CSV"
FOR I=1 TO nponto
INPUT#1,X1,X2,X3,X4,X5,X6,x7
XL(I)=X1/10:XF(I)=X6
REM PRINT I,XL(I),XF(I)
NEXT I
CLOSE 1
REM
N1=0.5:A1=63:TAL=100E-6:N2=0.8:A2=80
V=18600: VA=200:VC=700:DT=5E-6
COND=1.0E-6:XMOB=50
REM ARC DATA AT t=0, ARC LENGTH IN cm
rarc0=100: XLARC0=.21
REM ACTUALIZING ARC DATA
rarc=rarc0:XLARC=XLARC0
10  REM CALCULATION OF FORM FACTOR FOR XLARC
FOR I=1 TO nponto
IF XLARC>XL(I) THEN NEXT I
FF=XF(I-1)+(XF(I)-XF(I-1))*(XLARC-XL(I-1))/(XL(I)-XL(I-1))
```

```
PRINT "XLARC= ";XLARC;"  FF= ";FF
REM
REM CALCULATION OF POLLUTION LAYER RESISTANCE
RPOLN=FF/COND
print "rpoln=  ";rpoln
REM
REM CALCULATION OF CURRENT, CUR
CUR=(V-VC-VA)/(rarc*XLARC+RPOLN)
T(K)=TIME:C(K)=CUR
print"time=";T;"current=";cur
REM
REM CALCULATION OF ARC VOLTAGE GRADIENT, earc
earc=A1*CUR^(-N1)
REM
REM CALCULATION OF POLLUTION GRADIENT, ep, CONSIDERED UNIFORM
REM DISTRIBUTED POLLUTION OVER THE SURFACE, rp
rp=RPOLN/(XL(nponto)-XLARC)
ep=(A1^(1/(N1+1)))*(rp^(N1/(N1+1)))
print"ep= ";ep;" earc=";earc
REM
REM TESTING IF THE ARC ESTINGUISHES OR NOT
REM
IF ep<earc THEN PRINT " ARC ESTINGUISHES": GOTO 900
REM ARC PROPAGATES
REM CALCULATION OF XN, FROM THE STATIC ARC EQUATION
REM XN=60*V*CUR^0.8
XN=60
REM
```

```
        REM CALCULATION OF INCREMENT ON ARC RESISTANCE PER UNIT LENGTH
        drarc=DT*(rarc/TAL-(rarc^2)*(CUR^(N1+1))/(TAL*XN))
        print"drarc=";drarc
        REM
        REM CALCULATION OF ARC VELOCITY
        VEL=XMOB*earc
        REM
        REM CALCULATION OF NEW ARC LENGTH
        XLARC=XLARC+DT*VEL
        REM
        REM CALCULATION OF NEW ARC RESISTANCE PER UNIT LENGTH
        rarc=rarc+drarc
        print"new rarc=";rarc
        REM
        REM TESTING IF FLASHOVER OCCURRED
        TIME=TIME+DT:K=K+1
        PRINT "T= ";TIME;" I=";CUR;" ARC LENGTH=";XLARC
        IF XLARC>=XL(nponto) THEN PRINT"FLASHOVER":GOTO 900 ELSE GOTO 10
900     OPEN "O",2,"SAIDA.XLS"
        FOR I=1 TO K-1:WRITE#2,T(I),C(I):NEXT I
        CLOSE
1000    STOP
        END
```